# DYNAMIC DEMAND MODELING, ENERGY MANAGEMENT, AND INVESTMENT STRATEGIES IN UNCERTAIN ENERGY MARKETS

by

FARBOD FARZAN

A dissertation submitted to the

Graduate School-New Brunswick

Rutgers, The State University of New Jersey

In partial fulfillment of the requirements

For the degree of

Doctor of Philosophy

Graduate Program in Civil and Environmental Engineering

Written under the direction of

Jie Gong

And approved by

________________________________

________________________________

________________________________

________________________________

New Brunswick, New Jersey

OCTOBER, 2016

## ABSTRACT OF THE DISSERTATION

# Dynamic Demand Modeling, Energy Management, and Investment Strategies in Uncertain Energy Markets

By FARBOD FARZAN

Dissertation Director:

Jie Gong

This thesis is focused on development of an integrated decision making support framework to assist with the design of a sustainable community that has access to secure clean energy and utilizes innovative technologies and strategies. Innovative technologies include but not limited to renewable generation/storage resources, Plug-In Electric Vehicle (PEV), Building Monitoring Systems (BMS), Programmable Communication Devices (PCD), and etc. This framework has 3 unique components: i. energy dynamic demand modeling, ii. investment strategies for Distributed Energy Resources (DER), and iii. demand side energy management in uncertain markets.

In the existing litrature and industry practices, energy load profile is considered as an input to a decision making support tools and its dynamics is ignored which can lead to unreliable and less cost effective investment decisions in the long run. The analysis of such dynamics is not possible with existing demand forecast models, which are built based on time series forecasts relying on historical data. Therefore, in this thesis a bottom-up demand forecasting model entitled High Resolution Adaptive Model (Hi-RAM) is integrated with DER investment model.

Hi-RAM provides compelling results concerning the potential load shifting of PEVs, as well as how advanced energy management systems enable response to Electric Distribution Companies (EDC) price signals. Hi-RAM is a bottom-up stochastic demand model consisting of: 1- Markovian stochastic process for simulating human activities, and buildings occupany profiles. 2- Probabilistic Bayesian and Logistic technology adoption models and 3- Optimization and rule-based energy management models for building end-uses e.g., Heating, Ventilating, and Air Conditioning (HVAC), Lighting, and PEV charging which enable them to respond to EDC price signals without compromising users' comfort.

The DER investment model is built as a non-linear stochastic mixed integer programming to maximize the cash flow over the planning horizon considering long-term market variations, short-term operational volatilities, and the dynamics of underlying demand. Integration of Hi-RAM and the DER investment model offers a novel analytical framework which can be used at the design stage of new products to assess their effectiveness. Such a framework can also assist decision makers to investigate investment strategies on community's DER e.g., PV solar, wind turbines, electric storages, and etc.

taking into account the specifics of building behavioral and physical characteristics as well as the emergence of new end-uses and Demand-Side Management (DSM) capabilities.

While developing this tool is an essential step towards sustainable and efficient energy solutions in the planning stage of new buildings and communities, attention must also be paid to the existing building stock where the U.S. buildings sector alone accounted for 7% of global primary energy consumption. Recognizing its importance, this thesis also investigates advanced energy magement and control policies for buildings within a constrained peak demand envelope while ensuring that custom climate conditions are facilitated. This will mitigate service disruption and high cost of energy production and distribution.

Acknowledgment

These past wonderful years, have been a challenge to me with numerous uphill and downhill days. Luckily, I ended up with a bag full of experience, health, good memories, and wonderful people. Thank you Rutgers University!

It has been a period of intense learning for me, not only in the scientific arena, but also on a personal level. Writing this dissertation has had a great impact on me. I would like to reflect on the people who have supported and helped me so much throughout this period.

I would first like to thank my committee, Professor Jie Gong, Professor Mohsen Jafari, Professor Qizhong Guo, Professor Monica Mazurek and Mr. Andrew Stryker for their wonderful collaboration.. You supported me greatly and were always willing to help me. I would particularly like to single out one of my co-advisors, Professor Mohsen Jafari. Dear Mohsen, You are the true definition of "impact in life". It is hard to call you an advisor anymore, rather a true friend, bigger brother with heart full of passion.

To my mom and dad … How can I describe your love and support with my language! You are my hero. Nothing in this planet is worth hurting people. This is my language; this is what you have thought me.

To my lovely Farnaz … Who are you? Family member? NO! Sister? NO! You are my WORLD. From the days that you were trying to hug me with strategy of scaring me from the monster neighbor (hypothetical one!) all the way to detailed super technical advices, the only thing that has not been changed is your real love.

To Khashayar, my little brother with hidden craziness☺. I am the luckiest person who has the smartest, the most easygoing cousin here in NJ as a roomie.

To my family, who has brought me endless care and support.

To my wonderful friends back in Iran and here in U.S., God knows the level of joy, support, and togetherness that we have shared.

Thank you very much, everyone!

**TABLE OF CONTENTS**

## LIST OF TABLES

## LIST OF ILLUSTRATIONS

# INTRODUCTION AND RESEARCH BACKGROUND

## 1.1 Objectives Introduction an Research Background

This thesis intends to deliver solutions to the following problems:

1. A bottom up stochastic demand model that can capture the behavior of individuals, and residential units within a community. The demand model consists of the following components:
   i) Markovian stochastic process for simulating human activities. Activities are simulated with respect to individual's demographics e.g., age, gender, employment status and time of week. At given time within the building block, this model generates synthetic energy/non-energy related activities. Moreover, occupancy pattern of the building block would be realized.
   ii) Probabilistic Bayesian and Logistic regression technology adoption models. These models provide an estimate for penetration levels of PEVs and PCDs within communities.
   iii) Optimization and rule-based energy management models for end-uses which enable them to respond to EDC price signals without compromising users comfort.

2. DER investment strategies by considering long-term market variations, short-term operational volatilities, and the dynamics of underlying demand. The following models will be considered:

i) Non-linear stochastic mixed integer programming, which aims to maximize the cash flow due to investment on the portfolio of DER considering optimal unit commitment and economic dispatch subjected to DER operational constraints and availability of renewable sources e.g. solar, wind.

ii) Integration of bottom up demand model with investment model. This benefits investment decisions by providing realistic demand profiles considering the behavior of end users. Such integration enables investigating several scenarios under the emergence of new end-uses and the implementation of DSM strategies.

3. Day-ahead operational plans for a portfolio of multi-buildings by incorporating market uncertainty trends. The portfolio of interest consists of two groups of buildings namely; controllable and uncontrollable. The following models will be considered:

i) Physics-based and statistical models for estimation and prediction of end-use consumptions including HVAC, lighting, and building equipment in controllable buildings.

ii) A multi-objective mathematical programming to minimize the energy expenditure given EDC price signals while satisfying the occupants' comfort.

## 1.2 Brief Overview of Thesis Accomplishments

### 1.2.1 A High Resolution Adaptive Model of Residential Energy Demand

This chapter intends to build a dynamic demand model which may have advantages such as introducing the capability of estimating and forecasting of total energy consumption in residential communities without relying historical data. It also provides a better understanding of how load profiles would vary considering 1: the emergence of new end-uses e.g., PEV, 2: the DSM capabilities.

Built-in end-use models reflect the function of intelligent thermostats which learn temperature preference of building occupants. Furthermore, they simulate the dynamics of price responsive thermostats with pre-cooling and pre-heating capabilities; smart electric plugs with the capability of altering the switch status; automated dimmer switch with the capability of altering lighting levels based on real time EDC price signals.

PCDs have the potential to curtail the residential energy load profile and shift peak load to off peak periods. When the adoption of these devices is coupled with the introduction of new loads such as those from the PEVs, there is still very limited understanding on how they interact with each other, and influence one another, as well as their collective impact on energy demand.

The adaptive model is capable of analyzing why demand behaves the way it does by zooming in or out depending on the level of granularity required by the analysis. The proposed model empowers utility companies to investigate DSM strategies and their effectiveness. Moreover, it may provide insight to system operators about the impact of the emergence of new loads when actual historical or metered data is missing.

### 1.2.2 Integration of Demand Dynamics and Investment Decisions on Distributed Energy Resources

This chapter intends to demonstrate that closing the loop between demand dynamics and supply resource planning can influence long-term investment decisions on DER. The value of a DER portfolio depends on its projected return on investment and the potential growth in its operating income while serving underlying demand. For a DER, the investment payoff is directly linked to the operation of the physical assets, and return on investment depends on how these operations will be utilized in the short term. Depending on when investments were made and also amount of the investment, long-term value of a DER could be assessed. Investment decisions would be effected by considering grid energy and fuel costs, the price of technologies, and federal/state incentives [1].

Economics of DER could be enhanced by inclusion of DSM. In this context, DSM can be regarded as demand response resources. In presence of DSM, energy load profiles become highly dynamic and difficult to predict e.g. demand can be either curtailed or shifted over time as a result of response to electricity prices. Integration of DSM as a resource necessitates inclusion of dynamic demand models into planning frameworks.

The novelty of this work is the capability to investigate investment decisions by taking into account aforementioned demand dynamics. Investment planning also takes into account factors that are usually contributed to long-term market variations, and short-term operational volatilities. Unlike earlier works where power consumption is calculated from load forecast models obtained from historical data, this work uses a bottom-up demand model for short-term load calculations. The bottom up model is capable of lending itself to certain What-If analysis on the use of advanced technologies, new plug-ins e.g., PEVs, and consumer response to power price fluctuations. This would allow the investor to examine return on investment as a function of technology and behavioral pattern changes over time; such analysis cannot be carried out using stationary forecast models, which are solely obtained on the basis of historical data. The proposed methodology also enables the EDCs to investigate opportunities to reduce/defer investment on energy generation resources and network upgrades.

### 1.2.3 Operational Planning for Multi-building Portfolio in an Uncertain Energy Market

This chapter intends to investigate day-ahead operational planning of a multi-building portfolio under electricity market uncertainty. The portfolio of interest consists of two groups of buildings: controllable and uncontrollable. To perform the proposed study, a hybrid physics-based and statistical models for HVAC as well as models for lighting and electrical equipment are developed. This also includes calculation of hourly load distribution in uncontrollable buildings using non-parametric bootstrapping method. The problem of day-ahead operational planning is formulated as a multi-objective mathematical programming based on building, market, and weather information. The objectives are minimal operational expenditure and minimal occupants' discomfort. Bi-polar objectives are picked in order to consider the tradeoff between the two objective functions namely operational expenditure, and occupants comfort.

The proposed pricing scheme considers the differences between the day-ahead and real-time prices to reflect the trend of energy market uncertainty. It concludes that incorporating available insights about market uncertainty into day-ahead planning can result in load responses which may help to manage the underlying load more rigorously than just using forecasted market data.

## 1.3 Synopsis of contribution

### 1.3.1 A High Resolution Adaptive Model of Residential Energy Demand

- PEV and PCD probabilistic adoption models based on householder characteristics (see section: 3.2.1, 3.3.6) and
- End-use optimization/rule-based models that optimize the use of PCD components if adopted.

### 1.3.2 Integration of Demand Dynamics and Investment Decisions on Distributed Energy Resources

- Investigation of investment strategies on DER considering near-future scenarios such as large-scale penetration of PEV, and smart grid enabling technologies e.g. DSM.
- Inclusion of underlying demand dynamics on DER investment decisions.

### 1.3.3 Operational Planning for Multi-building Portfolio in an Uncertain Energy Market

- A generic hybrid physics-based statistical model for modeling HVAC system that is applicable for any building type and HVAC technology.
- A pricing scheme, which enables the decision maker to manage day-ahead load more efficiently in terms of daily peak reduction, overall load curtailment, and load smoothness.

## 1.4 Motivation

Many envision the future of power system to be an interconnected network of small-scale DER, along with a large-scale macro grid [2]. To name a few but not limited to, avoided transmission and distribution (T&D) losses, utilization of renewable energy, and lower greenhouse gas emissions are advantages of DER deployment [3]. According to International Energy Agency (IEA), renewable-based generation triples between 2008 and 2035 [4].

Paradigm shift is taking place not only in means of energy generation, delivery and control but also in behind-the-meter consumption patterns. A good example is PEV: The fast sales growth rate of PEVs can potentially alter the energy demand behavior [5], and could affect directly the electrical grid in at least two ways. First, as a new end-use it will increase overall energy consumption. Second, the pattern of charging PEV could correlate with traffic patterns which could potentially pose significant challenges to EDCs as it could introduce new peaks. A new demand profile may indicate different requirements to supply energy and to maintain the distribution network.

In the smart grid era, the development of information and communication technologies has enabled two-way communications between system operators and consumers. These technologies enable DSM capabilities. System planners and operators may consider DSM as a resource for balancing supply and demand. DSM can also help customers to reduce their carbon footprint [6]. Furthermore, considering high upfront cost of DER, DSM may provide opportunities to reduce/defer investment on these resources.

Operating a DER is complex due to the integration of renewable and conventional generation resources, energy storage devices, and DSM. Randomness of renewable power generation may violate the predefined DER operations schedules. Moreover, energy demands could become highly dynamic and difficult to predict in the presence of DSM.

The significant interdependency and interactions among behavior of end users, the operation of energy supply/storage resources, and the existence of DSM capabilities require a holistic and integrated decision making support framework that can capture the impact of these components on one another. Otherwise, the analysis could under or over estimate the value of DER, and could ignore the impact of risks due to uncertainties in demand and supply.

Having a model-based energy consumption calculation at end user’s level that can reflect their stochastic behavior rather than using time series-based forecasts lacks in the existing literature. This research aims at paving the way towards better understanding of the dynamics of community’s energy consumption patterns that could be utilized in the design of energy generation/storage resources to serve community’s energy needs. While developing such framework is an essential step towards sustainable and efficient energy solutions in the planning stage of new buildings and communities, attention must also be paid to the existing building stock. Recognizing its importance, this thesis also investigates green scheduling strategies for exisitng communities. This will lead to less service disruption as well as avoided investment cost on new power plants.

## 1.5 DER in conjugation with DSM

DERs are capable of operating in parallel with or independently from the macrogrid (islanded mode) ensuring reliable and affordable energy security. Having the obligation to fully satisfy its demand at each point of time, any shortage in available power supply within the DER will lead to the purchase of electricity from the macro-grid at spot market price [7].

Intermittent nature of renewable resources arise load balancing problems. One solution for this problem is application of energy storage devices. Yet another solution is DSM which can help consumers adjusts their consumption according to power supply.

High upfront cost of DER is one another barrier, since renewable energy resources are generally more capital intensive than fossil fuel resources. In this context DSM is a very promising resource [8, 9, 10]. It provides the opportunity to reduce/defer investments on new power plants. Customers will be encouraged by financial incentives e.g. real time pricing to use less energy during peak hours or to move the time of energy use to off-peak hours. This is as opposed to flat rates that do not reflect the actual costs to supply power lead to inefficient capital investment in new generation, and T&D infrastructure [11].

Above all, indicates that there is a need to integrate DSM into resource planning as a resource [11,12]. Innovations in monitoring and controlling loads are underway offering an array of new technologies that will enable substantially higher level of DSM in all customer segments. While DSM applications in industrial and commercial sectors have been well studied [13, 14, 15], there is a lack of studies which address the issue of consumers managing their household loads without sacrificing their comfort level. Examples are to name a few but not limited to application of time use management for electric vehicle recharging, pre-cooling/-heating, adjusting lighting level, and etc. These opportunities could not be investigated if underlying demand was not flexible enough to point out the effect of such dynamics on load profile.

In order to appropriately evaluate DSM, energy demand consumption models should be developed to simulate different scenarios for industrial, commercial and residential users. Traditional models forecast demand consumption based on the previous consumption data in a top-down approach. Instead, a bottom-up approach should be addressed to overcome the limitations of the former, such as the inability to predict consumption patterns changes like the implementation of flexible demand consumption, and adoption of new technologies.

The following chapters are organized as follows: Chapter 2 focuses on development of a High Resolution adaptive model of residential energy demand. In chapter 3, investment decisions on DER are investigated by considering long-term market variations, short-term operational volatilities, and dynamics of underlying demand. Last but not least, In Chapter 4, day-ahead operational strategies for existing portfolio of buildings will be discussed under uncertainty of energy market.

# 1. A HIGH-RESOLUTION ADAPTIVE MODEL OF RESIDENTIAL ENERGY DEMAND [101]

## 2.1 Abstract

In this chapter an adaptive residential energy demand model that can be used to determine changes in behavioral and energy usage patterns of a community is presented. The model is capable of simulating both electricity and heat demands of individual residential households and a community when: (i) new load patterns from Plug-in Electrical Vehicles (PEV) or other devices are introduced; (ii) new technologies and smart devices are used within premises; and (iii) new Demand Side Management (DSM) strategies, such as price responsive demand are implemented. Unlike time series forecasting methods that solely rely on historical data, the model only uses a minimal amount of data at the atomic level for its basic constructs. These basic constructs can be integrated into a household unit or a community model using rules and connectors that are, in principle, flexible and can be altered according to the type of questions that need to be answered. Furthermore, the embedded dynamics of the model works on the basis of: (i) Markovian stochastic model for simulating human activities, ii) Bayesian and logistic technology adoption models, and iii) Optimization, and rule-based models to respond to price signals without compromising users' comfort. The proposed model is not intended to replace load forecast models. Instead it provides an analytical framework that can be used at the design stage of new products and communities to evaluate design alternatives.

The framework can also be used to answer questions such as why demand behaves the way it does by examining demands at different scales and by playing What-If games.

These analyses are not possible with time-series forecast models built on historical samples, simply because, these forecast models and their level of accuracy are limited by their training datasets and can hardly demonstrate variations that are not present in the historical dataset.

KEYWORDS: Bottom-up demand modeling, Technology adoption, Demand side management, Electric vehicles, Price responsive demand.

Nomenclature

Index

| | |
|---|---|
| d | Index for Day of Week; $d \in \{0,1\}$ |
| $\Phi$ | Index for PEV State; $\Phi \in \{1,2,3\}$ |
| i | Index for Household; $i = 1 \dots I$ |
| j | Index for End-uses |
| r | Index for Occupant; $r = 1 \dots R$ |
| t | Index for Time of Day; $t = 1 \dots T$ |

Variables and Parameters

| | |
|---|---|
| $A_{PCD}$ | PCD Adoption |
| $A_{PEV}$ | PEV Adoption |
| AR | Acceptable Light Level |
| $CAP_{PEV}$ | PEV Electric Storage Capacity |
| $CC_t$ | Cost Associated to Charging PEV |
| $CH_t$ | PEV Electric Storage Charge |
| CHR | PEV Electric Storage Charge Rate |

| | |
|---|---|
| $CP_{air}$ | Air Specific Heat Capacity |
| $DCH_t$ | PEV Electric Storage Discharge |
| DF | Daylight Factor; Ratio of Internal Light Level to External Light Level |
| DHR | PEV Electric Storage Discharge Rate |
| $EL_j$ | Energy Load Associated to j-th End-use |
| EP | Electricity Price |
| FR | Flexible Lighting Level Range |
| K | Heat Transfer rate with Outside |
| $LUX_{AL}$ | Needed Artificial Light |
| $LUX_{IN}$ | Illuminance Due to Daylight at a Point on the Indoors Working Plane |
| $LUX_{OUT}$ | Outdoor Illuminance from an Unobstructed Hemisphere of Overcast Sky |
| $m_a$ | Air Mass |
| $m_{H\dot{V}AC}$ | Air Mass Flow Rate |
| MCI | Number of Monte Carlo Iterations |
| MDH | Miles Driven per Hour |
| MPSL | Minimum Percentage of Storage Level |
| NLUX | Indoor Comfortable Light Level |
| O% | Active Occupancy Percentage |
| $p_{S_nS_m}$ | Probability of Transition from $S_n$ to $S_m$ |
| Pspecific | Buildings' Specific Heat Loss Rate |
| $S_n$ | State of Markov Chain; $n = 1 \dots N$ |
| SOC | State of Charge |

| | |
|---|---|
| $SP_{LB\ \&\ UB}$ | Thermostat Set-points (Lower and Upper bound) |
| $T_a$ | Internal Temperature |
| $TEL_d^i$ | Total Energy Load Profile of the i-th Household |
| $T_{HVAC}$ | HVAC Supply Air Temperature |
| $T_{S_n S_m}$ | Transition Matrix |
| $T_\infty$ | Ambient Air Temperature |

## 2.2 Introduction

The residential sector is using almost one third of the total electrical energy in US [16]. According to the Federal Energy Regulatory Commission (FERC), much of the untapped potential for reducing electricity use lies in residential behavioral changes and modifications to traditional consumption patterns [17]. This is particularly true considering that by 2030 Automatic Metering Infrastructure (AMI) will be widely deployed across the U.S. and dynamic pricing will be widely available or at least it will be an option [17]. At the same time, the residential electricity demand is also on the verge of showing increased uncertainty as new types of home appliances/electronics are introduced and adopted. Traditionally, the major use of electricity in the U.S. residential sector can be attributed to air conditioning, lighting, appliance/electronics, and water heating [18]. The recent rapid adoption of new home appliances/electronics, albeit many of them have become more energy efficient, has introduced new variables into the residential electricity demand. A good example is Plug-in Electric Vehicles (PEV) with fast sales growth rate which can potentially alter the residential energy demand profile [19], and could affect directly the U.S. electrical grid in at least two ways. First, as a new end use it will heighten the average daily demand level. Second, it could pose significant challenges to utility companies if people choose to recharge their PEVs during peak hours. Without anticipating proper strategies to curtail/shift such heightened peak demands, new power plants are needed in order to meet these demands, which, in turn, lead to less efficient use of energy resources.

Fortunately, devices that provide feasibility for utility companies to influence consumer consumption behavior and for householders to save energy and to take benefits of Demand Side Management (DSM) strategies are emerging and have seen rising applications in the residential sector. These devices are commonly referred to as Programmable Communication Devices (PCD). PCDs are designed to adjust consumption level not only by household specific conditions but also by the exogenous market driven changes e.g., electricity price. A common set of these devices include, but are not limited to, Intelligent Thermostats ($\mathrm{PCD_{IT}}$), Price Responsive Thermostats ($\mathrm{PCD_{PRT}}$), Smart Electric Plugs ($\mathrm{PCD_{SEP}}$), and Automated Dimmer Switches ($\mathrm{PCD_{ADS}}$). These devices have the potential to shift/curtail energy consumption and contribute to the development of energy efficient behaviors. But when the adoption of these devices is coupled with the introduction of new loads such as those from the PEVs, there is still very limited understanding of how they interact and influence each other, and of their collective impacts on the residential energy demand. Furthermore, to design appropriate DSM strategies, energy demand consumption models should be developed to simulate different scenarios for energy users.

This research aims at developing a high-resolution residential energy demand model to gain better understanding of how different electricity demand patterns evolve with the emergence of new loads, such as PEVs, the adoption of new technologies, and the implementation of price responsive DSM strategies.

## 2.3 Review of Energy Demand Models

In deregulated markets, demand forecasting is vital for the energy industry. Forecasting models are used to set electricity generation and purchasing, establish electricity prices, switch loads and plan for infrastructure development [20]. Demand forecasting can serve short-term and long-term goals. Short-term forecasting plays a very important role in operating functions such as energy transactions, unit commitment, security analysis, and economic dispatch [21]. On the other hand**,** long-term forecasting focuses on the role of policy formulation and supply capacity expansion. Long-term forecasting tries to predict consumption behavior changes under the influence of adoptions of new technologies or changes in policies for energy use. Short-term and long-term forecasting requires different modeling approaches. More specifically, short-term forecasting usually employs a top-down approach, while for long-term forecasting; a disaggregated bottom-up approach is often used. The top-down approach treats individual sectors as energy sinks and is not concerned with individual end uses. The bottom-up approach, on the other hand, identifies the contribution of each end-use towards the aggregate energy consumption.

In the context of residential segment, both top-down and bottom-up models have been developed to model and predict residential energy demand. For example, a few studies utilized historic aggregate energy values and regressed the energy consumption of the housing stock as a function of top-level variables such as macroeconomic indicators (e.g. gross domestic product, and inflation), energy price, and general climate [22, 23].

The bottom-up approaches extrapolate the estimated energy consumption of a representative set of individual houses to the regional and national levels [23]. There are two types of models used in the bottom-up approach: statistical and engineering models. Statistical models apply a variety of statistical techniques to regress the relationship between the end-uses and the energy consumption. Techniques such as regression [24, 26], conditional analysis [26, 27] and neural networks [28, 29] are common practices throughout the literature. On the other hand, engineering models rely on information about building characteristics and end-uses to estimate energy consumption. Engineering models are the only viable methods that can fully develop energy consumption estimate for a sector without any historical energy consumption information. Engineering models proposed in the literature have employed techniques such as distribution [30, 31], archetypes [32, 33], and samples [34, 35]. Generally, bottom-up engineering models are more suitable options for evaluating the impacts of new technologies or energy saving opportunities [22]. In these types of models, each end-use has its own sub-model, which enables the aggregated model to track the effects of any component change on reducing energy consumption. However, one drawback common to most engineering models is the assumption of unrealistic occupant behavior which could lead to unreal conclusions [22].

This limitation has encouraged researchers to develop engineering models equipped with advanced occupant behavior models. Caposo et al. [30] used a Monte Carlo method to capture the relationship between the residential demand and the behavioral factors of the household occupants. Richardson et al. [36] introduced a Markov chain technique to generate synthetic active occupancy patterns based on the survey data on people’s time use in the UK. Highly resolved synthetic demand data were created in their study by using a stochastic model that maps occupant activities to appliance uses. Widén and Wäckelgård [37] employed a similar approach to relate residential power demand to occupancy profiles. Of particular note is that their synthetic activity generation model was calibrated using time use and electricity consumption datasets collected in Sweden. The study showed that realistic demand patterns can be generated from simulated sequence of human activities. Muratori et al. [38] proposed a similar approach with the addition of physics-based engineering HVAC systems, and their Markov process is calibrated based on the American Time Use Survey (ATUS) data. The study proved that the generated demand profiles are statistically similar to metered residential electricity data. Energy demand models can be a valuable tool for evaluating the challenges and opportunities for implementing DSM and Demand Response (DR) programs in smart electricity grids [39] with the potential of achieving to approximately 10% reduction of overall demand [40]. However, few studies have employed bottom-up models to study the impacts of energy saving programs. In [41, 42], a dynamic energy management framework is developed to find the overall optimal schedule of deferrable loads with the objective of minimizing the electricity-related expenditure of each residential customer. [43] presented a case study which simulates the effect of widespread adoption of tiered electricity pricing; this work complements earlier studies [44]. They are motivated by the economic and policy impacts of residential price-based demand response programs in smart grid era.

The focus of this chapter is to determine demand changes subject to (i) emergence of new PEV loads, (ii) adoption of new technologies (PCD), and (iii) implementation of DSM strategies in terms of price responsive demand. To achieve this, a high resolution bottom-up model is developed. The model includes advanced engineering and occupant behavior sub-models. Previous studies have evaluated the impacts of these new technologies, but more from the stand points of individual technologies or economic and policy impacts [43, 44]. In this study, however, the coupling effects of these technologies on energy demands when they are simultaneously adopted are considered. The model features the following new contributions: (i) PEV and PCD probabilistic adoption models based on householder characteristics and (ii) end-use optimization/rule-based models that optimize the use of PCD components if adopted. Collectively, the proposed model can pave the way towards a new community development plan and design platform that closely couples energy supply with energy demand dynamics and evolution and allows for a priori evaluation of effective energy saving and efficiency alternatives. Furthermore, a tool built on the basis of such a dynamic model can address the elasticity of a community to evolving changes in prices, energy efficiency policies, and so on. Next, modeling methodology is given followed by model validation, simulation analysis, discussion of results, and conclusions.

## 2.4 Modeling Methodology

The general composition of the proposed energy demand model is shown in Figure 1. In this model, three load categories are defined as base loads ($\mathrm{SH\&S, WH, LI, and\ CA}$), loads associated with specific activities (A), and PEV load. Nominated load categories are according to major end uses within residential sector [30]. To capture the effect of PEV emergence, a Bayesian probabilistic adoption ($\mathrm{A_{PEV}}$) model is introduced. In addition, a probabilistic logistic model is formulated to measure the willingness of householders to adopt new technologies ($\mathrm{A_{PCD}}$). For each specific household, a stochastic sequence of activities is generated based on its resident characteristics and time of week. Each activity in the sequence has its own energy consumption load ($\mathrm{EL_A}$). A sequence of activities also forms an occupancy pattern for a household such that it directly influences the base loads and PEV load. Last, but not the least, the model considers the availability of PCD such that it provides opportunities to end users to adjust consumptions based on price of energy while maintaining occupant comfort. The details of each end use model with two scenarios of $\text{"Equiped with PCD", and"Not equiped with PCD"}$ are provided in the upcoming sections. Based on the above structure, the total energy load profile of the i-th household with "R" ($\mathrm{r = 1}$, refers to householder index) residents can be formulated as:

$$\mathrm{TEL_d^{HH(i)} = \sum_{t=1}^{T} \sum_{j=1}^{J} EL_{j,d}(t)}, \text{where: } \mathrm{j \in \{SH\&SC, WH, L, CA, A, PEV\},\ EL_{A,d}(t) = \sum_{r=1}^{r=R} EL_{A\ r,d}(t)} \qquad (1)$$

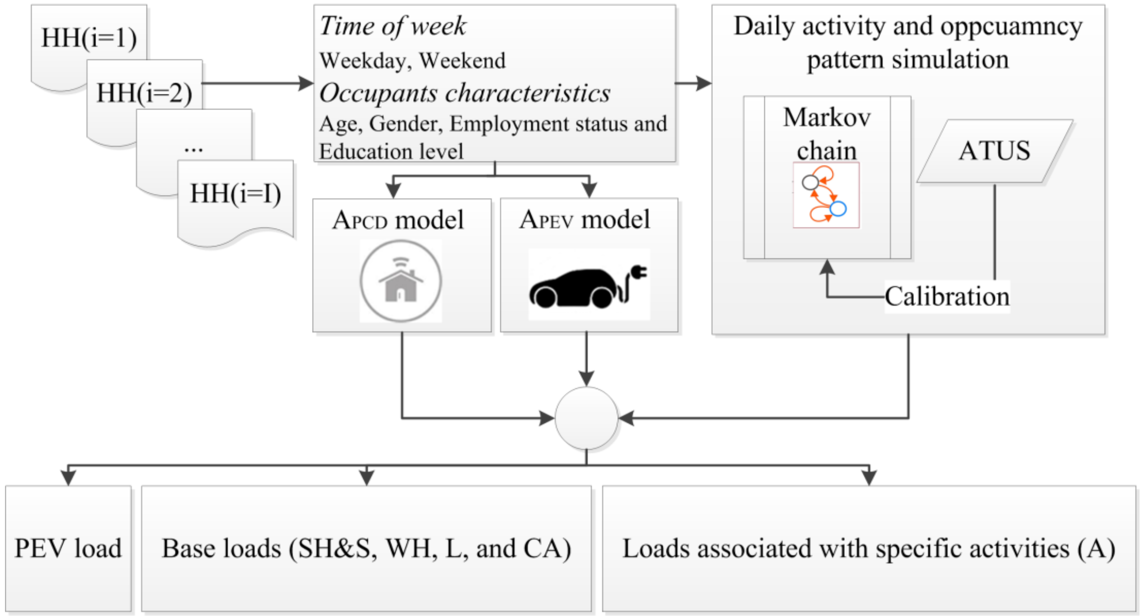


Figure 1 Schematic framework of proposed modeling methodology

## 2.5 Dynamic Demand Models

### 2.5.1 Daily Activity and Occupancy Pattern Simulation

Individual behaviors are stochastic in nature, which is caused by a multitude of factors such as individual demographic characteristics (e.g. age, gender, and employment status), type of day (weekend/weekday), and environmental conditions [38]. To capture this stochasticity, non-homogenous and discrete-time Markov chain models are used in this work. If there are N possible states defined as $S_1 \ldots S_{n=N}$, the memoryless Markov property indicates that at each time step (t) conditional probability distribution of future states of the process depends only upon the present state. At each time step, the transition matrix $T_{S_n S_m}(t) = \Pr(X_{t+1} = S_m \,|\, X_t = S_n)$ can be written as:

$$T_{S_nS_m}(t) = \begin{bmatrix} p_{S_1S_1}(t) & \cdots & p_{S_1S_N}(t) \\ \vdots & \ddots & \vdots \\ p_{S_NS_1}(t) & \cdots & p_{S_NS_N}(t) \end{bmatrix} \tag{2}$$

According to the above transition matrix, the probability that the process occupies a particular state $S_n$ at time step t is:

$$p_{S_n}(t) = p^{S_n}(1) \prod_{t=1}^{t-1} T_{S_nS_m}(t) \ , \sum_{n=1}^{N} p_{S_n}(t) = 1 \tag{3}$$

In this model, the transition probabilities are calibrated using the ATUS data with the 10-minute time intervals. Based on the ATUS data, the possible states are classified into 12 categories (See Table 1).

Table 1 The occupant states defined in the Markov chain

| States | | |
|---|---|---|
| 1.Away (work related/education) | 5.Vacuum/Sweeping | 9.Dishwashing/Drying |
| 2.Away (non-work related) | 6.Loundry | 10.Computer |
| 3.Sleeping | 7.Cooking | 11.Audio/Music |
| 4.Washing/Grooming | 8.Watching TV | 12.InsideActivity (non-energy) |

### 2.5.2 Customized Transition Probabilities

Previous studies have shown that age, gender, and employment status are dominant factors affecting average time spent on different activities [47] and different geographic regions have no influence on an ATUS occupant's daily activity pattern [48]. Since residential activities are highly relative to time of week [49], the transition probabilities are modeled as a function of Time of Week ($TW \epsilon \{weekday, weekend\}$), age, Gender ($G \epsilon \{male, female\}$), and Employment Status ($ES \epsilon \{employed, unemployed/retired\}$). For each respondent in the ATUS data set, these variables are extracted, and stratified into 6 homogenous age subgroups ($AgeCAT \epsilon \{1: < 22,\ 2: 22-29, 3: 30-43, 4: 44-57, 5: 58-71, 6: > 71\}$). In this way, a customized set of transition probabilities as follow are provided:

$$T_{AgeCAT,G,ES,TW}(t) = \begin{bmatrix} p_{(11|AgeCAT,G,ES,TW)}, t & \cdots & p_{(1N|AgeCAT,G,ES,TW)}, t \\ \vdots & \ddots & \vdots \\ p_{(N1|AgeCAT,G,ES,TW)}, t & \cdots & p_{(NN|AgeCAT,G,ES,TW)}, t \end{bmatrix} \quad (4)$$

At each time step 't', a uniformly-distributed pseudorandom number is used to determine an individual's state ($S \in \{1, \ldots, N = 12\}$). Figure 2 depicts the effect of occupant characteristics on occupancy pattern. The reference is a weekday for an occupant with $AgeCAT = 3, G = male, ES = employed$ (Blue curves in Figure 2). For each scenario a Monte Carlo simulation ($MCI = 1000$) is conducted. At each time step, the Expected Chance of Being Home (ECBH) is calculated as in (5).

$$ECBH(t) = {\textstyle\sum_{MCI} 1n(t)}/_{MCI}, 1n(t) := \begin{cases} 1, & \text{if } S(t) \notin \{1,2\} \\ 0, & \text{else} \end{cases} \quad (5)$$

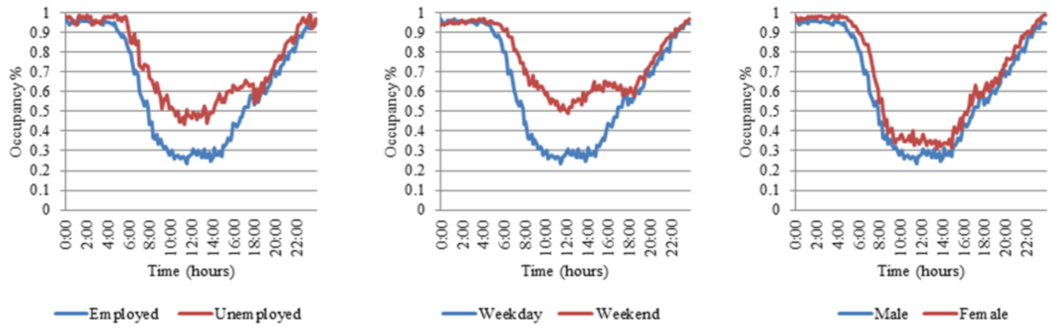


Figure 2 Expected chance of being home and different characteristics

## 2.6 Enabling Technologies

### 2.6.1 Probabilistic PCD Adoption Model

The adoption of the PCD technology is modeled as a probability event that is related to affordability and environmental attitudes of householders. A common approach to measure a person's attitude towards investing in energy efficient technologies is to ask customers about their past purchases of Compact Fluorescent Light bulbs (CFL) as an indicator of their willingness to pay more in order to save on energy costs over the life of a product [50, 51]. Herein data in [52] is applied where participants reported their perceptions of energy consumption and savings and recycling activities. In one of many questions, respondents were asked if they bought CFLs (binary response). These response data is used as the basis for developing a probabilistic PCD adoption model. More specifically, the problem is formulated as a logistic regression problem. Logistic regression uses a linear predictor function $f(k, i)$ to predict the probability that observation i (here: i-th Household) has outcome k, where:

$$f(k, i) = \beta_k \times X_i \tag{6}$$

$\beta_k$ is the set of regression coefficients associated with outcome k. $X_i$ is the set of explanatory variables $18 \leq \text{Age} \leq 76$, Education Level (Edl) $\{1\text{: high school/less}, 2\text{: some college}, 3\text{: college degree}, 4\text{: graduate school}\}$ associated with observation i. For K possible outcomes ($K = A_{PCD} \in \{\text{Yes}, \text{No}\}$), K-1 independent binary logistic regression model is built. One outcome is chosen as a pivot (reference category: $A_{PCD} = \text{No}$) and the other outcome is separately regressed against the pivot outcome (7). Based on this approach, logistic regression coefficients are estimated and summarized in Table 3.

$$\ln\left(\frac{P[A_{PCD_i} = \text{Yes}]}{P[A_{PCD_i} = \text{No}]}\right) = \beta_{(0, A_{PCD}=\text{Yes})} + \beta_{(\text{Age}, A_{PCD}=\text{Yes})} \times X_i^{\text{Age}_{r=1}} + \beta_{(\text{Edl}, A_{PCD}=\text{Yes})} \times X_i^{\text{Edl}_{r=1}} \quad (7)$$

It should be noted that, for the i-th household, $X_i^{\text{Age}}$ and $X_i^{\text{EL}}$ are assumed to be householder's $\text{Age}_{r=1}$ and$\text{EL}_{r=1}$, respectively. According to (5), the probability of adopting ($P[A_{PCD_i} = \text{Yes}]$) and not adopting PCD ($P[A_{PCD_i} = \text{No}]$) for i-th household are computed using the fact that all probabilities must sum to one ($P[A_{PCD_i} = \text{Yes}] + P[A_{PCD_i} = \text{No}] = 1$). For this sample dataset, the log odds of "$A_{PCD_i} = \text{Yes}$" versus "$A_{PCD_i} = \text{No}$", left hand side of (7), increases as the education level increases.

Table 2 Model coefficients and p-values

| | $A_{PCD} = \text{Yes}$ | P-Values |
|---|---|---|
| $\beta_{(0,A_{PCD}=\text{Yes})}$ | -1.7764 | 6E-05 |
| $\beta_{(\text{Age},A_{PCD}=\text{Yes})}$ | 0.020946 | 3E-02 |
| $\beta_{(\text{Edl},A_{PCD}=\text{Yes})}$ | 0.19858 | 5E-02 |

### 2.6.2 Intelligent Thermostats

$PCD_{IT}$ is considered as a device that is able to learn occupants' temperature preferences and adjust temperature settings accordingly. As the first step to develop the $PCD_{IT}$ model, Residential Energy Consumption Survey (RECS) data is used to tabulate the intelligent thermostats settings based on occupant characteristics. As shown in the RECS data [53], two variables, TEMPHOMEAC and TEMPHOME, were collected to represent comfort temperatures for householders during summer and winter seasons. Box-and-whisker diagrams are constructed for each 24 combinations of “AgeCAT” and “Edl”. Figure 3-a shows the first quartile (Q1) and the third quartile (Q3) values for “TEMPHOMEAC” for each combination. Figure 3-b shows the same information for “TEMPHOME”. Figure 3-a suggests that the sampled respondents with higher age levels prefer higher temperatures in summer and respondents with higher education levels prefer higher temperature settings as well. However, such trend cannot be clearly observed in winter (Figure 3-b). Based on Figure 3, the lower surface (Q1) and the upper surface (Q3) are used as the Lower Bound ($SP_{LB}$) and the Upper Bound Set Points ($SP_{UB}$), respectively, when HVAC systems are functioning.

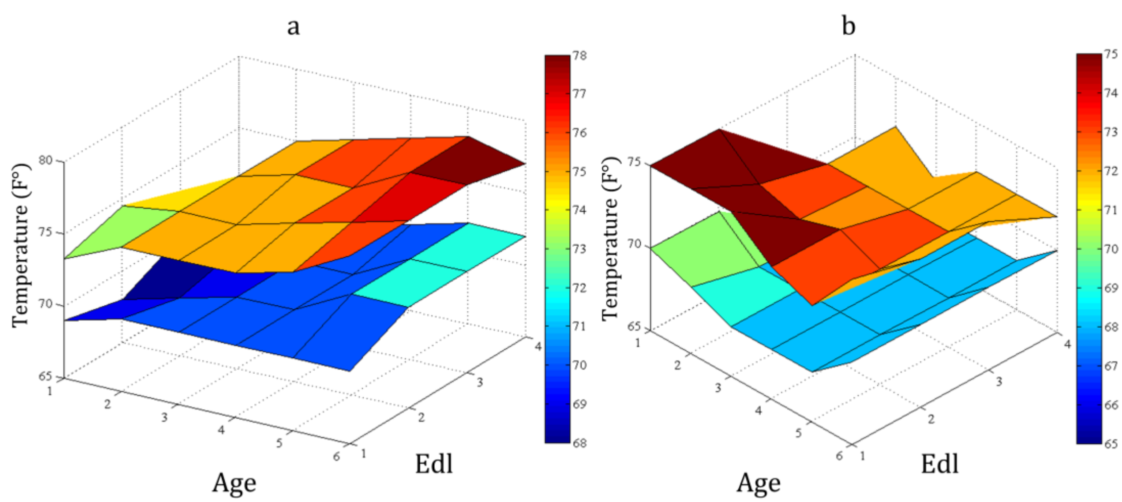


Figure 3 a) Lower and upper bounds for set points (summer), b) Lower and upper bounds for set points (winter)

## 2.7 Energy Consumption Modeling

This section describes the modeling of energy consumption associated with specific activities and the base load calculation. The latter accounts for end uses including SH&S, LI, CA, and WH. In addition to these models, a load model centered on PEVs is also described.

### 2.7.1 Energy Consumption Associated with Specific Activities

To model the energy consumption associated with specific activities, the power conversion parameters are used as shown in Table 4 to convert activity states into power demands, an approach similar to what was employed in [38]. These parameters are generated based on the average wattages of the current appliance stock [54].

Table 3 Energy consumption power associated to specific activities

| States | Electricity power consumption (Watt) |
|---|---|
| Washing | 1800 |
| Vacuum/Sweeping | 1500 |
| Laundry | 3600 |
| Cooking | 3500 |
| Watching TV | 120 |
| Dishwashing/Drying | 1800 |

### 2.7.2 Space Heating and Cooling Model

In order to calculate the energy consumption caused by the space heating and cooling end-uses, the dynamic change of indoor temperature is formulated as a Newton's law of heating and cooling problem. Such dynamic is introduced to enable the functionalities of $\mathrm{PCD_{PRT}}$ e.g. pre-cooling and pre-heating capabilities.

$$\mathrm{m_a} \times \mathrm{C_p} \times \frac{\mathrm{dT_a}}{\mathrm{dt}} = \dot{\mathrm{m}}_{\mathrm{HVAC}} \times \mathrm{CP_{air}} \times (\mathrm{T_{HVAC}} - \mathrm{T_a}) - \mathrm{K} \times (\mathrm{T_a} - \mathrm{T_\infty}) \tag{8}$$

Discretization techniques are used to integrate this model into a simulation framework with a step size of 10 minute. This process is usually carried out as a first step toward making continuous differential equations suitable for numerical evaluation. It is well-known that the space heating and cooling loads are highly dependent on site specific characteristics e.g. wall/window insulation, thickness of walls, humidity, etc. Since this chapter is not aimed at developing detailed model of HVAC, a slightly modified version of the temperature evaluation model which is proposed in [38] is adopted here (9). That is instead of calculating the thermal resistance of household envelope (K/W), a building's specific heat loss rate (Pspecific $\sim [\mathrm{W/K}]$) from the RECS dataset is used. To enable the pre-cooling/pre-heating capabilities, an optimization framework is developed to minimize the cost of HVAC energy consumption given the knowledge of the current electricity price in every ten minutes. If PCDs are not available, a flat electricity price profile will be assumed. In other words, this can be formulated as minimize $\sum_{t=1}^{T}|\mathrm{pdot}(t)| \times \mathrm{EP}(t)$ subjected to the following constraint:

$$T_a(t) = T_a(t-1) + \frac{\mathrm{pdot}(t) + \mathrm{Pspecific} \times \left(T_\infty(t) - T_a(t-1)\right)}{m_a \times \mathrm{CP}_{\mathrm{air}}} \quad (9)$$

The indoor temperature ($T_a$) at each time interval is constrained between the lower and upper bounds ($\mathrm{SP}_{\mathrm{LB}} \leq T_a(t) \leq \mathrm{SP}_{\mathrm{UB}}$). If PCD is available, the $\mathrm{PCD}_{\mathrm{IT}}$ sets lower and upper limits based on the preferences of householders. Otherwise, the predefined lower and upper bounds will be assigned based on the ASHRAE standards [55]:

$$[\mathrm{SP}_{\mathrm{LB}}, \mathrm{SP}_{\mathrm{LB}}] = \begin{cases} f(\mathrm{Age}_{r=1},\ \mathrm{Edl}_{r=1}), & \text{if equiped with PCD} \\ [70,75], & \text{else} \end{cases} \quad (10)$$

pdot at each time interval, is constrained as follow: $-\mathrm{Max}(\mathrm{AC}) \leq \mathrm{pdot}(t) \leq 0$ where:

$$\mathrm{MaxAC} = \mathrm{HH\ Area} \times \rho_{\mathrm{air}} \times \mathrm{CP}_{\mathrm{air}} \times \left(T_{\mathrm{HVAC,CoolingMode}} - T_{\mathrm{Designed,Cooling\ mode}}\right) \quad (11)$$

### 2.7.3 Lighting Model

The lighting end use model takes into account perception of natural light levels within a building, the number of people who are active (at home and awake) [30, 56], and household area. At each time step, the indoor illuminance ($\text{lux}{\sim}\text{lm}/\text{m}^2$) is defined as below:

$$\text{Lux}_{\text{IN}}(\text{t}) = \left(\frac{\text{DF}}{100}\right) \times \text{Lux}_{\text{OUT}}(\text{t}) \tag{12}$$

If an active individual is presented at a time step, the luminance level should be hold within an Acceptable Range ($\text{AR} \in \{100 - 150\ \text{lux}\}$ [57]). The Flexible Range (FR) is defined as a distance between the maximum and minimum levels of AR. Anywhere within this range; AR represents a comfortable lighting situation for occupants. $\text{PCD}_{\text{ADS}}$ is included to provide the capability of controlling lighting levels within the AR range. It is assumed that the FR has a negative relationship with the ratio of electricity price over the peak price. A mathematical formulation of $\text{FR}(\text{t})$ is as follows:

$$\text{FR}(\text{t}) = \begin{cases} \text{f}\left(\frac{\text{EP}(\text{t})}{\max(\text{EP})}\right) & , \quad \text{if equiped with PCD} \\ \max(\text{AR}) - \min(\text{AR}), & \quad \text{else} \end{cases} \tag{13}$$

The number of people who are active at each time interval is derived from simulated individual activities at a household. This leads to the definition of occupancy percentage at each time interval as:

$$\mathrm{O\%(t)} = \frac{\sum_{n=1}^{n=N} \mathrm{1n(t)}}{\mathrm{N}}, \quad \mathrm{1n(t)} := \begin{cases} 1, & \text{if } \mathrm{S_n(t)} \notin \{1,2,3\} \\ 0, & \text{else} \end{cases} \tag{14}$$

Given $\mathrm{O\%(t)}$, one could calculate lighting electricity load within a household as the following:

$$\mathrm{NLUX(t)} = \mathrm{Min(AR)} + \mathrm{FR(t)} \tag{15}$$

$$\mathrm{LUX_{AL}(t)} = \mathrm{Max}\left[\left(\mathrm{NLUX(t)} - \mathrm{LUX_{IN}(t)}\right), 0\right] \times \mathrm{O\%(t)} \tag{16}$$

$$\mathrm{EL_{LI}(t)} = \mathrm{Area} \times \left(\frac{\mathrm{LUX_{AL}(t)}}{\eta\mathrm{(efficiency)}}\right) \tag{17}$$

### 2.7.4 Cold Appliance (Refrigeration) Model

According to the data from the energy.gov website, cold appliances generally work 1/3 of the time. To calculate the energy consumption of cold appliances, a Bernoulli distribution with 1/3 probability of success is being used. This approach has been previously introduced in [48].

### 2.7.5 Water Heating Model

Based on the possible states (S), loads associated with water heating are calculated if a household individual is engaged in one of the following activities: washing/grooming, dishwashing/drying, and laundry. As reported in a previous study [58], the following metric for relating water usage to specific activities is used (Table 5).

Table 4 Average GPM water usage for each activity state

| State(S) | GPM |
| --- | --- |
| 4 | 2.5 |
| 6 | 2 |
| 9 | 2.25 |

To calculate the amount of electricity needed to heat water, it is assumed that water typically enters residences at about 10 °C (Tin). It is true that Tin may vary with latitude and season, but for simplicity this variation is ignored. Also according to [58], water with a temperature of 40–49 °C (mean(Tout) = 45°C) is usually used for dish-washing, laundry and showering. Based on this information, the consumed electricity for water heating in each time step within a household can be calculated using the following formula:

$$\mathrm{EL_{WH}(t)} = \mathrm{GPM_{S_i}} \times \mathrm{Duration(t)} \times \left(\frac{\mathrm{8.3lb\ water}}{\mathrm{gal}}\right) \times (\mathrm{Tout} - \mathrm{Tin}) \tag{18}$$

### 2.7.6 PEV Model

Curtin et al. [44] conducted interviews with randomly selected 2,513 participants to assess their state of knowledge and opinions about PEVs. They found that “age of householder” and “income” are strong correlates of consumers who expressed interest in purchasing PEVs. Age is an important factor due to the strong relationship between with driving miles - elderly people drive less than young people [59]. With respect to income, Curtin et al. found that consumers with higher income have a significantly higher probability to purchase PEVs [44]. Their study also found a correlation between income and education level (Edl). Using data in [44], a probabilistic PEV adoption ($A_{PEV}$) model is formulated (19). For each household, the model treats householders' age and Edl as two independent variables (see Figure 4). Number of adopted PEVs in each household is set to be one. Figure 4 shows the calculated probabilities for PEV adoption across the factors including education level and age of householder. This probabilty plot clearly confirms the findings in [50].

$$p(A_{PEV}|Age, Edl) = \frac{p(A_{PEV},Age,Edl)}{p(Age,Edl)} = \frac{p(Age|A_{PEV},Edl).p(PEVAdoption,Edl)}{p(Age,Edl)} =$$

$$\frac{p(Age|A_{PEV}).p(A_{PEV}|Edl).p(Edl)}{p(Age,Edl)} = \frac{p(A_{PEV}|Age).p(A_{PEV}|Edl)}{p(A_{PEV})} = \frac{p(A_{PEV}|Age).p(A_{PEV}|Edl)}{\sum_{Age} p(A_{PEV}|Age).p(Age))} \quad (19)$$

Table 5 Age and education levels for PEV adoption model

| Variables | Categories | Description |
|---|---|---|
| Education level (Edl) | 1 | High School or less |
| | 2 | Some College |
| | 3 | College degree |
| | 4 | Graduate school |
| Age | 1 | 18-34 |
| | 2 | 35-44 |
| | 3 | 45-54 |
| | 4 | 55-64 |
| | 5 | 65 and more |

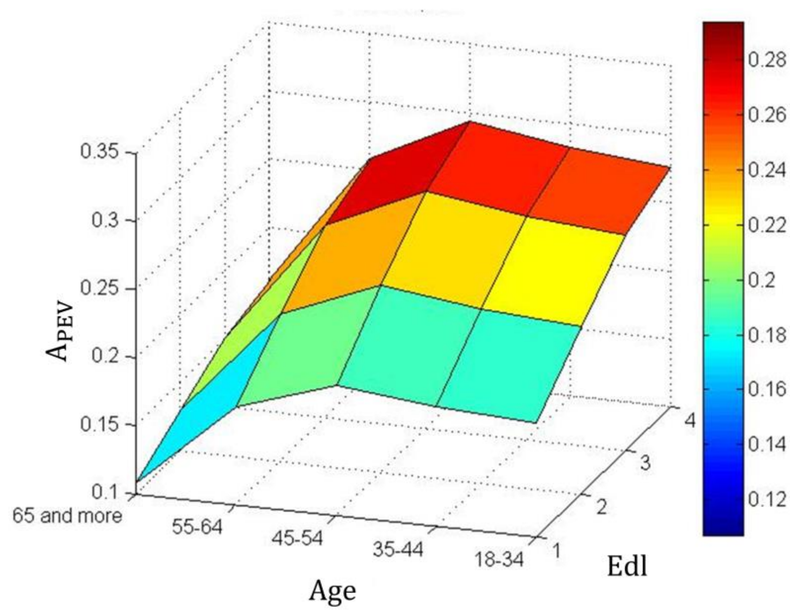


Figure 4 $\mathbf{A_{PEV}}$ probabilities across different age and education levels

The time and amount of charging are two key factors for evaluating the impact of the large-scale introduction of PEVs on the aggregated load profile [60]. As a result two schemes can be adopted (i) optimal and (ii) non-optimal charging scheme. In both schemes, the charging schedule is based on occupancy patterns that are obtained from daily activity simulator in section 3.5.2 along with consideration of individual driving habits. Scheme (i) is effective when both PEVs and PCDs are adopted. Furthermore, to demonstrate the functionality of $\mathrm{PCD_{SEP}}$, the charging schedule is set to follow a dynamic programming framework, which finds the shortest feasible path along which the cost based on a given hourly price is minimized. The feasibility of a path is dictated by householder occupancy patterns and PEV technical constraints e.g., battery capacity, charge, and discharge. On the other hand, scheme (ii) is effective when PEV exists but no PCD is adopted. In this case, one random feasible schedule that is not necessarily averse of price will be assigned. To solve the cost optimization problem, a forward induction technique is employed. More specifically, the recursive relationship for the forward induction on the minimum-cost problem is formulated as in $(21)$ where $\mathrm{CC_t}(\Phi_\mathrm{t})$ is an optimal value over the current and completed stages given that PEV is in state $\Phi \in [1\text{: Charge}\ ,\ 2\text{: Discharge},\ 3\text{: Idle}]$ with $\mathrm{t}$ stages to go. At each time stage (t) available options for PEV state are dictated by whether a PEV is present in the premise's charging station or not (20). It is assumed that the householder is the one who commutes with PEV, and PEV will not be used in durations when the householder is "OUT" for less than an hour (4 consecutive 15min intervals where householder is in $\mathrm{S_i} \in \{\mathrm{i} = 1\ ,2\}$). One hour minimum charging time is also considered (4 consecutive 15min intervals where householder is in $\mathrm{S_i} \notin \{\mathrm{i} = 1\ ,2\}$.

$$\Phi_\mathrm{t} = \begin{cases} \mathrm{S_i} \in \{1 \text{ or } 3\} & ,\mathrm{PEV_t^{in,out}} = 1 \\ \quad \mathrm{S_i} = 2 & ,\ \mathrm{PEV_t^{in,out}} = 0 \end{cases} \quad ,\mathrm{PEV_t^{in,out}} \in \{1\text{: IN}, 0\text{: OUT}\} \tag{20}$$

Consequently, the minimum charging cost problem can be formulated as:

$$\text{minimize } \mathrm{CC_t}(\Phi_\mathrm{t}) + \mathrm{CC_{t-1}}(\Phi_\mathrm{t-1}) \tag{21}$$

s.t.

$$\mathrm{CC_t}(\Phi_\mathrm{t}) = \begin{cases} \mathrm{CH_t} \times \mathrm{EP_t} & ,\ \Phi_\mathrm{t} = 1 \\ 0 & ,\ \Phi_\mathrm{t} \neq 1 \end{cases} \tag{22}$$

$$\mathrm{CH_t} \quad = \begin{cases} \mathrm{CHR} & ,\ \Phi_\mathrm{t} = 1 \\ 0 & ,\ \Phi_\mathrm{t} \neq 1 \end{cases} \tag{23}$$

$$\mathrm{DCH_t} \quad = \begin{cases} \mathrm{DHR} \times \mathrm{MDH} & ,\ \Phi_\mathrm{t} = 2 \\ 0 & ,\ \Phi_\mathrm{t} \neq 2 \end{cases} \tag{24}$$

$$\mathrm{MPSL} \times \mathrm{CAP_{PEV}} \leq \mathrm{SOC_t} \leq (1 - \mathrm{MPSL}) \times \mathrm{CAP_{PEV}} \tag{25}$$

$$\mathrm{SOC_t} \leq \mathrm{SOC_{t-1}} + \mathrm{CH_t} - \mathrm{DCH_t} \tag{26}$$

The MDH parameter in (24) was derived from [61]. According to [61], "average driving miles" is strongly correlated with driver's age and gender. Since the amount of battery discharge during each time interval is highly dependent on driven miles, it is reasonable to relate the "miles/hour" of householders who adopted PEVs to his/her demographics (see Figure 5). This leads to the following tabulation: Age1: 16-19, Age2: 20-34, Age3: 35-54, Age4: 55-64, and Age5: ≥65. In addition to these parameters, several PEV specific technical parameters are considered in the proposed model. They include: $\mathrm{CAP_{PEV}} = 20\mathrm{kwh}$ [65], $\mathrm{CHR} = 1.4\mathrm{KW}$ [63], and $\mathrm{DHR} = \frac{0.34\mathrm{KW}}{\mathrm{mile}}$ [63].

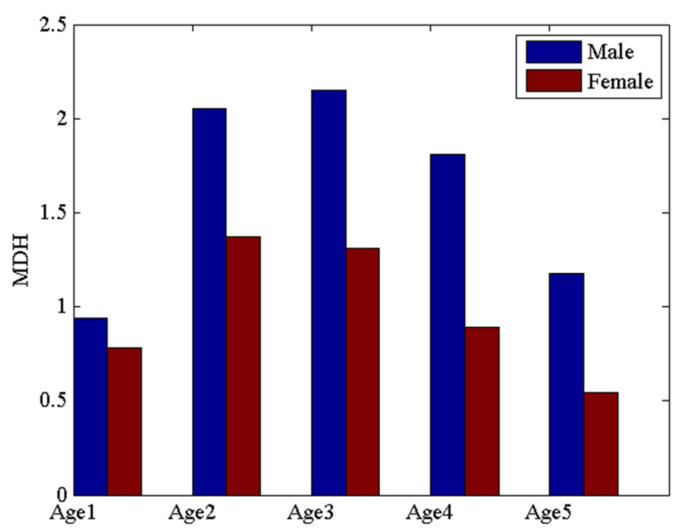


Figure 5 Average driving miles across different groups

## 2.8 Model Validation

The above bottom-up model integrates many sub-models, some of which are built on the basis of earlier works. However, there are unique contributions of this work in terms of new sub-models and also the embedded optimization routines and algorithms that automatically optimize technology adoption and managing new loads. Naturally, such a comprehensive model requires large set of high fidelity data on a variety of variables at atomic level. The focus of this work has not been on how to collect and validate such large volume of high fidelity data. Instead, it is focused on the development of model constructs and integration of these constructs into a larger framework. For validation, the following two-step approach has been taken:

(i) Validation of individual sub-models; simulation of occupancy patterns via discrete-time Markov chain is previously validated in earlier literature [37, 38, 46]. Using same publicly available dataset as in [46], Section 2.5.2 provides results for this sub-model (see Figure 2). Survey data in [52] is used for developing PCD adoption model in section 2.6.1. Introduced in section 2.7.4, cold appliances sub-model is constructed as in [48]. Data in [58] is used for sub-model in section 2.7.5. In section 2.7.6, calculated probabilities from PEV adoption model clearly confirms the findings in [50] (this model is developed using dataset in [50]). Technical parameters of dynamic programming in PEV charging sub-model are adopted from real data as in [63, 65].

(ii) Validation of the whole model; the RECS dataset is used to validate the whole model. RECS study gathers information on how and how much total energy is distributed across various end-uses [58]. In addition to end-use data, RECS feeds the model with unique information about characteristics of household members e.g. age, gender, education level, and employment status and appliances within premises. The latter, gives an opportunity to candidate households that syncs well with the defined states in section 2.7.1 (see Table.2). These are households which have dishwashers, cloth washer, clothes dryer, space heating and cooling system, and one TV since it is defined to be a shared state. Filtering RECS households accordingly, leaves 361 households for validating the whole model (141 households with one member, 134 households with 2 members, 44 households with 3 members, 30 households with 4 members, and 12 households with 5 members). Since RECS has annual consumption data, one year simulation is conducted for all selected households with respect to their occupant characteristics. Two sample t-tests are performed to compare the simulation results with the RECS data. The t-test suggests that there is no statistically significant difference at $\alpha$=0.05 between the simulated and the RECS data (Table 6). This further indicates that the proposed model is capable of simulating energy demands based on the selected household characteristics. Since information regarding to weather (e.g. hourly ambient temperature) and household insulations are not available in RECS, space heating & cooling is taken out from both simulation and RECS data (see [48] for validation of such end-use in host of required information).

Table 6 Model vs. RECS (μ=sample mean, $\sigma^2$= sample standard deviation)

| HH members | μ (Model) | μ (RECS) | $\sigma^2$ (Model) | $\sigma^2$ (RECS) | Null hypothesis | p-value |
|---|---|---|---|---|---|---|
| 1 | 8.64 | 8.34 | 2.31 | 4.81 | Failed to reject | 0.503 |
| 2 | 12.43 | 12.76 | 3.95 | 7.33 | Failed to reject | 0.634 |
| 3 | 13.86 | 14.06 | 4.15 | 6.33 | Failed to reject | 0.852 |
| 4 | 16.02 | 15.55 | 4.13 | 5.7 | Failed to reject | 0.711 |
| All HHs | 11.54 | 11.57 | 4.95 | 6.7 | Failed to reject | 0.939 |

## 2.9 Simulation and Analysis

In this section, the proposed residential energy demand model is used to demonstrate its capability in assessing the effects of PEV and PCD adoption on load profiles. Price signals are effective drivers for end uses namely; SH&SC, LI, and PEV charging. Since it is assumed that water heaters and stoves are using natural gas, these end-uses are excluded out of the entire load profile.

## 2.10 Design of Experiment

One household is selected from the RECS database as the subject of investigation in Experiments 1 and 2; sections 2.10.1 and 2.10.2 respectively. The characteristic of this particular household is shown in Table 7. To simulate the energy demand profile, a working (TW = 1) summer day is chosen as a representative date. For ambient temperature, a profile as shown in Figure 6 is used that corresponds to July 2nd of a synthetic year in Deer Valley, Phoenix, AZ [65]. It should be noted that the proposed model is not limited to any particular household or date. The selection of the above household and date is just for the purpose of demonstration.

Table 7 Household characteristics

| | | | | |
|---|---|---|---|---|
| Number of Household members (R) | | | | 4 |
| Householder education level | | | | 3 |
| Householder Age (r = 1) | | | | 32 |
| Total Square foot | | | | 3239 |
| Total Cooled Square foot | | | | 2839 |
| | AgeCAT | Gender | ES | TW |
| Householder | 3 | 1 | 1 | 1 |
| HH member2 | 3 | 2 | 2 | 1 |
| HH member3 | 1 | 1 | 2 | 1 |
| HH member4 | 1 | 1 | 1 | 1 |

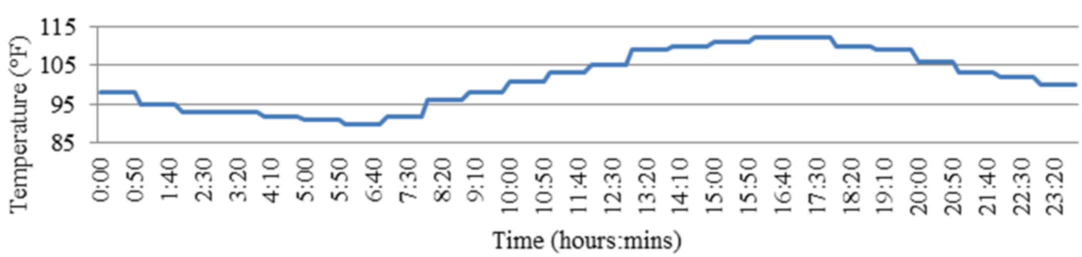


Figure 6 Hourly ambient temperature

### 2.10.1 Experiment 1 (Introduction of PEV and Impact on Load Profile)

The purpose of this experiment is to evaluate the impact of different PEV penetration levels on the electricity load profile. Monte Carlo technique ($\mathrm{MCI} = 1000$) was used to simulate the household electric load profile (see Table. 8 for household characteristics) which is governed by the probabilistic activity model. Different $\mathrm{A_{PEV}}$ levels ($\mathrm{A_{PEV}} = 10\%$ to $100\%;$ Increment step $= 10\%$) are considered along with the reference load ($\mathrm{A_{PEV}} = 0\%$). In this experiment, no PCDs are considered ($\mathrm{A_{PCD}} = 0\%$). Figure 7 shows 6 scenarios where $\mathrm{A_{PEV}}\% \in \{0,20,40,60,,80,100\}$. The average peak and the load factor along with the statistical t-test results against the reference load are provided in Table 8. It is noticeable that when $\mathrm{A_{PEV}}\%$ reaches to 30% and higher, the average load becomes significantly higher than the reference load. Since the peak growth is slower than that of the average load, one could clearly see the gradual increase of load factor (Average load / peak load). This is more due to the valley filling during the early hours (time period of 12:00AM to 6:00AM). On the other hand, the peak grows rapidly during the period of 18:00PM to 21:00PM. This growth of peak which is the result of evening PEV charging, could pose significant problems to utility companies. As mentioned earlier, a possible solution to this problem is the time of use management. Such model capability provides great insights to power suppliers on the impact of the potential emerge of new loads when actual metered data are missing.

Table 8 Different $\mathbf{A_{PEV}}$ levels against reference ($\mathbf{A_{PEV}} = \mathbf{0}\%$)

| [$\mathbf{A_{PEV}}$, $\mathbf{A_{PCD}}$] | $H_{null}$: $\mu_{Reference} = \mu_{PEV\%}$ | P-value | Average load (Watt) | Peak load (Watt) | Load Factor | Average load growth against reference | Peak growth against reference |
|---|---|---|---|---|---|---|---|
| [0%,0%] | | | 2004.6 | 3102.2 | 0.646 | | |
| [10%,0%] | Failed to reject null | 5.6E-01 | 2048.5 | 3165.1 | 0.647 | 1.02 | 1.02 |
| [20%,0%] | Failed to reject null | 2.0E-01 | 2101.9 | 3222.4 | 0.652 | 1.05 | 1.04 |
| [30%,0%] | Null rejected | 4.2E-02 | 2158.6 | 3307.7 | 0.653 | 1.08 | 1.07 |
| [40%,0%] | Null rejected | 04.9E-03 | 2217.3 | 3372.1 | 0.658 | 1.11 | 1.09 |
| [50%,0%] | Null rejected | 5.5E-04 | 2264.8 | 3428.2 | 0.661 | 1.13 | 1.11 |
| [60%,0%] | Null rejected | 1.54E-05 | 2329.8 | 3495.2 | 0.667 | 1.16 | 1.13 |
| [70%,0%] | Null rejected | 5.84E-07 | 2381.0 | 3552.7 | 0.670 | 1.19 | 1.15 |
| [80%,0%] | Null rejected | 1.48E-08 | 2432.9 | 3614.2 | 0.673 | 1.21 | 1.17 |
| [90%,0%] | Null rejected | 2.77E-10 | 2483.4 | 3665.9 | 0.677 | 1.24 | 1.18 |
| [100%,0%] | Null rejected | 1.21E-11 | 2520.7 | 3707.9 | 0.680 | 1.26 | 1.20 |

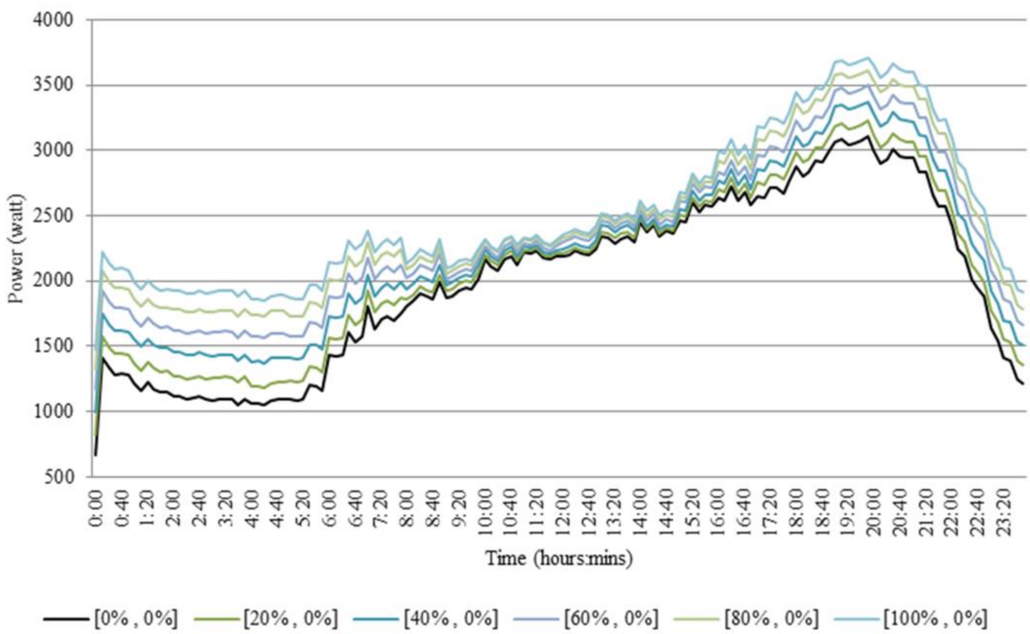


Figure 7 Electricity loads for different $\mathbf{A_{PEV}}$ levels. Inside brackets refer to [$\mathbf{A_{PEV}}\%$, $\mathbf{A_{PCD}}\%$]

### 2.10.2 Experiment 2 (Effect of Different $\mathbf{A_{PCD}}$, and $\mathbf{A_{PCD}}$ Penetration Levels)

In this experiment, eleven categories of adoption percentages are considered for PEV and PCD. These are $\mathrm{A_{PEV}}, \mathrm{A_{PCD}} = 10\%\ \text{to}\ 100\%;\ \text{Increment step} = 10\%$ (see Table 7 for household characteristics). This leads to 11x11 scenarios. An artificial price profile is constructed based on the generated reference loads. This derives from the load at each time divided by the peak load (Figure 8).

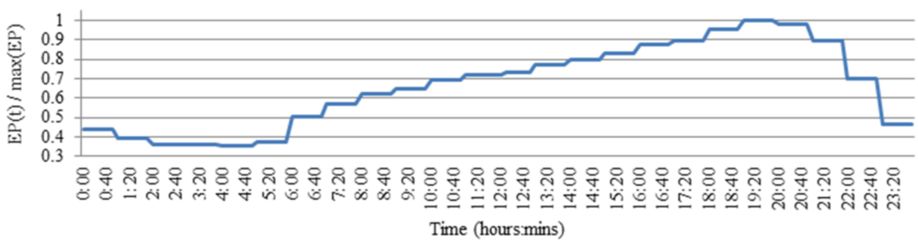


Figure 8 Hourly electricity price over peak price

Figure 9 graphically illustrates the changes of the average and peak loads across different $\mathrm{A_{PEV}}$ and $\mathrm{A_{PCD}}$ levels. The load factors across different $\mathrm{A_{PEV}}$ and $\mathrm{A_{PCD}}$ are also provided in Figure 10.

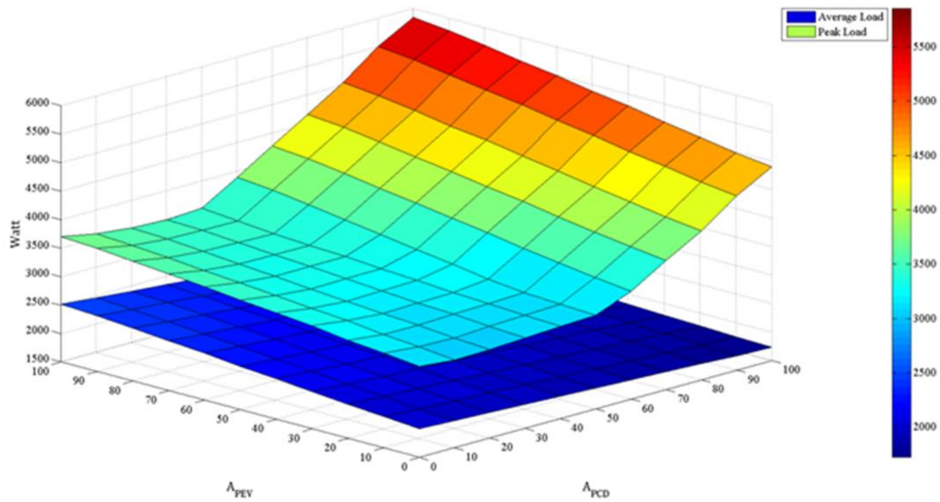


Figure 9 Average and Peak load across different $\mathbf{A_{PEV}}$ , $\mathbf{A_{PCD}}$

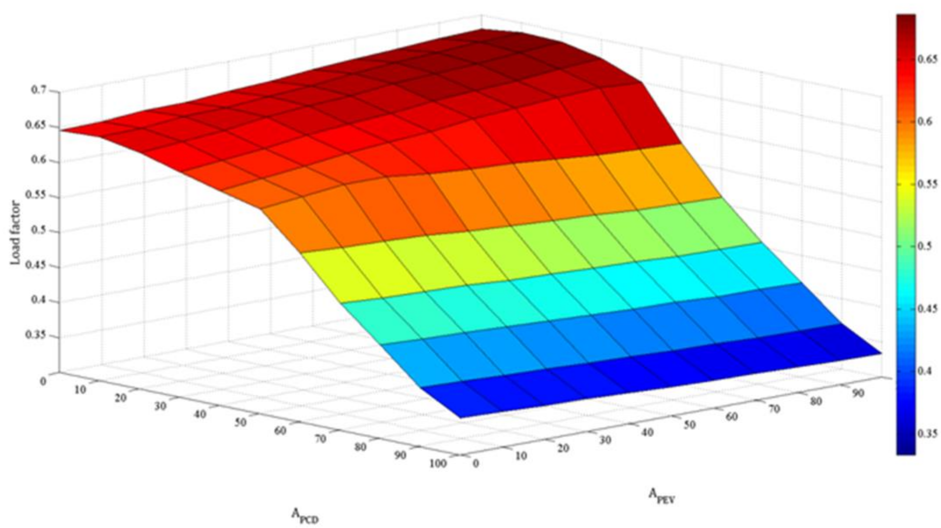


Figure 10 Load factor across different $\mathbf{A_{PEV}}$ , $\mathbf{A_{PCD}}$

It can be seen from Figure 9 that as the $A_{PCD}$ level increases the average load smoothly decreases. But this behavior cannot be observed on the peak load profile. As the

$A_{PCD}$ level increases, the peak value starts to decrease, but at a certain point it starts to go up again. To better understand the reason behind this behavior, the $A_{PEV}$ level was kept at 50% along with different $A_{PCD}$ levels. The resulting load profiles are provided in Figure 11. The average peak and load factors along with the statistical t-test results against the reference load $[A_{PEV} = 50\%, A_{PCD} = 0\%]$ are provided in Table 9. The results suggest that when $A_{PCD}$ reaches 40%, the curtailment of the average load starts differing significantly from the reference load while the new peak is still lower than the reference peak. One may notice that when the $A_{PCD}$ level increases to 50%, the new peak load starts to be greater than the reference peak, leading to a significant drop in the load factor.

Table 9 Average load, Peak, and load factor of different $\mathbf{A_{PCD}}$ levels

| $[A_{PEV}, A_{PCD}]$ | $H_{null}$: $\mu_{Reference} = \mu_{PCD\%}$ | P-value | Average load (Watt) | Peak load (Watt) | Load factor |
|---|---|---|---|---|---|
| [50%,0%] | Failed to reject null | | 2264.85 | 3428.22 | 0.66 |
| [50%,10%] | Failed to reject null | 5.2E-01 | 2220.91 | 3336.26 | 0.66 |
| [50%,20%] | Failed to reject null | 1.9E-01 | 2175.62 | 3279.81 | 0.66 |
| [50%,30%] | Failed to reject null | 6.3E-02 | 2138.52 | 3293.00 | 0.65 |
| [50%,40%] | Null rejected | 1.3E-02 | 2098.27 | 3300.39 | 0.63 |
| [50%,50%] | Null rejected | 2.0E-03 | 2057.47 | 3463.39 | 0.59 |
| [50%,60%] | Null rejected | 2.39E-4 | 2014.76 | 3840.22 | 0.52 |
| [50%,70%] | Null rejected | 2.17E-05 | 1972.50 | 4222.50 | 0.46 |
| [50%,80%] | Null rejected | 1.81E-06 | 1931.09 | 4595.12 | 0.42 |
| [50%,90%] | Null rejected | 8.38E-08 | 1881.00 | 5047.73 | 0.37 |
| [50%,100%] | Null rejected | 7.10E-09 | 1840.89 | 5393.09 | 0.34 |

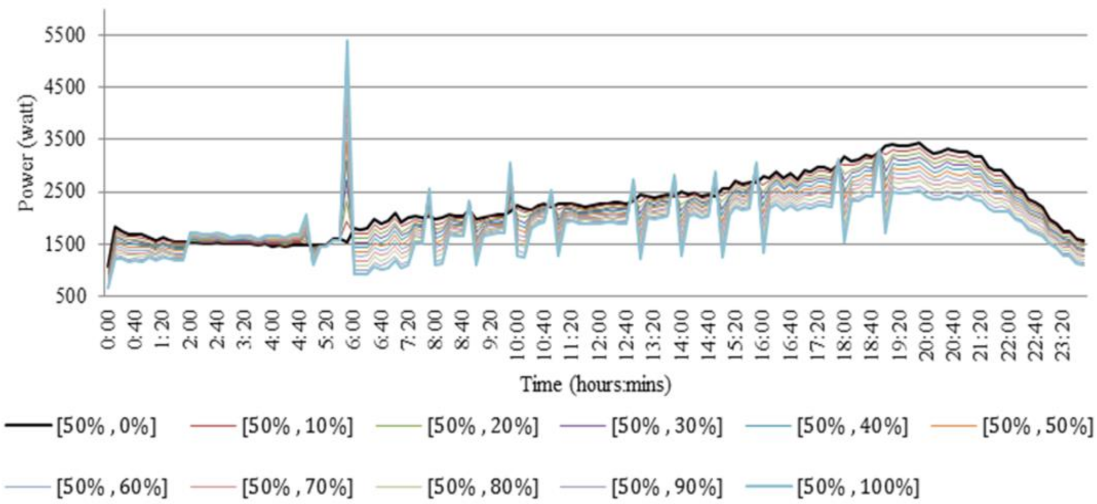


Figure 11 Electricity load for different $\mathbf{A_{PCD}}$ levels. Inside brackets refer to [$\mathbf{A_{PEV}}$%, $\mathbf{A_{PCD}}$%]

It is safe to conclude that the presence of PCDs can not only curtail the load but also shift the peak in response to the price signals. This also leads to a lower load factor. To better visualize this, three scenarios including $\mathrm{A_{PEV,PCD}} = [50\%, 0\%]$, $\mathrm{A_{PEV,PCD}} = [50\%, 40\%]$, and $\mathrm{A_{PEV,PCD}} = [50\%, 70\%]$ are extracted and displayed in Figure 12. In the scenario of $\mathrm{A_{PEV,PCD}} = [50\%, 40\%]$, it can be seen that the original peak load at 19:50PM with the magnitude of 3428.2 Watt is successfully curtailed and shifted to 18:50PM. Meanwhile, another peak rises up at 5:50AM as a result of the relatively significant price differences between 5:50AM (0.37) and 6:00AM (0.50). In the scenario of $\mathrm{A_{PEV,PCD}} = [50\%, 70\%]$, one could observe that this price difference generates a big spike which is higher than the original peak value. To investigate the spike formation, one could zoom in onto the end-use level. This will lead to the discovery of end-uses which are capable of curtailing/shifting loads. These end-uses include PEV charging (Figure 13), Space Cooling (Figure 14) and Lighting (Figure 15).

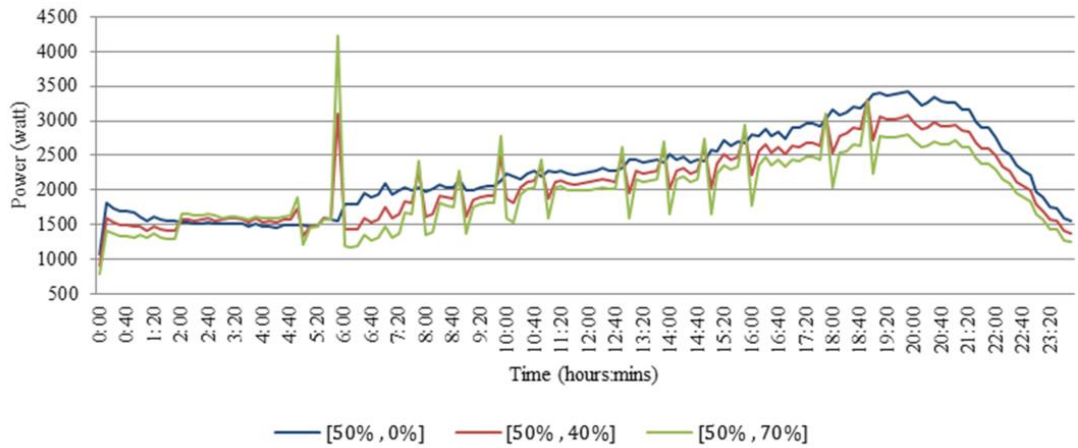


Figure 12 Electricity loads of three different $\mathbf{A_{PCD}}$ levels. Inside brackets refer to [$\mathbf{A_{PEV}}$%, $\mathbf{A_{PCD}}$%]

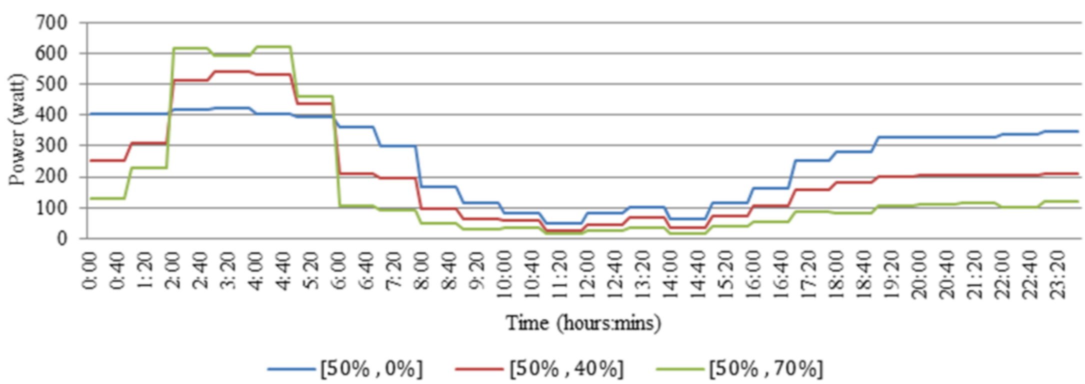


Figure 13 Electricity load of PEV charging. Inside brackets refer to [$\mathbf{A_{PEV}}$%, $\mathbf{A_{PCD}}$%]

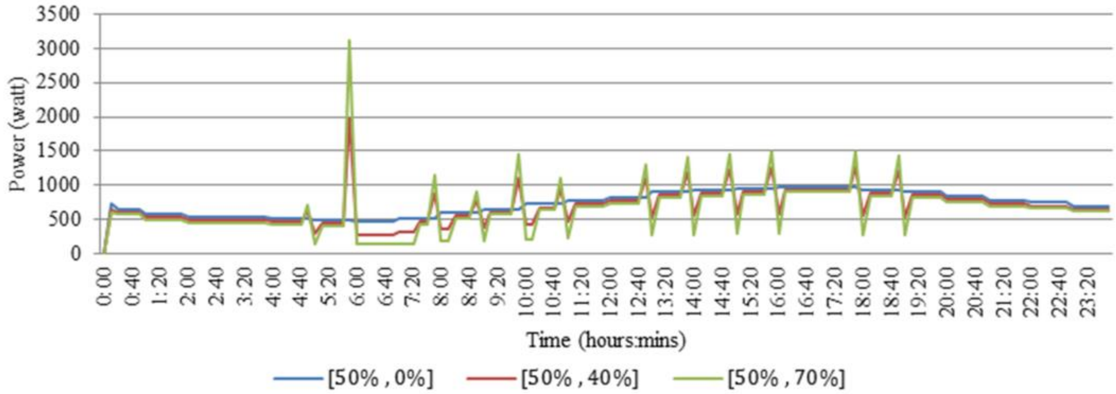


Figure 14 Electricity load of space cooling. Inside brackets refer to [$\mathbf{A_{PEV}}$%, $\mathbf{A_{PCD}}$%]

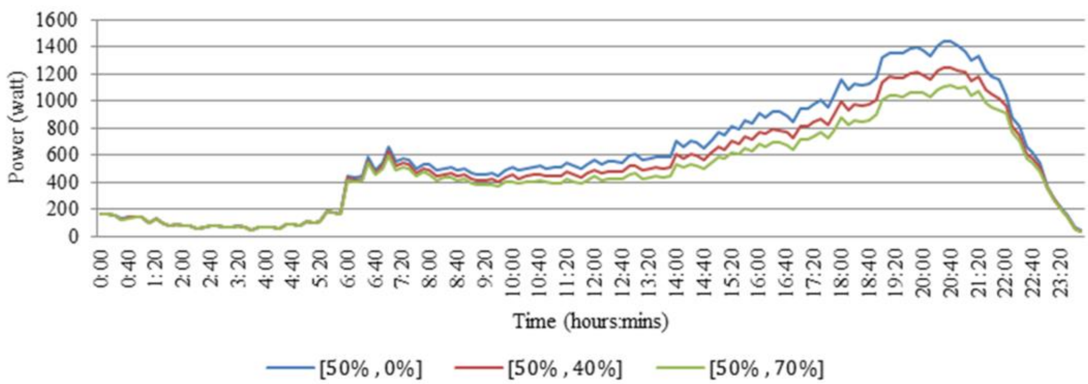


Figure 15 Electricity load of lighting - Inside brackets refer to [$\mathbf{A_{PEV}}$%, $\mathbf{A_{PCD}}$%]

It can be observed from the peak period between 19:00PM to 20:40PM that a portion of load is shifted because the electricity price encourages shifting the recharging schedule to off peak hours (early morning). Another portion of the peak load is curtailed, largely thanks to the dimmable lighting system where FR has a negative relationship with the ratio of electricity price over the peak price (a peak usually occurs in a time period when the sun is down and artificial lighting is necessary). Also, the pre-cooling capability switched off the cooling system in the first 20 minutes of the peak period (see Figure14). The spike occurring at 5:50AM is due to the relative price difference between 5:00AM and 6:00AM. This price difference forces the cooling system to pre-cool the building and works in a relatively low mode till 7:10AM. Meanwhile, the load associated to the PEV charging is also accumulated up to this point of time (5:50AM). It should also be noticed that since most of the householders are in sleep during this time period, the lights are off; therefore the lighting system has no capability to curtail the load.

### 2.10.3 Experiment 3 (Aggregating Load Profiles from Households to Residential Community)

The purpose of this experiment is to aggregate the load profiles of individual households with different characteristics and varying willingness to adopt PEVs and PCDs. Forty households $(\mathrm{HH(i)}: \mathrm{i} \ldots \mathrm{I} = 40)$ with different occupant numbers and characteristics are considered in this experiment. Among these households, 50% of them are with four occupants, 20% with three, 20% with two, and 10% with one occupant. 40 households are chosen due to the fact that 40 is the typical number of connected households to a primary distribution feeder. For the i-th household, $\mathrm{A_{PEV}}$ and $\mathrm{A_{PCD}}$ are calculated based on its householder characteristics ($\mathrm{X_i^{Age_{r=1}}}$ and $\mathrm{X_i^{Edl_{r=1}}}$) using $(19)$ and $(7)$, respectively. The square footages of households are assumed to be same. Furthermore, it is assumed that all households have an identical HVAC system where the thermostat levels are set according to their occupant characteristics as in $(10)$. Let's first analyze the effects of resident characteristics on the load patterns. In the following scenario, both $\mathrm{HH}(31)$and $\mathrm{HH}(39)$ have 4 occupants but with different characteristics (see Table 10). In Figure 16, load profiles are provided. For $\mathrm{HH}(39)$, morning peak occurs, then the load level drops since household members are probably going to work/school. However, this pattern is not true for $\mathrm{HH}(31)$ due to the non-employed status of household members (see Table 10). According to Figure 4 the probability of $\mathrm{A_{PEV}}$ in $\mathrm{HH}(39)$is higher than $\mathrm{HH}(31)$. Considering consequent load for PEV charging, one may observe that the demand valley in time period between 12:00PM-6:00AM is filled more in $\mathrm{HH}(39)$than $\mathrm{HH}(31)$. The average load reduction percentages in $\mathrm{HH}(31)$ and $\mathrm{HH}(39)$ are 6% and 10% respectively.

Table 10 HH31 and HH39 characteristics

| HH31 | | | | | HH39 | | | | |
|---|---|---|---|---|---|---|---|---|---|
| $\mathrm{Edl_{r=1}}$ | | | | 1 | $\mathrm{Edl_{r=1}}$ | | | | 4 |
| $\mathrm{Age_{r=1}}$ | | | | 56 | $\mathrm{Age_{r=1}}$ | | | | 49 |
| r | AgeCAT | Gender | ES | TW | r | AgeCAT | Gender | ES | TW |
| 1 | 4 | 2 | 2 | 1 | 1 | 4 | 1 | 1 | 1 |
| 2 | 6 | 1 | 2 | 1 | 2 | 4 | 2 | 1 | 1 |
| 3 | 4 | 1 | 2 | 1 | 3 | 1 | 1 | 2 | 1 |
| 4 | 1 | 2 | 2 | 1 | 4 | 1 | 2 | 2 | 1 |

The aggregated electricity load profiles of all these forty households in both 10-minute and hourly resolution are shown in Figure 17, and Figure 18. The energy load profiles for both 10-minute and hourly resolution are also provided Figure 19 and Figure 20. One may observe that by reducing the resolution to one hour, load fluctuations and spike formations are not visible anymore. This clearly demonstrates the value of high resolution demand model, which is to provide suppliers with better insights such that the generation can be matched with consumption. Moreover, the capability of such models in aggregating individual unit loads to different desirable scales (e.g. neighborhoods) without compromising the underlying details and dynamics paves the way towards more sustainable investment decisions on power generator systems.

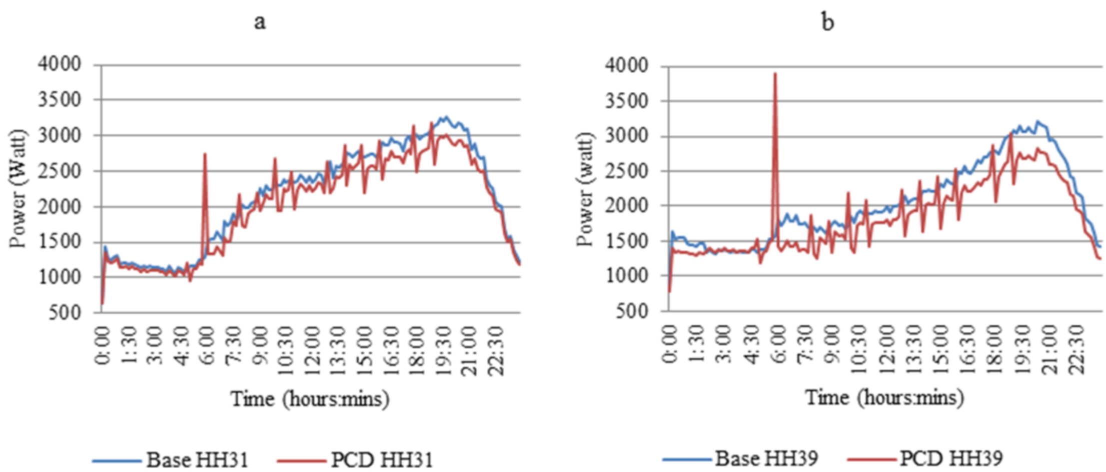


Figure 16 a) $\mathbf{HH}(\mathbf{31})$and b) $\mathbf{HH}(\mathbf{39})$electricity load profile

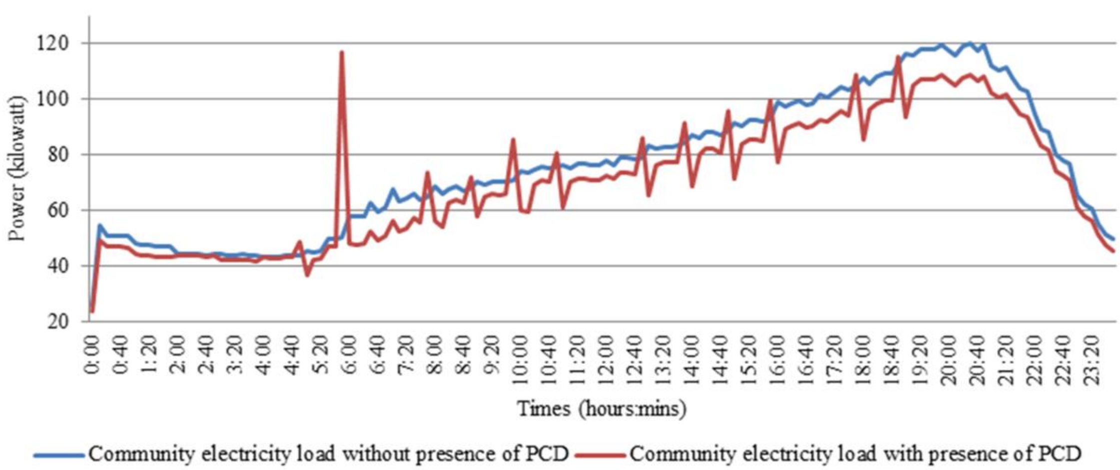


Figure 17 Electricity load for community of 40 households - 10minute resolution

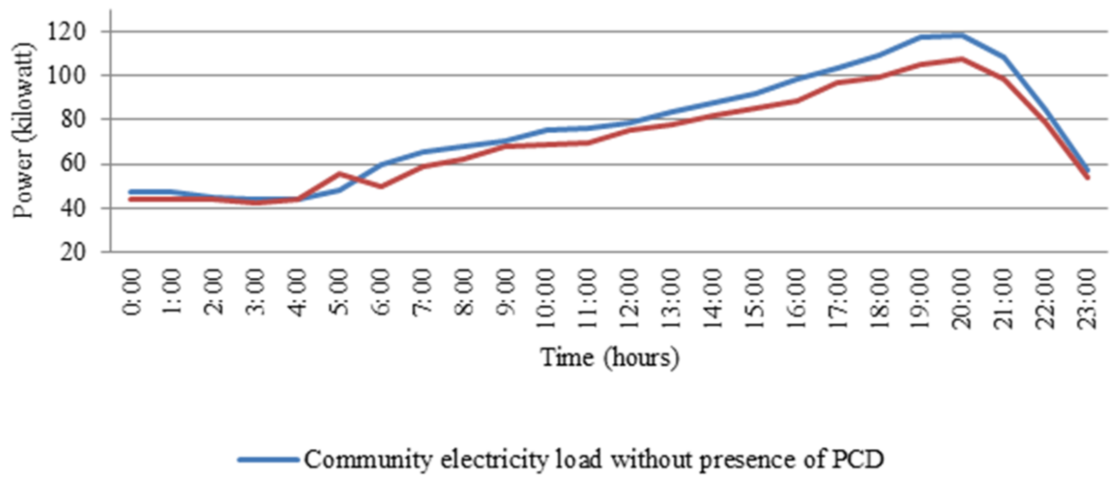


Figure 18 Electricity load for community of 40 households - 1 hour resolution

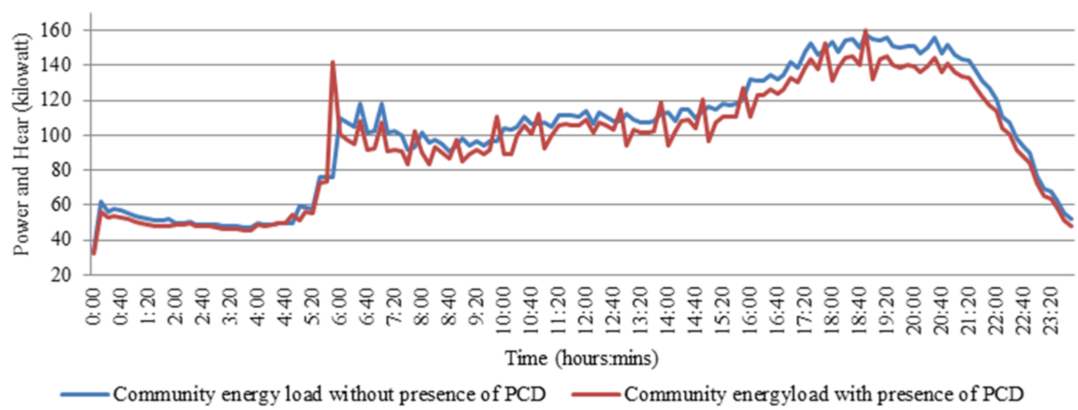


Figure 19 Energy load for community of 40 households - 10minute resolution

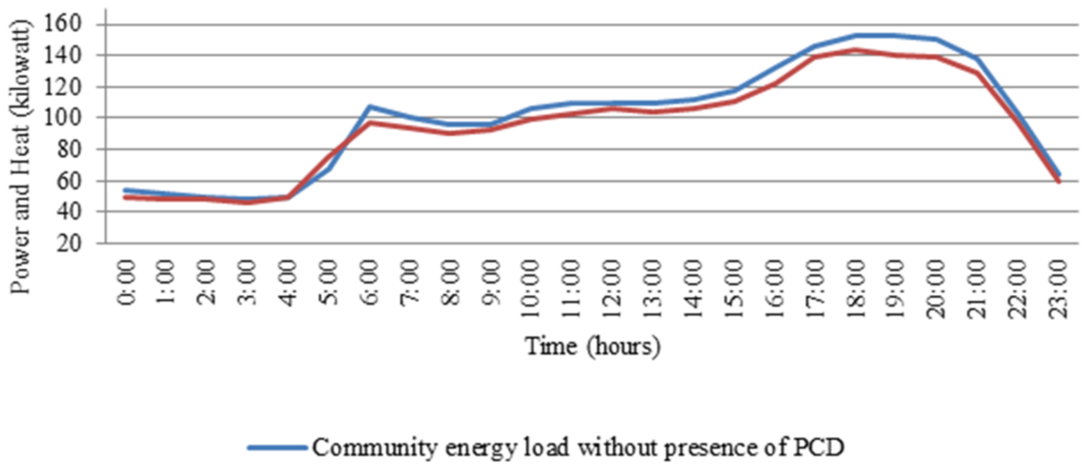


Figure 20 Energy load for community of 40 households - 1 hour resolution

## 2.11 Discussion of Results and Future Research

It is observed that as $A_{PEV}$ penetration level surpass a certain level; the average load becomes significantly higher than reference load. Since the growth of peak is slower than that of average load, one could see the gradual increase of the load factor due to valley filling during time period between midnight and sunrise. On the other hand, intensified consumption during peak hours could pose significant problems to utility companies. The effect of PCD on electricity load pattern is found interesting in two ways. First, it shows that as $A_{PCD}$ percentage reaches to a certain level (here; $A_{PCD} = 50\%$, see Table 10), a relatively different electricity load profile is obtained where leveraging off-peak electricity prices lead to creation of even higher rebound peak shifted toward the off-peak period. These rebound peaks have also been observed by [43, 66]. As also discussed in [33], this is the result of one-way communication e.g., price signals to customers. Reduced peak demand and greater efficiency may be achieved by a two-way communication between customers and system operators. Second, it is observed that the electricity price structure has major effects on the curtailed/shifted demand profile. The relatively large price difference between 5:00 AM and 6:00AM caused rebound peak formation prior to 6:00AM, while the smooth price difference from 13:00PM till 20:00PM resulted in smaller and smoother spikes. The proposed framework helps utilities to investigate and evaluate their pricing policy effectiveness in absence of historical responded demand data. In Experiment 3, the average load reduction percentages confirm the findings in previous studies - the potential of approximately 10% reduction of overall demand is achievable [39, 40]. Moreover, a comparison of the aggregated electricity load profiles of all households in both 10-minute and hourly resolution reveals that by reducing the resolution to one hour, load fluctuations and spike formations will not be visible anymore, leading to a potential loss of valuable information for utility owners.

The models developed in this research can be improved in several ways. First, for the probabilistic PCD adoption model, the use of CFL measure may be a limiting assumption due to the fact that willingness to purchase a CFL is a "quick win" energy efficiency measure, and does not necessarily indicate that the householder is willing to pay for a more expensive and complex efficiency measure e.g. PCD. Designing specific surveys may help to relax this assumption. SH&SC model within proposed framework which is currently simplified version of [38] can be improved by different approaches. Although [38] proposes an accurate model of a household, the proposed approach needs information, which is usually not available. Instead, one may apply a hybrid physics-based and data driven approach as in [67]. Assuming independency among occupant’s activities which is the result of applying discrete Markov chain is one another limitation of this study. Last but not least, the use of static power conversion parameters to calculate energy consumption associated with specific activities can be significantly improved by developing consumption distribution for such activities. One major direction for the future work is to link this framework to energy resource capacity planning. By doing so, it closes the loop between the demand dynamics and the energy supply, such that it enables the investigation of opportunities to reduce/defer investment on energy supply resources. This is particularly true in situations where customers have capabilities to receive real time energy price.

## 2.12 Conclusion

A bottom-up demand model with constructs that are capable of simulating both electricity and heat demands of individual residential households and a community is proposed. With new model constructs and integration of these constructs into a larger framework, this work propose new sub-models and technology adoption models along with embedded optimization routines and algorithms that automatically optimize technology adoption and managing new loads. In the context of different experiments, it is shown how this model can be used for understanding the demand behavior, investigation of DSM strategies, energy price effectiveness and so on. For the purpose of presented experiment, surveyed public data and results from existing literature that are not necessarily of high fidelity nature as intended are used. However, this does not limit the broad applicability of the simulation platform for real life applications.

**ELSEVIER LICENSE**
**TERMS AND CONDITIONS**

Jul 05, 2016

This Agreement between farbod farzan ("You") and Elsevier ("Elsevier") consists of your license details and the terms and conditions provided by Elsevier and Copyright Clearance Center.

| | |
|---|---|
| License Number | 3902420181325 |
| License date | Jul 05, 2016 |
| Licensed Content Publisher | Elsevier |
| Licensed Content Publication | Applied Energy |
| Licensed Content Title | A multi-scale adaptive model of residential energy demand |
| Licensed Content Author | Farbod Farzan,Mohsen A. Jafari,Jie Gong,Farnaz Farzan,Andrew Stryker |
| Licensed Content Date | 15 July 2015 |
| Licensed Content Volume Number | 150 |
| Licensed Content Issue Number | n/a |
| Licensed Content Pages | 16 |
| Start Page | 258 |
| End Page | 273 |
| Type of Use | reuse in a thesis/dissertation |
| Portion | full article |
| Format | both print and electronic |
| Are you the author of this Elsevier article? | Yes |
| Will you be translating? | No |
| Order reference number | |
| Title of your thesis/dissertation | Dynamic demand modeling, energy management, and investment strategies in uncertain energy markets |
| Expected completion date | Jul 2016 |
| Estimated size (number of pages) | 160 |
| Elsevier VAT number | GB 494 6272 12 |
| Requestor Location | farbod farzan<br>1507 azalea drive<br><br>NORTH BRUNSWICK, NJ 08902<br>United States<br>Attn: farbod farzan |
| Total | 0.00 USD |
| Terms and Conditions | |

# 2. INTEGRATION OF DEMAND DYNAMICS AND INVESTMENT DECISIONS ON DISTRIBUTED ENERGY RESOURCES [68]

## 3.1 Abstract

This chapter directly couples investment decisions on Distributed Energy Resources (DER) with Demand Side Management (DSM) strategies that can be adopted over time by residential communities. The formulation also takes into account factors that usually contribute to long-term market variations and short-term operational volatilities. This work uses a High Resolution Adaptive Model (Hi-RAM) proposed in chapter 2 for short-term load calculations on a premise that expected dynamical effects due to DSM strategies and their interactions that cannot effectively be captured by time-series forecast models. The integration of Hi-RAM into investment formulation allows for certain What-If investment scenario analysis on the use of advanced technologies, new plug-ins, and consumer response to power price fluctuations. To demonstrate the significance of coupling of DER investment decisions and DSM strategies, three scenarios are presented. The base scenario (Mode I) results can be reproduced using traditional forecast models and is included for baseline analysis and benchmarking. In Mode II new load patterns for PEV are introduced. Mode III is an extended version of Mode II where smart devices are used within households. The comparison of investment decisions from the three modes clearly demonstrate that interaction effects of DSM strategies matter.

KEYWORDS—Distributed energy resources (DER), demand dynamics, capacity planning, plug-ins, price responsive demand.

Nomenclature

A. Index

| | |
|---|---|
| $\phi$ | Index of Power Generator Assets; $\phi \in \{WT, PV, GF, CHP\}$ |
| i | Index of Household |
| j | Index of CHP Regions |
| r | Index of Household Residents |
| t | Index of Time (Hour) |
| $\vartheta$ | Portfolio Assets; $\vartheta \in \{PV, WT, GF, CHP, Boiler, ST\}$ |
| y | Index of Time (Year) |

B. Variables

| | |
|---|---|
| AI | Cash invested in other alternatives in period ($) |
| BGen | Boiler Hourly Heat Generation (kW) |
| C | Storage Charge (kW) |
| $CHPG_H$ | CHP Total Hourly Electricity Generation (kW) |
| $CHPG_{HW}$ | CHP Hourly Wasted Heat Generation (kW) |
| $CHPG_{HNW}$ | CHP Hourly Non-wasted Heat Generation (kW) |
| D | Storage Discharge (kW) |
| $\phi G$ | $\phi$ Total Hourly Power Generation (kW) |
| $\phi G\_L$ | $\phi$ Hourly Power Generation Serves Load (kW) |
| $\phi G\_S$ | $\phi$ Hourly Power Generation to Storage (kW) |
| GP | Gas Price ($/kWh) |

| | |
|---|---|
| Hd | Heat Demand |
| Pd | Power Demand |
| PB | Total Financial Charges on Borrowed Funds ($) |
| EPG | Hourly Electricity Purchased from Macro Grid (kWh) |
| PLLj | Partial Load Levels of CHP |
| ROI | Return of Cash Invested on Alternative Investment |
| SOC | Storage State of Charge (kW) |
| SP | Electricity Spot Price ($) |
| SOG | Annual On-site Generation Operational Savings ($) |
| $\vartheta$CAP | Accumulated Installed Capacity (kW) |

C. Parameters

| | |
|---|---|
| AIC | Initial Available Cash ($) |
| $B_{eff}$ | Boiler Efficiency |
| Blimit | Maximum Borrowing Limit ($) |
| CapEx$\vartheta$ | Unit Capacity Cost of $\vartheta$ ($/kw) |
| $CHPLLj_{eff}$ | CHP Electric Efficiency Associated to Load Level |
| $C\vartheta_{O\&M}$ | $\vartheta$ Non-fuel Operational and Maintenance Cost |
| DF | Annual Discount Rate |
| $E_{grid}$ | Grid Average Heat Rate (mmbtu/kwh) |
| FC | Finance Charge Rate |
| GFHR | Gas-fired Heat Rate (mmbtu/kwh) |

| | |
|---|---|
| HPR | Heat to Power Ratio |
| IRR | Investment Rate of Return |
| LRP | Land Rental Price ($/Acre) |
| MLST | Minimum Percentage of Storage Level |
| Mult | Transmission Costs Multiplier |
| $ST_{eff}$ | Electricity Storage Efficiency |
| STPR | Electricity Storage Charge/Discharge Power Rate |

## 3.2 Introduction

The value of a DER portfolio depends on its projected return on investment and the potential growth in its operating income while serving underlying demand. For a DER, the investment payoff is directly linked to the operation of the physical assets, and return on investment depends on how these operations are utilized overtime [69, 70]. Depending on when and how much investment is made, long-term value of a DER could be assessed. Investment decisions are usually influenced by fuel costs, the price of technology, state incentives, and parameters such as finance charge rates/terms [71].

Economic benefits of a DER could be enhanced by contributing strategies such as demand side management (DSM) [72, 73]. In this context, DSM can be regarded as a means of not only reducing energy costs but also generating revenue by reducing load on the grid [74, 75, 76]. In the presence of DSM, energy demand becomes highly dynamic and difficult to predict e.g., demand can be curtailed/shifted over time as a result of customer response to electricity prices. Integration of DSM as a resource necessitates inclusion of such dynamics into investment modeling.

In this chapter investment decisions on DER are investigated by taking into account the specifics of household behavioral and physical characteristics, which happen to be the main load drivers in residential communities. Investment planning also takes into account factors that usually contribute to long-term market variations, and short-term operational volatilities. This work uses a bottom-up demand model proposed in chapter 2. The bottom up model (Hi-RAM) is capable of capturing behavioral patterns of end users and lends itself to certain What-If analysis on the use of advanced technologies, new plug-ins, and consumer response to price fluctuations according to their demographic characteristics. This would allow investors to examine return on investment as a function of technology and behavioral pattern changes over time; such analysis cannot be carried out using stationary forecast models, which are solely obtained on the basis of historical data.

## 3.3 Related Studies

Planning, operation, and control of DER are extensively studied in literature. Focusing on operation and control of DER, [78] applied a stochastic optimization framework to optimize the operation of a DER configuration, where they observed significantly different results versus that of deterministic case. [77] proposed a two-stage optimization model to optimize the hourly operation of a DER aiming at optimizing one-day-ahead plans and daily operations. By considering a trade-off between revenue and risk, [79, 80] proposed a two-stage stochastic optimization model where weighted mean-risk sum is the objective function of the problem. Commercially available software systems also exist, such as Hybrid Optimization Model for Electric Renewables [81], which enables to analyze the combination of renewable and conventional energy resources. By incorporating investment into operation and control problem, [82] studied the capacity investment in order to optimize the sizing and siting for DER. Their objective function includes investment and operating costs. Cost-benefit analysis is conducted in order to obtain both optimal size and site. [83] and [84] applied non-linear optimization approach toward the problem of optimal portfolio sizing considering static and stochastic demand; respectively. [85] investigates investment decisions on DER by combining short-term operational volatility and long-term market variations.

Using DER in conjugation with DSM provides both economic and environmental advantages [86]. [87] described how price responsive demand can be effectively integrated into wholesale power markets. [88] proposed active energy management system endowed with an optimal power flow integrating DSM and active management schemes for the optimization of a smart grid in a competitive power market. [89] presented the relationship between networks and consumer electronics. They discussed capabilities to control the temperature and volume of heat, cooling, or ventilation, and lighting patterns depending on what the occupant is doing. However, models for capturing such dynamics were not provided. [90] proposed optimal load scheduling strategy to minimize the electricity costs of an industrial end user under real time pricing. An analytical approach was followed to describe the potential electricity cost savings to an industrial end user under real time pricing through intelligent demand management.

[91] proposed a short-term physically based load model of the demand of a group of air conditioners as a function of outside temperature, and air conditioning system parameters. The formulation provides the optimal schedule of electricity usage given the predetermined electricity price schedule. [92] discussed the critical role that energy optimization algorithms will play at residential level to effectively achieve benefits of energy saving via participation of informed customers. They presented a vision of a home electrical system which consists of renewable generation assets, electric vehicle, and sets of controllable and uncontrollable appliances. Also [93] recommended an algorithm for power usage of home appliances where real-time price signals are sent from utility to customer end. Finally, [96] proposed a layered architecture for load management system in smart buildings with emphasis on optimal energy consumption management.

The proposed framework enables investigation of long-term investment decisions on DER considering near-future scenarios such as large-scale penetration of PEV, and smart grid enabling technologies e.g., DSM. Unlike studies such as [86, 96] that assume expected measures for responded demand, in this work curtailed/shifted demand will be directly calculated thanks to end-use models in Hi-RAM. Hi-RAM breaks down the complex interactions between the network participants by modelling each end-use. Moreover, it not only investigates DER operational costs in conjugation with DSM as in [94, 95] but also suggests capacity planning solutions for a DER portfolio. Through a number of numerical experiments, it is demonstrated that the inclusion of underlying dynamics significantly impact investment decisions. For the purpose of demonstration three modes of investment are considered, where mode I simulates a baseline model which works similar to existing models in the literature. The other two modes are variations of our proposed investment model.

### 3.4 Problem Statement

The problem of interest is to formulate DER investment decisions e.g., sizing, configuration and timing by directly taking into account DSM solutions and interactions between these solutions. Null hypothesis is that distribution (expected value and variance) of savings from DSM strategies will significantly influence the investment decisions. DSM strategies may include a host of options, including but not limited to: adoption of advanced control and scheduling for EV charging and smart home technologies e.g., with ability to respond to price signals. The main premise of this chapter is that savings from DSM solutions evolve over time and depend on the interaction between these solutions. Furthermore, such dynamics can hardly be captured through forecast models that are solely built on the basis of observed historical data. Real life data collection of such effects and their interactions would usually require extensive experiments and observations, and would be expensive if not infeasible. On the other hand, the use of dynamic bottom up models that works on the basis of atomic level data and closely capture behaviors and patterns under various DSM strategies can be much more cost effective and practical. In essence the simulated data from a bottom up model is used as surrogate for observed data. In practice, one can use combined framework where historical data is used primarily and augmented by secondary data from such bottom up simulations.

The proposed solution to the above problem constitutes the integration of the following sub-models: (i) A dynamic model that accurately captures load behavior under a discrete set of configurations and design choices that pertain to behavioral patterns and technological solutions that are adopted at individual household level (see chapter 2). This model is briefly discussed later in this chapter. (ii) A stochastic investment model in the form of Mixed Integer Non-linear Programming (MINLP) that optimizes cash flow over a horizon $(\mathrm{CF}_{\mathrm{Y}})$ and projected cash flow beyond the planning horizon $(\widehat{\mathrm{CF}}_{\mathrm{Y}})$. Cash flows include operational savings due to DER investment, finance payments and alternative investment. It is assumed that each year the investor has opportunity to invest on other activities. Also limited funds are available to be borrowed in each year in order to invest on DER assets. Monte Carlo technique is applied for solving stochastic MINLP problem.

This chapter will focus on the investment model and, in particular, it will demonstrate how to incorporate the bottom-up dynamical demand model into investment decisions. Despite earlier works e.g. [71, 77, 85, 86, 98] where power consumption is calculated from load forecast models obtained from historical data, this work uses a bottom-up demand model. Furthermore, in comparison to [71, 77, 85] which considered gas-fired (GF), photovoltaic cells (PV), wind turbine (WT), electric battery storage (ST), and purchase form the grid in DER portfolio, in this research two new resources are added into the mix. Those are combined heat and power (CHP) and DSM. Moreover, unlike [71, 77, 85] where DER cost savings function was calculated separately and was fed to a stochastic long-term investment model, operation and investment optimization problems are solved together combined. Objective function for the investment problems is formulated as:

$$\text{maximize}(\mathrm{CF_Y} + \widehat{\mathrm{CF}}_\mathrm{Y}) = \mathrm{SOG_Y} + \mathrm{ROI_Y} + \mathrm{B_Y} - \mathrm{PB_Y} - \mathrm{SOA_Y} - \mathrm{AI_Y} + \widehat{\mathrm{SOG}}_\mathrm{Y} + \widehat{\mathrm{ROI}}_{\mathrm{Y+1}} - \widehat{\mathrm{PB}}_{\mathrm{Y+1}} \quad (1)$$

### 3.5 Problem Formulation

#### 3.5.1 Operational Constraints

In this section formulation for each asset generation is described. Gas-fired is assumed to generate power according to its capacity and specific heat rate as in [71, 77]. For WT and PV generation, capacity factor approach is applied, where WT and PV are assumed to generate power according to their capacity factor $(\mathrm{CF\phi} \mid \phi \in \{\mathrm{WT, PV}\})$. For WT it is assumed that capacity factor follows $(\mathrm{CFWT})$ based on Figure 21, where the ratio is the function of hourly wind speed. It is also assumed that for wind speeds below 4m/s and above 25m/s, the WT does not function [97]. PV capacity factor $(\mathrm{CFPV})$ is assumed to be a ratio of hourly solar intensity to the intensity which PV generates its maximum power. This gives both WT and PV hourly generation as below:

$$\phi \mathrm{G}_{\mathrm{y,t}} = \phi \mathrm{CAP_y} \times \mathrm{CF}\phi_{\mathrm{y,t}} \,, \qquad \phi \in \{\mathrm{WT, PV}\} \quad (2)$$

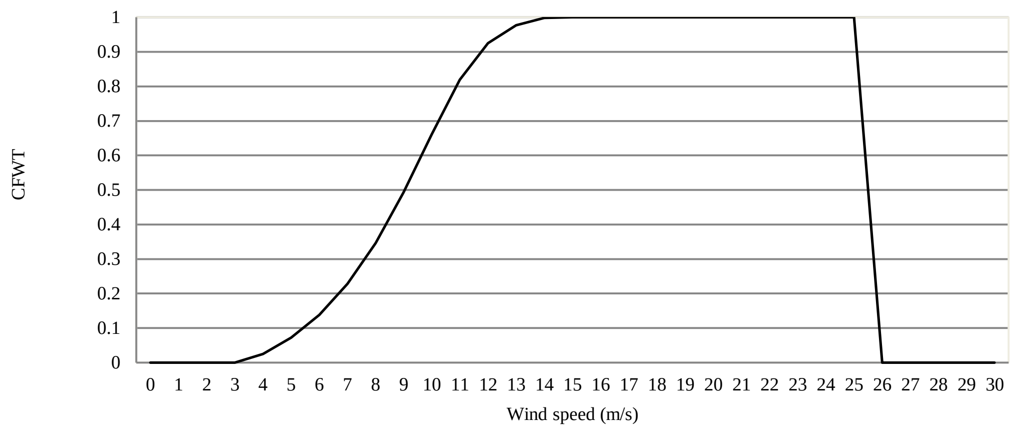


Figure 21 Wind Turbine Capacity Factor

CHP consumes gas and generates both power and heat. Since CHP electrical efficiency is highly dependent on its load level [98], piecewise linear electrical efficiency algorithm is applied for CHPG formulation. Three load regions with specific efficiency are assumed ($PLL_j, CHPLL_{j_{eff}}$) as in Figure 22. in each 'y', according to accumulated installed capacity ($\phi CAP | \ \phi = CHP$) the allowable load for each region follows:

$$LLj_y = PLL_j \times CHPCAP_y, j = 1 \ldots 3 \qquad (3)$$

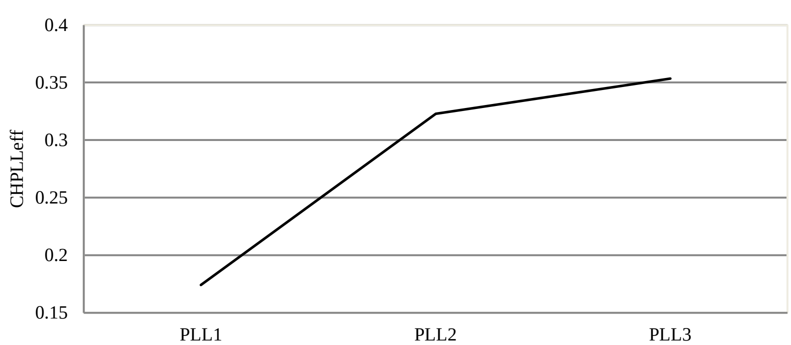


Figure 22 CHP electrical efficiency at each region

Two sets of binary constraints as in $(4)$, $(5)$ along with binary decision variable for CHP status ($\mathrm{CHP_{OS}}$) are introduced which force the unit to be shut down if the load level is below $\mathrm{LL1}$. '$\mathrm{M}$'refers to a large number.

$$\mathrm{PLL_1 \times CHPCAP_y - PRLL1_{y,t} \;\; \leq \;\; M \times \left(1 - CHP_{OS_{y,t}}\right)} \tag{4}$$

$$\mathrm{PLL_1 \times CHPCAP_y - PRrLL1_{y,t} > -M \times \; CHP_{OS_{y,t}}} \tag{5}$$

Total hourly electricity generation (CHPG) calculates as in (6) with respect to unit status and electricity generation at each region ($\mathrm{PRLLj}$):

$$\mathrm{CHPG_{y,t}} = \sum_{\mathrm{j=1}}^{\mathrm{J}} \mathrm{PRLLj_{y,t}} \begin{cases} = \mathrm{CHPCAP_y \times (PLL_1) \quad \times CHP_{OS_{y,t}}} & \mathrm{, j = 1} \\ \leq \mathrm{CHPCAP_y \times CHP_{OS_{y,t}} \times \left(PLL_j - PLL_{j-1}\right)} & \mathrm{, j \neq 1} \end{cases} \tag{6}$$

The amount of hourly generated heat ($\mathrm{CHPG_{HW} + CHPG_{HNW}}$) is constrained as in (7).

$$\mathrm{CHPG_{HW_{y,t}} + \; CHPG_{HNW_{y,t}} = HPR \times CHPG_{y,t}} \tag{7}$$

After defining all generation constraint, electric storage constraints will be introduced. At each time period, the available energy kept in storage ($SOC$) is conserved by:

$$\mathrm{SOC_{y,t}} = \mathrm{SOC_{y,t-1}} + \mathrm{C_{y,t}} \times \mathrm{ST_{eff}} - \frac{\mathrm{D_{y,t}}}{\mathrm{ST_{eff}}}\ , \mathrm{t} \neq 1 \tag{8}$$

$C_{y,t}$ and $D_{y,t}$ are charging and discharging quantities from storage during each hour. Storage charge and discharge are constrained by maximum charge/discharge power rate of the device (9).

$$\mathrm{C_{y,t}} \times \mathrm{ST_{eff}} + \frac{\mathrm{D_{y,t}}}{\mathrm{ST_{eff}}} \leq \mathrm{STPR} \times \mathrm{t} \tag{9}$$

Moreover, the state of charge (SOC) is constrained between min/max of allowable storage level. This will constrain SOC at each time step with respect to accumulated capacity at ‘y’ (10).

$$\mathrm{MLST} \times \mathrm{STCAP_y} \leq \mathrm{SOC_{y,t}} \leq (1 - \mathrm{MLST}) \times \mathrm{STCAP_y} \tag{10}$$

In (11), allowable energy for charging the device (C) is constrained based on available portion of generation which is not served the load ($\phi$G_S).

$$\mathrm{C_{y,t}} = \sum\nolimits_{\phi} (\phi \mathrm{G\_S_{y,t}} = \phi \mathrm{G_{y,t}} - \phi \mathrm{G_{L_{y,t}}}) \tag{11}$$

### 3.5.2 DER Operational Saving

Cost of operating DER is the cost of both fuel and non-fuel on-site generation plus if any, the cost of purchasing power from grid (EPG). It is assumed that if PV or WT is installed there would be associated costs for renting the needed land ($\mathrm{RL\phi}\ |\phi \in \{\mathrm{WT, PV}\}$). In this order, DER operational cost at each year ($\mathrm{DEROC_y}$) follows:

$$
\begin{aligned}
&\mathrm{DEROC_y} \\
&= \sum_{d=1}^{D}\sum_{t=1}^{T}\left[\left(\vartheta \mathrm{G_{y,t}} \times \left(\frac{\mathrm{GP_y}}{\vartheta_{\mathrm{eff}}} + \mathrm{C}\vartheta_{\mathrm{O\&M}}\right)\middle|\vartheta \in \{\mathrm{GF, Boiler}\}\right) + \sum_{\phi \in \{\mathrm{WT,PV}\}} \phi \mathrm{G_{y,t}} \times \mathrm{C}\phi_{\mathrm{O\&M}}\right. \\
&\left. + \sum_{j=1}^{J} \mathrm{PRLLj_{y,t}} \times \left(\mathrm{CostSlopej_y} + \mathrm{CCHP_{O\&M}}\right) + \mathrm{EPG_{y,t}} \times \mathrm{SP_{y,t}}\right] \\
&+ \sum_{\phi \in \{\mathrm{WT,PV}\}} \mathrm{RL}\phi_{\mathrm{y}} \qquad (12)
\end{aligned}
$$

$\mathrm{RL\phi}$'s are calculated as: $\phi\mathrm{lkw} \times \mathrm{LRP_y} \times \phi\mathrm{CAP_y}$. For calculating the fuel-related CHP operation costs, slope cost (CostSlopej) is defined as below:

$$
\mathrm{CostSlopej_y} = \begin{cases} \mathrm{GP_y} \times \left(\dfrac{1}{\mathrm{CHPLL_{j_{eff}}}}\right) & ,\mathrm{j} = 1 \\[2ex] \mathrm{GP_y} \times \dfrac{\frac{\mathrm{PLL_j}}{\mathrm{CHPLL_{j_{eff}}}} - \frac{\mathrm{PLL_{j-1}}}{\mathrm{CHPLL_{j-1_{eff}}}}}{\mathrm{PLL_j} - \mathrm{PLL_{j-1}}} & ,\mathrm{j} \neq 1 \end{cases} \qquad (13)
$$

In (12), electricity spot price (SP) is assumed to be a random function of natural gas price (GP), grid average heat rate ($\mathrm{E_{grid}}$), a multiplier (Mult) which accounts for transmission costs, and hourly profile of electricity price as a percentage of peak price. Adopted from [99], Ornstein-Uhlenbeck Brownian motion with mean reverting drift is used to model natural gas prices. With knowing underlying price values along with both power (Pd) and heat demand (Hd), the annual operational cost without DER ($\mathrm{NoDEROC_y}$) calculates as below:

$$\mathrm{NoDEROC_y} = \sum_{d=1}^{D}\sum_{t=1}^{T}(\mathrm{Pd_{y,t}} \times \mathrm{SP_{y,t}} + \mathrm{Hd_{y,t}} \times \frac{\mathrm{GP_y}}{\mathrm{B_{eff}}}) \tag{14}$$

Using (13) and (14), one could calculate savings due to on-site generation ($\mathrm{SOG}$) as follow:

$$\mathrm{SOG_y} = \mathrm{NoDEROC_y} - \mathrm{DEROC_y} \tag{15}$$

### 3.5.3 Serving Dynamic Demand

Both power and heat demand should be met as the main constraint of any energy system [100]. Recognizing its importance, the summation of hourly power generation which serves load ($\phi$G_L), discharge from ST (D) and electricity purchased from macro grid (EPG) should be equal or greater than power demand at each time step (16). This also holds for heat as in (17).

$$\sum_{\phi} \phi\mathrm{G\_L_{y,t}} + \mathrm{D_{y,t}} + \mathrm{EPG_{y,t}} \geq \mathrm{Pd_{y,t}} \tag{16}$$

$$\mathrm{BGen_{y,t}} + \mathrm{CHPG_{HNW_{y,t}}} = \mathrm{Hd_{y,t}} \tag{17}$$

Pd and Hd derive from stochastic bottom-up adaptive model (Hi-RAM). At household (HH) level, model takes into account HH physical characteristics ($X_{Ph}^{HH=i}$), residents' demographics ($Y_{Demo}^{HH=i}$), and ambient variables ($Z_{Amb}^{HH=i}$). Considering "I" HHs this gives:

$$Pd_{y,t}\ , Hd_{y,t} \sim \sum_{i=1}^{I} f(X_{Ph}^{HH=i}, Y_{Demo}^{HH=i},\ Z_{Amb}^{HH=i}) \qquad (18)$$

Where:

$X_{Ph}^{HH=i} \in \{\text{ HH Size}\}$

$Y_{Demo}^{HH=i} \in \{\text{Age, Gender, Empolyement status}\}$

$Z_{Amb}^{HH=i} \in \{\text{Ambient Temperature , Solar Intensity }\}$

The embedded dynamics of the model works on the basis of Markovian stochastic model for simulating human activities. Given "R" residents in the i-th HH, sequence of activities will be simulated where transition probabilities (T) are in form of: $T_{S_n S_m}^{R=r}(t) \sim g(Y_{Demo}^{HH=i})$. Transition probabilities are calibrated using American Time-Use Survey data (ATUS), publicly available in US Department of Labor website (http://www.bls.gov/tus/). Simulated activities then will be converted to its associated load (e.g. watching TV, dishwashing, etc. Herein these are called "Loads associated to specific activities" (LASA). "Base-load" is the other load category which consists of: HVAC, Lighting, and cold appliances load. HVAC model works on basis of a Newton's law of heating and cooling. The lighting energy use model takes into account perception of the natural light level (solar intensity) within a building and number of people who are active. At each time interval “t”, latter calculates from the simulated activities of residents. This follows as:

$$\sum_{r=1}^{r=R} 1n(t), \quad 1n(t) := \begin{cases} 1, & S_r(t) \notin \{away, sleeping\} \\ 0, & S_r(t) \in \{away, sleeping\} \end{cases} \tag{19}$$

where S refers to states (activities)

Moreover, cold appliances load follows probabilistic Bernoulli distribution. Knowing number of households (HH) under the study, both power and heat demands are obtained from (18). Two What-if scenarios are defined. These scenarios are denoted by Mode II, and Mode III. In Mode II new load patterns from PEV are introduced. PEV charging schedule is based on occupancy pattern simulated by Hi-RAM and takes into consideration the driving habits of individuals. Charging schedules are not necessarily averse of price.

Mode III is the upgraded version of Mode II where smart devices are used within premises. This enables the implementation of price responsive DSM strategies via programmable communication devices (PCD). PCD enables end-use models to reflect the function of: Intelligent thermostats which learn temperature preference of occupants; Price responsive thermostats with pre-cooling capabilities; Smart electric plugs with the capability of altering the switch status; Automated dimmer switch with the capability of altering lighting levels based on the real time market price (For more details see: [100]). Conceptual framework that demonstrates the integration of bottom-up demand model to capacity planning (investment problem) is depicted in Figure 23.

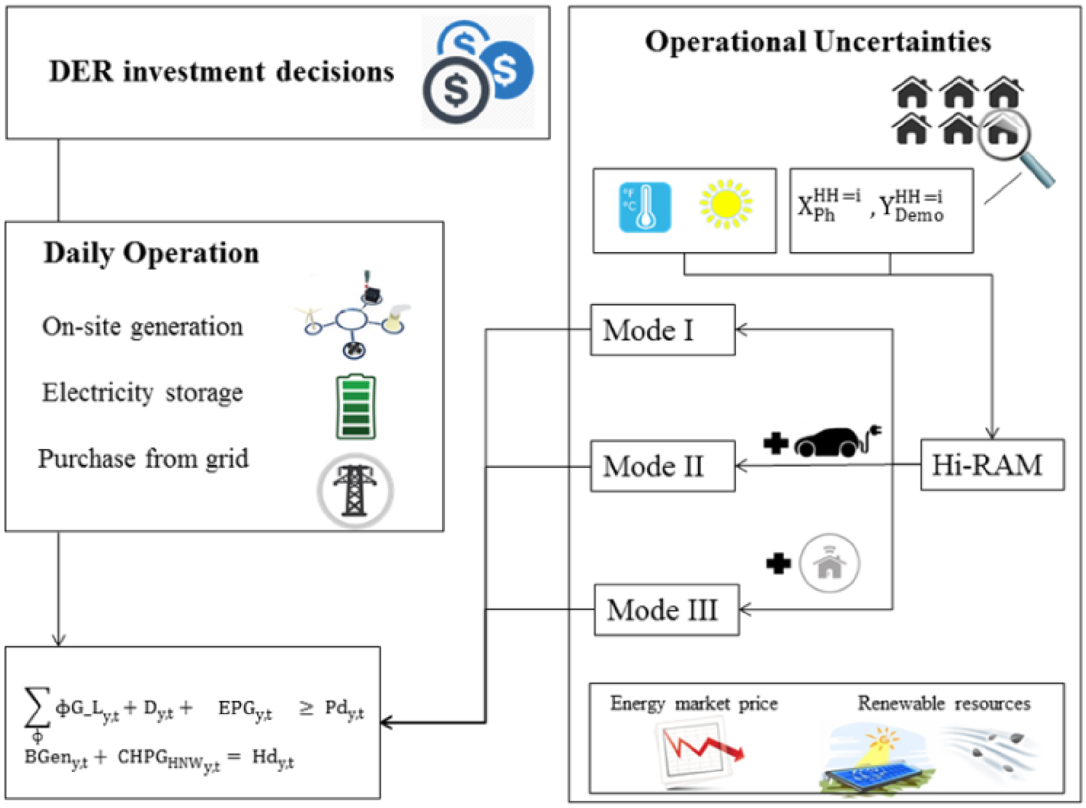


Figure 23. Integration of demand dynamics to capacity planning

### 3.5.4 Cash Flow Constraints

Investment decisions will be made in order to maximizing the end of horizon cash flow plus the projected value of any cash flow beyond the horizon at horizon year [77]. Cash flow constraints (20 - 22) are adopted from [77, 85].

$$CF_Y = SOG_Y + ROI_Y + B_Y - PB_Y - SOA_Y - AI_Y \tag{20}$$

$ROI_Y$ which is the return of cash invested on an alternative investment other than DER in the previous period ($AI_{Y-1}$), calculates as: $ROI_Y = AI_{Y-1} \times (1 + IRR)$. AI is constrained based on the availability of cash, where at the beginning of horizon ($y = 1$) it cannot exceed initial available cash (IAC), and in following years it follows as:

$$\mathrm{AI_y} \leq \mathrm{SOG_{y-1}} + \mathrm{ROI_y} \quad , y \neq 1 \tag{21}$$

At each period it is assumed that borrowed fund cannot exceed the limit ($\mathrm{B_y} \leq$ Blim). Moreover, Funds borrowed are restricted to be used to purchase on-site resources and cannot be invested on analternative option. Therefore, total DER investment in each period is constrained by funds available through borrowing and $\mathrm{SOA_y}$:

$$\mathrm{SOA_y} + \mathrm{B_y} = \sum\nolimits_{\vartheta} \mathrm{CC\vartheta_y} \tag{22}$$

where $\mathrm{CC\vartheta}$ is the cost associated to purchase incremental capacity of $\vartheta$ ($\mathrm{AC\vartheta}$): $\mathrm{CC\vartheta_y} = \mathrm{CapEx\vartheta_y} \times \mathrm{AC\vartheta_y}$. Having purchased $\mathrm{AC\vartheta}$ at each year, accumulated capacity of each asset could be calculated as follow:

$$\mathrm{\vartheta CAP_y} = \begin{cases} \mathrm{AC\vartheta_y} & , \quad y = 1 \\ \mathrm{\vartheta CAP_{y-1}} + \mathrm{AC\vartheta_y} & , \quad y \neq 1 \end{cases} \tag{23}$$

Fund borrowed in period x would entitle the borrower to payment flows in coming periods. Total payment in each period would be:

$$\mathrm{PB_y} = \sum_{x=1}^{y-1} \frac{\mathrm{FC} \times \mathrm{B_y}}{1 - (1 + \mathrm{FC})^{-\mathrm{FT}}} \qquad y = x + 1, \ldots, x + \mathrm{FT} \tag{24}$$

$\widehat{\mathrm{CF}}_{\mathrm{Y}}$ includes perpetual savings from the DER ($\widehat{SOG}_{\mathrm{Y}}$), the return on cash invested in the last period ($\widehat{\mathrm{ROI}}_{\mathrm{Y+1}}$), and the remainder of finance charges ($\widehat{\mathrm{PB}}_{\mathrm{Y}}$). These follow as:

$$\widehat{\mathrm{SOG}}_{\mathrm{Y}} = \frac{1}{1+\mathrm{DF}} \sum_{s=0}^{\infty} \frac{\mathrm{SOG}_{\mathrm{Y+1}}}{(1+\mathrm{DF})^{s}} = \frac{\mathrm{SOG}_{\mathrm{Y+1}}}{\mathrm{DF}} \tag{25}$$

$$\widehat{\mathrm{ROCI}}_{\mathrm{Y+1}} = \frac{1}{(1+\mathrm{DF})} \mathrm{ROI}_{\mathrm{Y+1}} \tag{26}$$

$$\widehat{\mathrm{PB}}_{\mathrm{Y}} = \sum_{t=\mathrm{Y+1}}^{\mathrm{Y+FT}} \frac{\mathrm{PB}_{\mathrm{t}}}{(1+\mathrm{DF})^{\mathrm{t}}} \tag{27}$$

Non-negativity constraints are also considered for variables which cannot take negative values:

$$\mathrm{AC}\vartheta_{\mathrm{y}}, \vartheta\mathrm{CAP}_{\mathrm{y}}, \mathrm{SOA}_{\mathrm{y}}, \mathrm{B}_{\mathrm{y}}, \mathrm{AI}_{\mathrm{y}} \geq 0 \tag{28 − 32 }$$

## 3.6 Results and Discussion

In this section daily DER operation along with investment decisions will be presented for three modes of electricity demand. Results corresponding to Mode I (base) are reproducible using time series forecast models and are provided here as a benchmark to evaluate the results from Mode II (new end-use consumption in form of PEVs) and Mode III (customer's response to price signals and other DSM strategies). Community of 40 households is selected; note that there are typically 40 households connected to a primary distribution feeder. Households are selected from Residential Energy

Consumption Survey (RECS) data (for detailed description of selected households, see chapter 2). RECS feeds the proposed demand model in chapter 2 with unique information about characteristics of household members (e.g. age, gender, education level, and employment status) and appliances within premises (see [101] for detailed information regarding application of RECS in bottom-up models). It should be noted that the model is not limited to any particular household and this selection is just for the purpose of demonstration. Both power and heat load will be supplied by either DER or macro-grid. Hourly power demand medians with corresponding 25th and 75th percentiles for Mode I, II, and III are demonstrated in Figure 25, 26, and 27; respectively. Heat demand is same for all three different electricity modes (Figure 28). Planning horizon is assumed to be 5 year. Availability of renewables such as solar intensity and wind speed are illustrated in Figure 24. Operational and financial parameters are provided in Table 11. Moreover, Unit capacity costs are presented in Table 12.

Table 11 Operational and financial parameters

| | | | | | |
|---|---|---|---|---|---|
| HPR | 1.1 | $CGF_{O\&M}$ | 0.015 $/kWh | IAC | $10^5$ $ |
| STPR | 100 kW | $CWT_{O\&M}$ | 0.009 $/kWh | Blim | $10^5$ $ |
| MLST | 0.1 | $CPV_{O\&M}$ | 0.005 $/kWh | IRR | 0.03 |
| Beff | 0.8 | $CCHP_{O\&M}$ | 0.012 $/kWh | FC | 0.06 |
| GFHR | 0.03 | PVlkW | 0.07Acre/kW | FT | 5 |
| $CB_{O\&M}$ | 0.006 $/kWh | WTlkW | 0.24 Acre/kW | DF | 0.05 |

Table 12 Unit capacity cost ($/kW)

| $\vartheta$ | Year 1 | Year 2 | Year 3 | Year 4 | Year 5 |
|---|---|---|---|---|---|
| PV | 3000 | 2810 | 2630 | 2460 | 2300 |
| WT | 2200 | 2090 | 1985 | 1880 | 1770 |
| GF | 100 | 100.1 | 100.2 | 100.3 | 100.4 |
| CHP | 1200 | 1210 | 1220 | 1230 | 1240 |
| ST | 600 | 570 | 540 | 513 | 490 |
| Boiler | 0.6 | 0.7 | 0.8 | 0.9 | 1.0 |

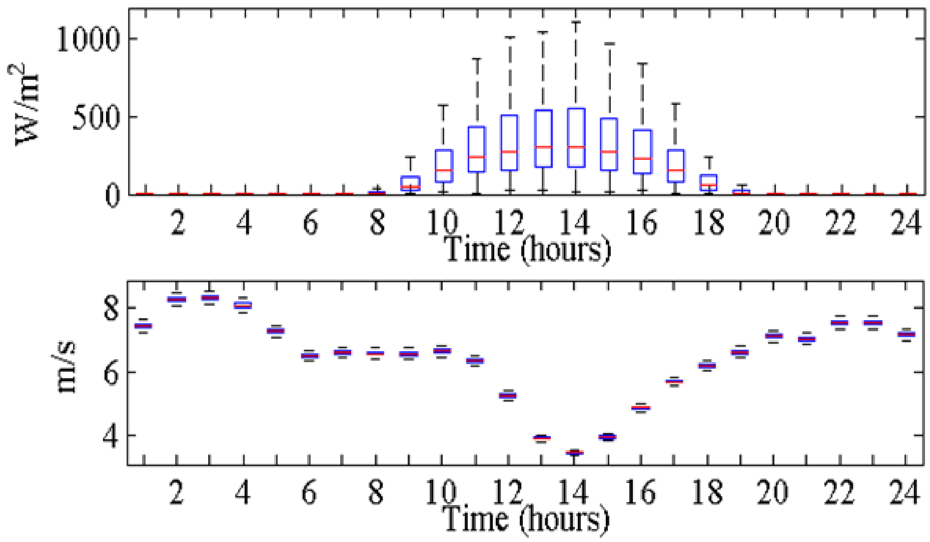


Figure 24 Hourly solar intensity (top) and wind speed (bottom)

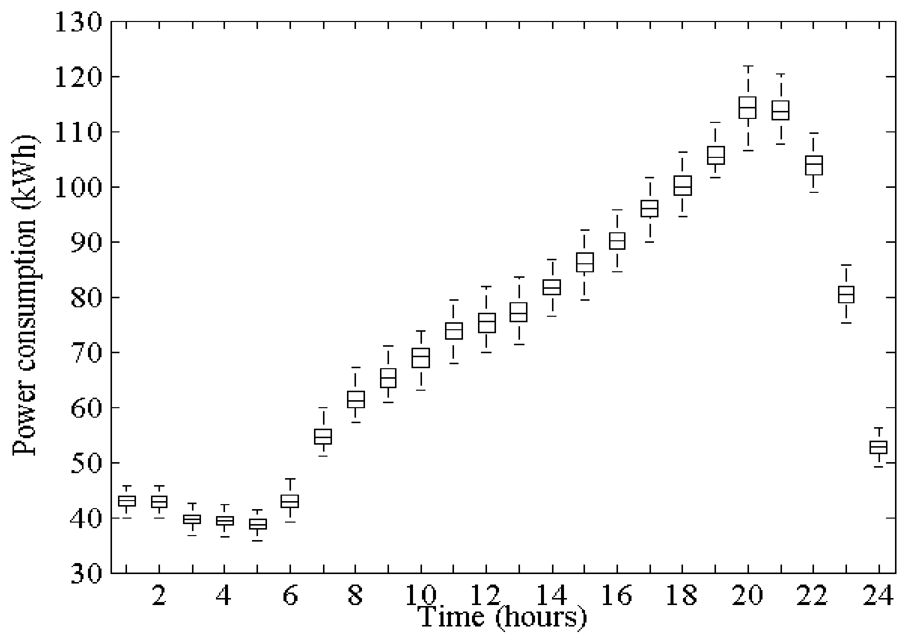


Figure 22 Power demand Mode I

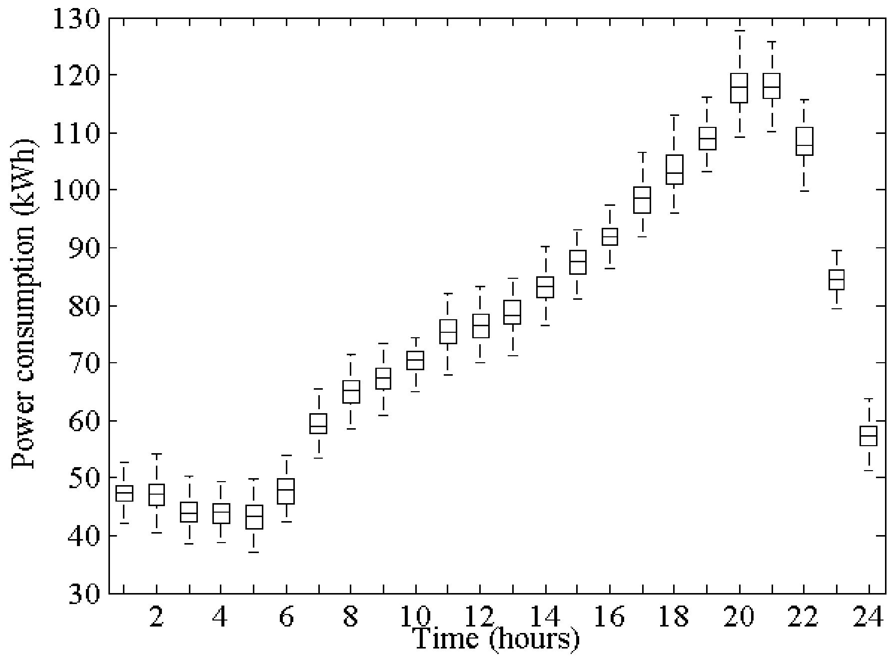


Figure 23 Power demand Mode II

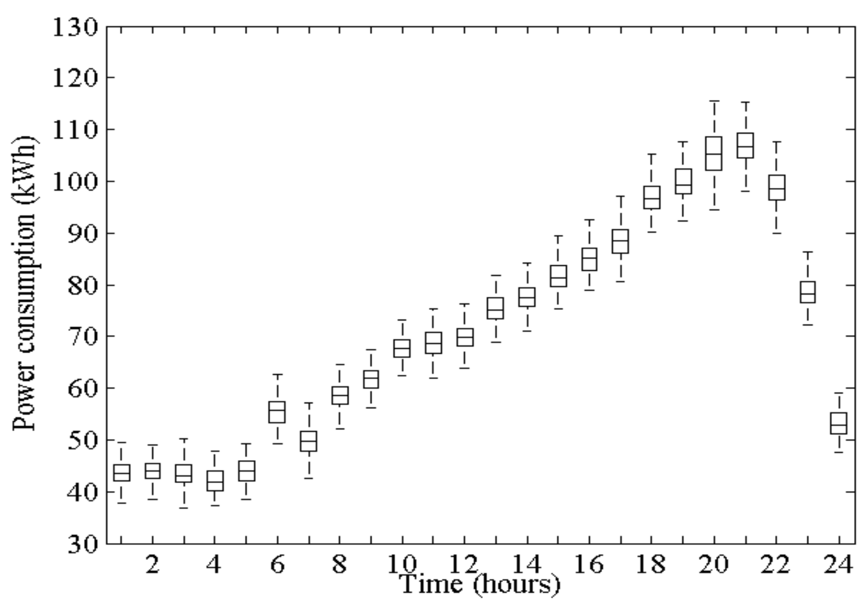


Figure 24 Power demand Mode III

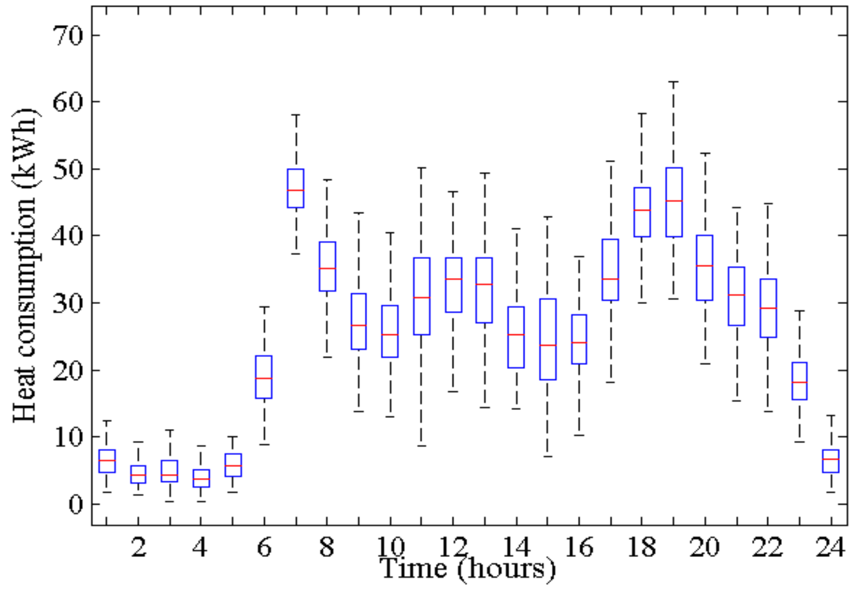


Figure 25 Heat demand across all models

### 3.6.1 Mode I; Daily DER Operation and Investment Decisions

Average daily operation in horizon year for Mode I is demonstrated in Figure 29. One may observe that generation from renewable sources namely PV and WT follow the availability of their corresponding resources (Figure 24). Moreover, it could be seen that CHP generation is negligible during early hours (EH) of the day (between1$^{st}$ and 6$^{th}$ hour period). As depicted in Figure 29, heat demand during EH is in the minimum level except for 6$^{th}$ period. This sudden spike in heat demand with considering relatively low power demand (see 6$^{th}$ hour in Figure 25) limits the potential of CHP. In such situation according to (4), and (5) the unit will be shut down ($\mathrm{CHP_{OS}} = 0$) since: $\mathrm{PLL_1} \times \mathrm{CHPCAP_y} \leq \mathrm{PRLL1_{y,t}}$.

Poor coordination between power and heat level in this time period, leads to highest EPG level throughout the day. Figure 30 illustrates average sources which contribute to charge electricity storage rather than directly serving the load. This type of analysis is feasible due splitting mechanisms ϕG_L , and ϕG_S as in (11). As it can be seen major contribution is from renewable resources. This indicates that, existence of electricity storage helps to accommodate excess generation from intermittent renewable resources and to participate into price arbitrage operations.

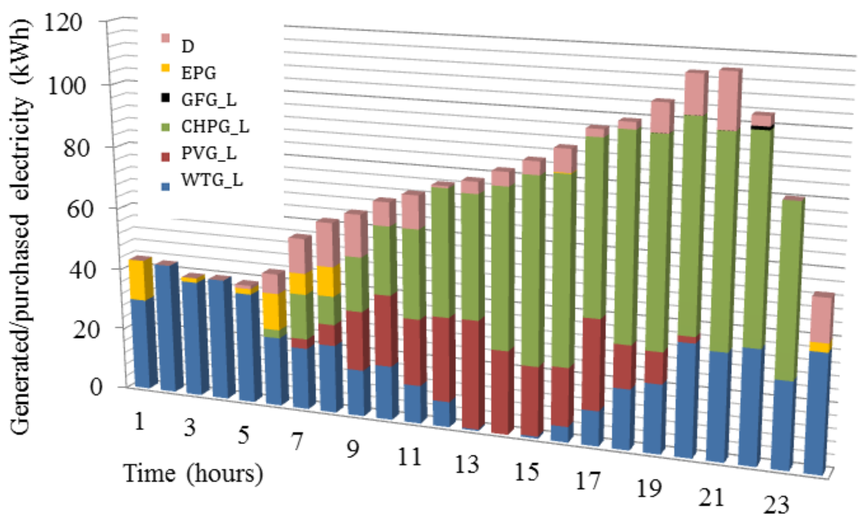


Figure 26 Mode I, Average hourly operation (horizon year)

### 3.6.2 Mode II; PEV Emergence and Investment Decisions

In Table 13 average cumulative capacity installments are demonstrated for all three modes. As it can be seen, by considering the emergence of PEV (Mode II) investment decisions may differ compare to Mode I. In this (Mode II), PEV recharging schedule is based on householder's occupancy pattern. This means charging is an option when they are at home. This mostly happens in early hours of the day, and peak hours through end of the day. Simulated by Hi-RAM, the frequency of PEV recharging is depicted as in Figure 31.

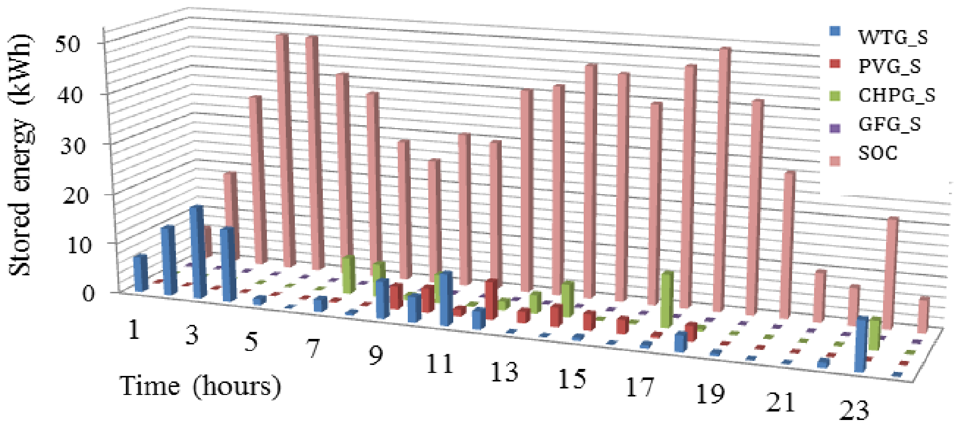


Figure 30 Mode I, State of charge and resources

The positive correlation between recharging pattern and wind availability (see Figure 24), suggested more capacity installment of WT in Mode II compare to Mode I (see Table 13). Moreover, higher peak values in Mode II as a result of PEV recharges, ended-up in more CHP installment compare to Mode I. One may notice that by incorporating such demand dynamics e.g. large PEV penetration to communities into capacity planning problem, more sustainable strategy than Mode I could be suggested that can hedge against possible future supply shortcomings.

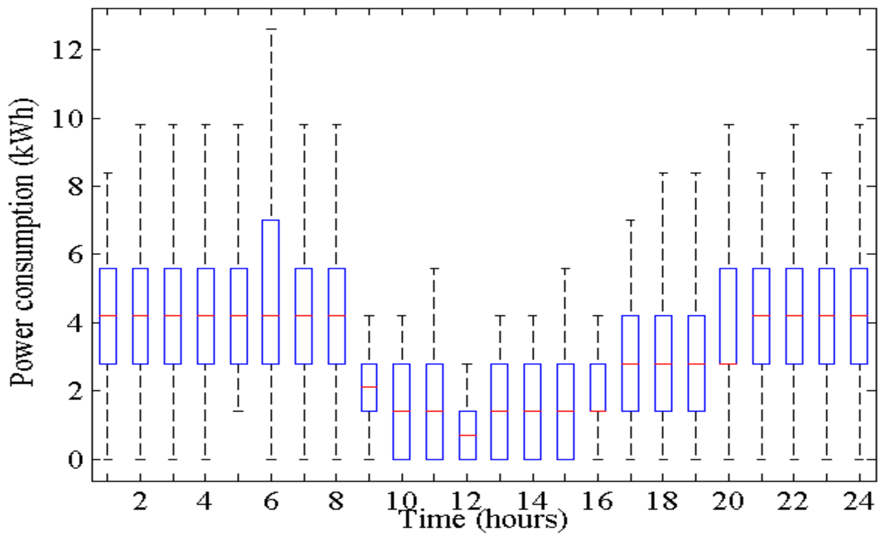


Figure 31 PEV recharging

Table 13 Average cumulative installed capacity (kW) among all modes

| | Year 1 | Year 2 | Year 3 | Year 4 | Year 5 |
|---|---|---|---|---|---|
| Mode I | | | | | |
| WT | 0.7 | 27.5 | 64.3 | 100.6 | 162 |
| PV | 2.6 | 14.3 | 22.4 | 26 | 59.3 |
| ST | 0 | 7.7 | 17.9 | 62.2 | 64 |
| CHP | 64.7 | 64.7 | 64.7 | 64.7 | 64.7 |
| GF | 10.7 | 10.7 | 10.7 | 10.7 | 10.7 |
| Boiler | 46.1 | 46.1 | 46.1 | 46.1 | 46.1 |
| Mode II | | | | | |
| WT | 0.3 | 28.8 | 65.1 | 104.2 | 171.7 |
| PV | 2.5 | 14.8 | 23.6 | 26.7 | 55.6 |
| ST | 0 | 10.1 | 19.2 | 55.9 | 56.8 |
| CHP | 68 | 68 | 68 | 68 | 68 |
| GF | 11.5 | 11.5 | 11.5 | 11.5 | 11.5 |

| | | | | | |
|---|---|---|---|---|---|
| Boiler | 44.9 | 44.9 | 44.9 | 44.9 | 44.9 |
| | Mode III | | | | |
| WT | 1.3 | 30.9 | 68.5 | 106 | 171.5 |
| PV | 3.8 | 17.4 | 22.9 | 27.8 | 68.4 |
| ST | 0 | 5.8 | 26.2 | 60.2 | 60.2 |
| CHP | 57.8 | 57.8 | 57.8 | 57.8 | 57.8 |
| GF | 11.4 | 11.4 | 11.4 | 11.4 | 11.4 |
| Boiler | 45.5 | 45.5 | 45.5 | 45.5 | 45.5 |

### 3.6.3 Mode III; DSM as a Resource

In this mode, three end-uses namely lighting, PEV charging, and space cooling are responding to SP. Average profile of end-uses consumption in both Mode II and Mode III are depicted in Figure 32. Cash flows at the end of horizon plus beyond the horizon ($\mathrm{CF_Y} + \widehat{\mathrm{CF}}_\mathrm{Y}$) in different Modes are illustrated in Figure 33. One may observe that addition of price responsive DSM into portfolio (Mode III) results in more cash flow than both Mode I and II. To better envision the reason behind this, financial activities during planning horizon are provided for both Mode II and Mode III in Figure 34 (negative values indicate outflows).

As it can be seen when DSM is available, more operational savings will be achieved. This will expand the opportunity to invest on other activities according to (20).

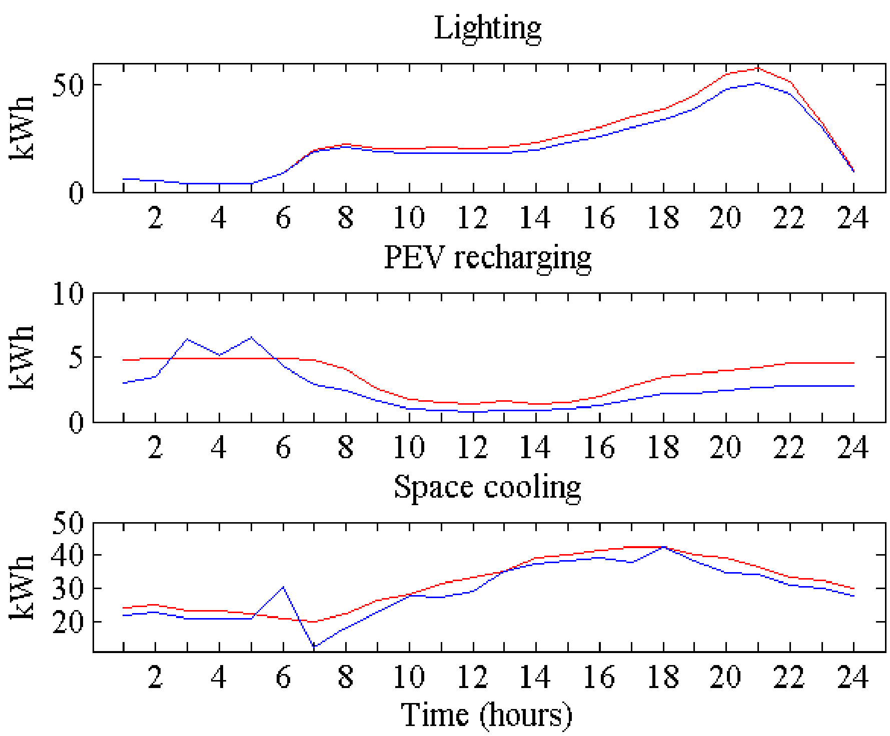


Figure 32 Average end uses consumption Mode II (red) vs. Mode III (blue)

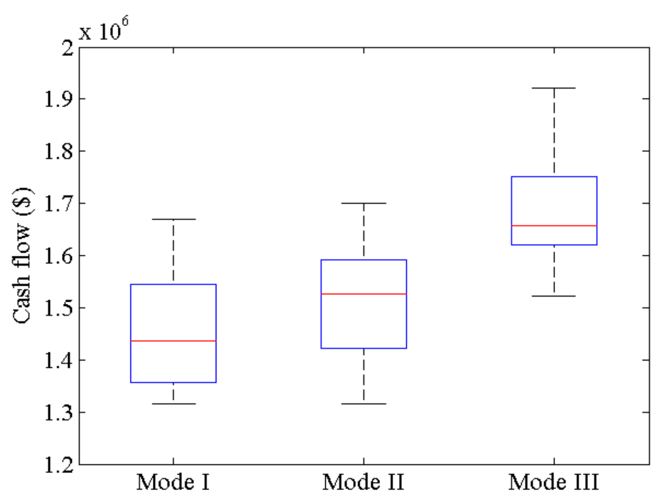


Figure 33 Cash flow at end of horizon + beyond horizon

By comparing the configuration of installed assets in Mode III and Mode II, one finds more investment on PV and less investment on CHP. The latter is mainly due to the curtailment of peak load. The former would lead to more installation of electricity storage. Higher unit cost of PV relative to CHP (see Table 13) leads to more funds to procure resources in Mode III compared to Mode II. However, more operational savings would be obtained in Mode III since production cost of PV is less than CHP. Another reason relates to price arbitrage operations. More electricity generation from PV leads to more contribution of this resource to recharge electricity storage (recharging with cheaper electricity). Mode III results suggest that the addition of DSM into the portfolio optimization results in not only higher operational savings but also in less environmental burdens.

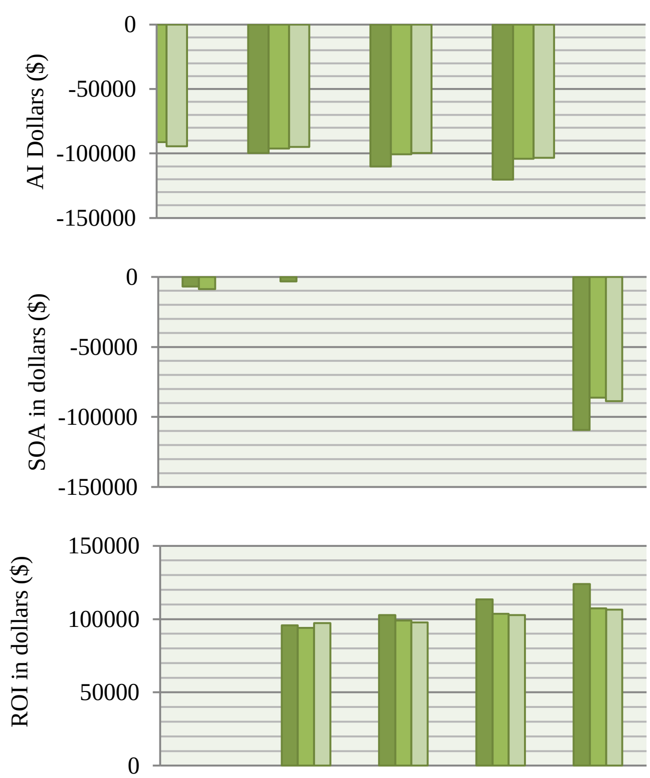

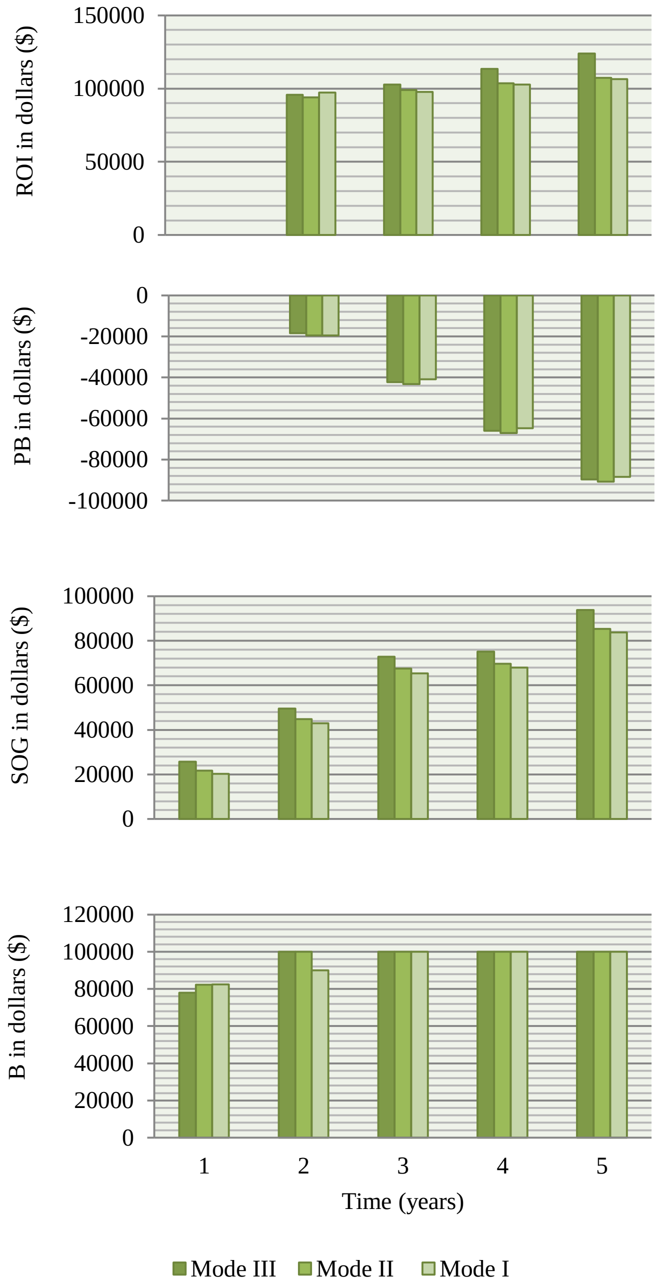


Figure 34 Financial activities in Mode II and III

## 3.7 Conclusion and Future Work

This research intends to formulate DER investment decisions by directly taking into account savings from DSM strategies. Hi-RAM that is capable of calculating DSM dynamical impacts is coupled with long-term formulation of a capacity planning problem. It was argued that traditional forecast models obtained solely from historical data fail to capture interaction effects of DSM strategies and, thus may lead to investment decisions that do not truly reflect optimal conditions. It is observed that emergence of PEV load varies the investment decisions. In particular more investment in wind turbines in Mode II than I due to the coordination of charging habits and wind availability. [94] observed similar patterns by using transportation data. In Section C, one may observe that existence of DSM e.g. smart charging reduces the operational costs. Investigation of such operational cost savings are observed in literature as in [94, 95]. This framework not only investigates operational cost savings as a result of DSM existence, but also suggests optimal configuration for DER portfolio in host of DSM. It is demonstrated that existence of DSM flattens the load profile (peak reduction and valley filling). This will avoid further investment in generation assets (particularly in dispatchable resources) in order to meet peak capacity. Proposed investment strategy in Mode II could be considered as a "more sustainable solution" where it can hedge against possible future supply shortcomings. In Mode III, decisions are even smarter than Mode II, where existence of price responsive demand would lead to utilization of more renewables and revenue.

Coordination of model outcomes with existing literature is interesting since the simulated data from a bottom up model is used as surrogate for historical domain specific data e.g., electric meter, transportation, and demand response data. Unlike the existing literature, this framework not only investigates load dynamics in the presence of advanced technologies, new plug-ins, and consumer response, but also suggests DER capacity planning solutions. This is important particularly for new communities where historical data is not available/sufficient. Furthermore, case of study can be easily expanded/changed in Hi-RAM. One direction for the future work is the addition of industrial and commercial load to this framework. Other direction would be participation of daily activities and consequent loads into demand response programs. One could derive willingness-to-shift functions for so-called delay-able activities. Investigating the effect of different climate on investment decisions is one another direction for future work.

**Requesting permission to reuse content from an IEEE publication**

**Title:** Integration of Demand Dynamics and Investment Decisions on Distributed Energy Resources

**Author:** Farbod Farzan; Farnaz Farzan; Mohsen A. Jafari; Jie Gong

**Publication:** Smart Grid, IEEE Transactions on

**Publisher:** IEEE

**Date:** July 2016



Logged in as:
farbod farzan
Account #:
3001023015

LOGOUT

## Thesis / Dissertation Reuse

**The IEEE does not require individuals working on a thesis to obtain a formal reuse license, however, you may print out this statement to be used as a permission grant:**

*Requirements to be followed when using any portion (e.g., figure, graph, table, or textual material) of an IEEE copyrighted paper in a thesis:*

1) In the case of textual material (e.g., using short quotes or referring to the work within these papers) users must give full credit to the original source (author, paper, publication) followed by the IEEE copyright line � 2011 IEEE.
2) In the case of illustrations or tabular material, we require that the copyright line � [Year of original publication] IEEE appear prominently with each reprinted figure and/or table.
3) If a substantial portion of the original paper is to be used, and if you are not the senior author, also obtain the senior author�s approval.

*Requirements to be followed when using an entire IEEE copyrighted paper in a thesis:*

1) The following IEEE copyright/ credit notice should be placed prominently in the references: � [year of original publication] IEEE. Reprinted, with permission, from [author names, paper title, IEEE publication title, and month/year of publication]
2) Only the accepted version of an IEEE copyrighted paper can be used when posting the paper or your thesis on-line.
3) In placing the thesis on the author's university website, please display the following message in a prominent place on the website: In reference to IEEE copyrighted material which is used with permission in this thesis, the IEEE does not endorse any of [university/educational entity's name goes here]'s products or services. Internal or personal use of this material is permitted. If interested in reprinting/republishing IEEE copyrighted material for advertising or promotional purposes or for creating new collective works for resale or redistribution, please go to http://www.ieee.org/publications_standards/publications/rights/rights_link.html to learn how to obtain a License from RightsLink.

If applicable, University Microfilms and/or ProQuest Library, or the Archives of Canada may supply single copies of the dissertation.

# 4. OPERATIONAL PLANNING FOR MULTI-BUILDING PORTFOLIO IN AN UNCERTAIN ENERGY MARKET [105]

## 4.1 Abstract

In this chapter, an optimization framework is proposed for day-ahead operational planning of a multi-building portfolio under market uncertainty. The portfolio of interest consists of two groups of buildings: controllable and uncontrollable. In the proposed framework, first, physics-based and statistical models are developed for estimation and prediction of end-use consumptions including Heating, Ventilation Air Conditioning (HVAC), lighting, and equipment in controllable buildings. In addition, calculation of hourly load distributions in uncontrollable buildings is developed using a non-parametric bootstrapping method. Then a multi-objective mathematical programming is formulated to minimize the energy expenditure given utility price signals while satisfying the occupants' comfort. The proposed pricing scheme considers the differences between the Day-Ahead and Real-Time prices to reflect the trend of energy market uncertainty. It is demonstrated that this pricing scheme results in better performance, in terms of achieving to demand management goals, than the current scheme. Current pricing scheme is solely based upon the Day-Ahead forecasted price. The performance of the proposed framework is explored using real energy market data.

Keywords: Multi-building portfolio, hybrid end-use models, uncertain market trend, energy market, demand response.

Nomenclature

A. Index

| | |
|---|---|
| D | Day Index |
| ϕ | Building Index |
| ɣ | End-use Index |
| T | Time Index (Hour) |
| Z | Zonal Index |
| D | Day Index |
| ϕ | Building Index |

B. Variables

| | |
|---|---|
| A | Floor Area (ft$^2$) |
| $E_.$ | Electricity Consumption (KWH) |
| LB | Temperature Lower Bound |
| O | Occupancy Percentage |
| SCH | Operational Schedule |
| $T_i$ | Internal Temperature (°F) |
| $T_\infty$ | Ambient Temperature (°F) |
| UB | Temperature Upper Bound |
| A | Floor Area (ft$^2$) |
| $E_.$ | Electricity Consumption (KWH) |
| LB | Temperature Lower Bound |
| UB | Temperature Upper Bound |

C. Variables

| | |
|---|---|
| DAP | Day-ahead Price |
| DAP&ED | DAP with Inclusion of Expected Market Uncertainty Trend |
| DAP&SDD | DAP with Inclusion of Standard Deviation of Market Uncertainty Trend |
| LF | Load Factor |
| OLR | Overall Load Reduction |
| PC | Constant Power Consumption (W/ft$^2$) |
| PHR | Peak Hour Reduction |
| PS | Pseudorandom Scalar |
| R. | Reduction |
| RTP | Real-time Price |
| SLR | Schedule Reduction Limit |
| SP | Set point (°F) |


| | |
|---|---|
| DAP | Day-ahead Price |
| DAP&ED | DAP with Inclusion of Expected Market Uncertainty Trend |
| DAP&SDD | DAP with Inclusion of Standard Deviation of Market Uncertainty Trend |
| LF | Load Factor |
| OLR | Overall Load Reduction |
| PC | Constant Power Consumption (W/ft$^2$) |
| PHR | Peak Hour Reduction |
| PS | Pseudorandom Scalar |

## 4.2 Introduction

The electricity network faces several major challenges, such as ever-increasing demand, emergence of intermittent renewable supply systems, and weather-related blackouts [106]. Real-time market is one of the potential solutions to address these challenges. Real-time market benefits the network in stressed out hours e.g., peak hours mainly through motivating enrolled customers to reduce/shift their loads. In such a market, costumers, facility managers may adjust their near future operational schedules based on available market information e.g., day-ahead market. This is a win-win situation since in one hand costumers can receive financial benefits, and on the other hand, the network can experience more balance between the demand and supply. The latter also provides economic benefits as it reduces the need for additional peaking capacity, increases component reliability, and results in a better operating performance.

However, a major concern or obstacle to achieve the above benefits is the uncertainty in energy markets. The energy market uncertainty can lead to large deviations between the Real-Time Price (RTP) and its forecasted values, e.g., Day-Ahead Price (DAP). Ignoring these deviations in near-future operational planning and adjusting or modifying the load according to the forecasted values may threaten the reliability of the system. As a result, in order to enhance the reliability or maximize the benefits of the real-time market, two capabilities are of great need: (i) the underlying demand needs to be elastic enough to market signals; and (ii) operational plans need to be made under consideration of market volatilities. Consumers who are able to foresee the market volatility with a reasonable level of accuracy can adjust their operating schedule in order to reduce the risk of power network failures (increasing network reliability) and/or maximize the profits in day-ahead market. Equipping major energy consumption sectors, including residential, commercial, industrial, and transportation, with these two capabilities can contribute to a sustainable and reliable demand-supply network.

In 2014, almost 55% of total energy is consumed in residential (11%), commercial (7%), and industrial buildings (36%) [107]. Residential and commercial sectors tend to have more regular schedules and operating patterns. Such regularity is a valuable characteristic in terms of load response to network signals. As a matter of fact, decision makers such as facility/portfolio managers have often more confidence about future/near-future operational plans for such loads than for irregular and unpredictable load patterns, which are often associated with industrial buildings [108].

As technologies reach maturity and dynamic pricing spreads nationwide, the business value behind load management increases. For example, Building Energy Management System (BEMS) empowers facility managers in this particular matter [109]. BEMS can be centrally located and communicate over telephone or Internet links with remote buildings having outstations so that one energy manager can manage multiple buildings remotely. Targets of BEMS often include HVAC, lighting, and electrical equipment (appliances). The HVAC accounts for 50% and the latter two combine (lighting and equipment) for 30% of energy consumption across all building sectors [110, and 111].

In recent years, increasing attention has been paid to building energy management via operational adjustments (operational planning). A conceptual framework for improving the effectiveness of building energy management in the realm of smart grids operations was presented in [114]. Furthermore, [115] proposed the pricing scheme to shift electricity demand of appliances from periods of high prices to periods of low prices with and without electricity storage devices. They used artificial dynamic pricing scheme that was a linear function of the spot price and load level. Multi-objective optimization frameworks were proposed in some studies to evaluate the effects of comfort relaxation on the energy demands of buildings [114, 115, 116]. In both studies, the authors employed a physics-based model of a single-zone building conditioned by an air-handling unit (AHU), and developed a detailed thermal comfort model. In addition, [117] assessed the possible benefits of optimized HVAC control strategies that account for both energy and indoor air quality goals. [118] also implemented a multi-agent comfort and energy simulation to model alternative management and control of building systems and occupants.

Human and device agents including HVAC, lighting, and appliance agents were used to explore trends in energy consumption and management of a university test-bed building. In addition, Markov decision problems were used to model and modify the interaction among agents. This enabled the investigation of opportunities to reschedule energy-consuming events. To study the trade-off between energy and comfort, [119] combined occupancy prediction with occupant discomfort which was described with probability density functions. In some of those studies, evaluations were not necessarily performed for real energy market [113-119]. The effects of the day-ahead market on the predictive dynamic building models were also investigated by [120, 121]. In particular, [121] focused on power consumption scheduling to minimize the electricity consumption with peak load reduction in buildings. The analysis was performed under the flat rate electricity price policy. Also, the total energy demands of buildings were calculated via abstract functional forms (sinusoidal functions). However, no measures for validating the proposed end-use models were provided in [120, 121]. The extensive literature in building energy management suggests the necessity of considering and investigating multi-building energy management strategies to reduce the risks associated with the high volatility of the real-time market [120]. Such effort is important due to the fact that the economic downturn has shifted the attention of firms and public owners of large building portfolios toward their existing buildings [122].

In this chapter, the portfolio of multi-buildings with different functionalities is considered. In these buildings, portfolio manager faces both controllable and uncontrollable loads. The problem of interest is to evaluate the day-ahead operational plans for the portfolio by incorporating market uncertainty and volatility. These plans should be adaptable to regional/temporal power network/market needs, such as peak reduction, average load shedding, load smoothing, etc. More specifically, the day-ahead plans are compared under different pricing schemes in terms of their ability to satisfy demand-side management goals such as peak hour reduction (PHR), overall load reduction (OLR), and daily load factor (LF) enhancement.

To perform the proposed study, a hybrid physics-based and statistical models for HVAC as well as models for lighting and electrical equipment are developed. This also includes calculation of hourly load distribution in uncontrollable buildings using non-parametric bootstrapping method. The problem is formulated as multi-objective mathematical programming based on building, market, and weather information. The objectives are minimal operational expenditure and minimal occupants' discomfort. Bi-polar objectives are picked in order to consider the tradeoff between the two objective functions, operational expenditure, and comfort. This is in fact, an essential step towards evaluating demand elasticity at large scale [123].

This chapter features the following contributions: (i) A generic hybrid physics-based statistical model for modeling HVAC system that is applicable for any building type and HVAC technology (ii) A pricing scheme, which enables the decision maker to manage day-ahead load with respect to demand-side management goals e.g., PHR, OLR, and LF enhancement (load smoothness). The chapter is structured as follows. In the following section, the modeling methodology is described along with the proposed end-use models and energy market dynamics. This follows by operational day-ahead planning under different price regimes along with discussion of results and findings through numerical examples. Conclusions and future work are presented at the end.

## 4.3 Modeling Methodology

In this study, buildings with different use types are selected. These buildings include a building with large, industrial load, an office building, a residential building, and a lodging building. Although the latter is characterized by its high-energy consumption due to its main mission e.g., providing maximum comfort to its customers to any price, there are still opportunities to reduce consumption levels through effective energy management strategies [124]. Three standard reference building energy models are utilized. These models developed by the U.S. Department of Energy are namely: mid-rise apartment (A:

33,740 ft2, |floors|:4), medium office (A: 53,628 ft2, |floors|:3), and small hotel (A: 43,200 ft2, |floors|:4) constructed in or after 1980 [125]. The mid-rise apartment contains 27 zones including apartments and corridors; the medium office has 15 zones including core and perimeter offices in all three floors; and the hotel has 68 zones belonging to guest rooms, laundry room, mechanical room, meeting room, corridors, attic and storage rooms.

For the building with industrial loads, the industrial load data from [126] is adopted. The industrial load has an uncontrollable nature while the loads associated with other buildings are controllable. Controllable (responsive) loads are namely HVAC, lighting, and electrical equipment. Using simulated data generated by EnergyPlus, multiple regression models are built for estimation of HVAC, lighting and equipment consumptions. This is necessary in order to bring the aforementioned end-uses into an optimization problem. The controllable parameters are considered as independent variables in regression models. These are temperature set points and schedules for lighting and equipment. At each time step, schedules for lights and equipment are in form of $|\mathrm{Lights; ON}|/|\mathrm{Total\ lights}|$, $|\mathrm{Equipment; ON}|/|\mathrm{Total\ equipment}|$, respectively. It should be mentioned that physical upgrades, such as building renovations are not considered here. Interested readers can refer to [127] for such studies.

The facility is expected to be enrolled in a real-time pricing program and the portfolio manager is aware of the hourly day-ahead energy market, such as the Locational Marginal Pricing (LMP) data. Operational plans are derived using DAP and is compared with the ones derived using actual price (RTP). In this setting, RTP data is the control price and DAP is the forecast of RTP using the state-of-the-art forecasting methods [128, 129, and 130]. In addition, two new pricing schemes are introduced in order to foresee the trend of market uncertainty and adjust operational plans accordingly. These two new schemes are DAP&ED, and DAP&SSD. The former adds the expected market uncertainty trend to DAP schemes while the latter includes standard deviation of market uncertainty trend into DAP schemes. Performances of the proposed pricing schemes are compared in terms of their ability to satisfy demand-side management goals. Herein the specific goals of interests are PHR, OLR, and daily LF enhancement. Next, the proposed methodology for modeling HVAC, lighting, and equipment are provided. Then, energy market dynamics and uncontrollable buildings with industrial load and multi-objective mathematical programming are also described.

### 4.3.1 Estimation of Total HVAC Electricity Consumption

This section describes the analytic constructs of the generic hybrid physics-based and statistical model, a model for the estimation of electricity consumption associated with HVAC. The model relates the space cooling electricity consumption in the building to exogenous parameters such as ambient temperature and internal parameters such as building characteristics, building occupancy, and HVAC technologies. The model not only assists with estimating HVAC electricity consumption, but also can be utilized for investigation of optimal operational schedules without compromising occupants comfort. Moreover, it enables load shifting strategies such as pre-cooling. The general functional form of the model is inspired by Newton's law of heating and cooling: $dT_a/dt \sim f\,(T_{HVAC} - T_i\ ,\ \ T_i - T_\infty)$. The Proposed HVAC energy consumption model is written as follows:

$$E_{HVAC}^{\phi}(t) = \beta_0^{\phi} + \beta_1^{\phi}.\frac{\sum_{z=1}^{Z(\phi)} T_i^{z,\phi}(t) - T_i^{z,\phi}(t-1)}{|Z(\phi)|} + \beta_2^{\phi}.(\frac{\sum_{z=1}^{Z(\phi)} T_i^{z,\phi}(t)}{|Z(\phi)|} - T_{\infty}(t))$$

$$+ \beta_3^{\phi}.\widehat{O^{\phi}}(t) + \beta_4^{\phi}.(T_{HVAC}^{\phi} - \frac{\sum_{z=1}^{Z(\phi)} T_i^{z,\phi}(t)}{|Z(\phi)|}) \quad (1)$$

Total HVAC energy consumption ($E_{HVAC}^{\phi}$) in (1) is calculated by adding all HVAC-related electricity consumers e.g., chillers, pumps, cooling towers, auxiliary handling unit, fan, exhaust fan, etc. In order to build the model, simulation for typical summer period (06/01 – 08/31) is conducted using EnergyPlus. First half of the data is used for training the model, and the second half will be conserved for testing purposes (model validation). In order to make the model flexible to a broad span of operating conditions, random hourly zonal set points (SP) is assigned in the simulation period. By doing this, the statistical models are able to capture the variability in HVAC consumption over a wide range of set points values. This is achievable by integration of EnergyPlus and Matlab via Building Controls Virtual Test Bed (BCVTB)[1]. Hourly random set point assignment follows an algorithm similar to truncated random walk process. This is demonstrated as in Figure 35.

[1] BCVTB is a software environment that allows users to couple different simulation programs for distributed simulation. For example, the BCVTB allows to simulate a building and HVAC system in EnergyPlus and the control logic in MATLAB/Simulink, while exchanging data between the software as they simulate. The BCVTB is based on the Ptolemy II software environment.

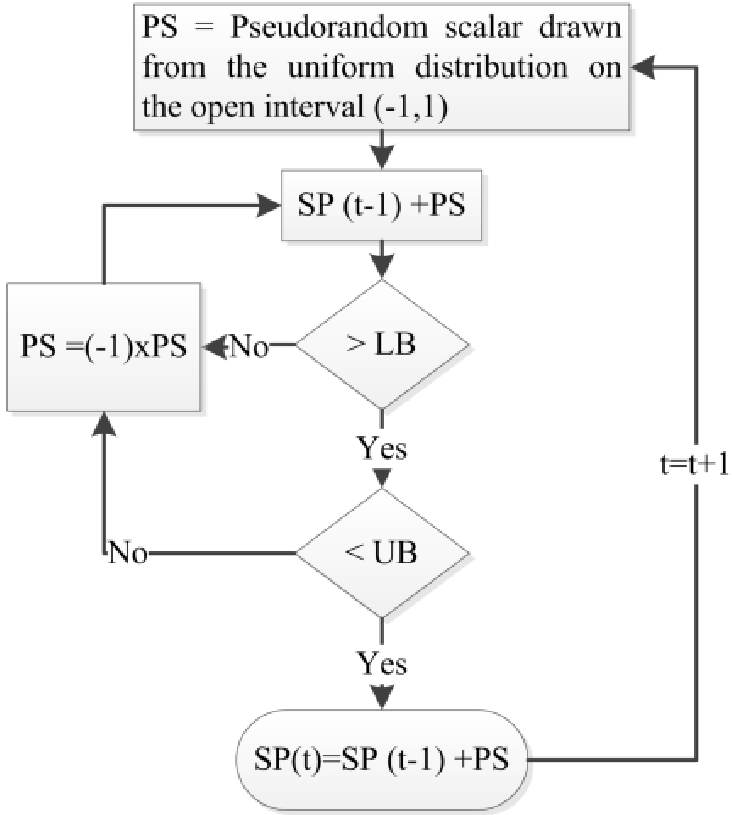


Figure 27 Hourly set point assignment algorithm

For model adequacy checking and validation, coefficient of determination ($R^2$), and standard error from mean (SEM) are used. Given the notation "y" for simulated values of total HVAC energy consumption, $R^2$can be calculated as follows.

$$R^2 = 1 - \frac{\sum_{i=1}^{N}\left(y(i) - E_{HVAC}^{\phi}(i)\right)^2}{\sum_{i=1}^{N}\left(y(i) - \frac{1}{N}\sum_{i=1}^{N} y(i)\right)^2}, \quad SEM = \sqrt{\frac{\sum_{i=1}^{N} y(i) - E_{HVAC}^{\phi}(i)^2}{N}} \tag{2}$$

The performance measures ($R^2$, and SEM) for the proposed HVAC model across different buildings along with model parameters are provided as in Table 14. To better visualize the performance of the proposed model, the estimated and the simulated values of $E_{HVAC}^{\phi}$ are depicted in time-series and scatter plots in Figure 36 and Figure 37, respectively. In Figure 36, blue curves represent the actual values (simulated data using EnergyPlus) for HVAC electricity consumption while red curves correspond to estimated values using (1) for all controllable buildings within the portfolio; $\phi \in$ {small hotel, mid-rise apartment, medium office}. In Figure 37, reference line $y = x$ is provided. This helps to understand whether or not two comparable data sets (actual and estimated) agree with each other. In this setup, the more the two data sets agree, the more the scatters tend to concentrate in the vicinity of the identity line. As it can be seen in this figure, the paired values of the estimated and simulated observations are relatively close to the identity line, particularly in the hotel building and the midrise apartments. The proposed forecast model has a slight underestimation in larger simulated values in the office building (Figure 37, right, see also SEM values in Table 14). This is mainly due to existence of electric reheat system in the air primary loops in this building.

Table 14 Summary of parameters and performance of HVAC estimation model

| ϕ | HVAC technology | $\hat{y}$ | $R^2$ | SEM | Coefficients (β) | | P-value |
|---|---|---|---|---|---|---|---|
| Small hotel | Packaged terminal air conditioner -Single speed direct expansion coil | 43.92 | 0.73 | 6.86 | $\beta_0$ | 61.92 | 1e-12 |
| | | | | | $\beta_1$ | -2.59 | 6e-14 |
| | | | | | $\beta_2$ | 2.18 | 4e-25 |
| | | | | | $\beta_3$ | -0.26 | 8e-2 |
| | | | | | $\beta_4$ | 2.37 | 2e-38 |
| Midrise apartment | Split system units with - Single speed direct expansion coil | 41.82 | 0.88 | 6.45 | $\beta_0$ | 42.92 | 6e-59 |
| | | | | | $\beta_1$ | -3.93 | 8e-27 |
| | | | | | $\beta_2$ | -3.77 | 0 |
| | | | | | $\beta_3$ | 3.08 | 8e-48 |
| | | | | | $\beta_4$ | 2.98 | 8e-06 |
| Medium office | Packaged VAV units – Two speed direct expansion coil | 90.53 | 0.79 | 13.42 | $\beta_0$ | 113.12 | 1e-10 |
| | | | | | $\beta_1$ | -9.52 | 6e-28 |
| | | | | | $\beta_2$ | -4.261 | 1e-23 |
| | | | | | $\beta_3$ | 8.64 | 9-17 |
| | | | | | $\beta_4$ | 5.63 | 1e-35 |

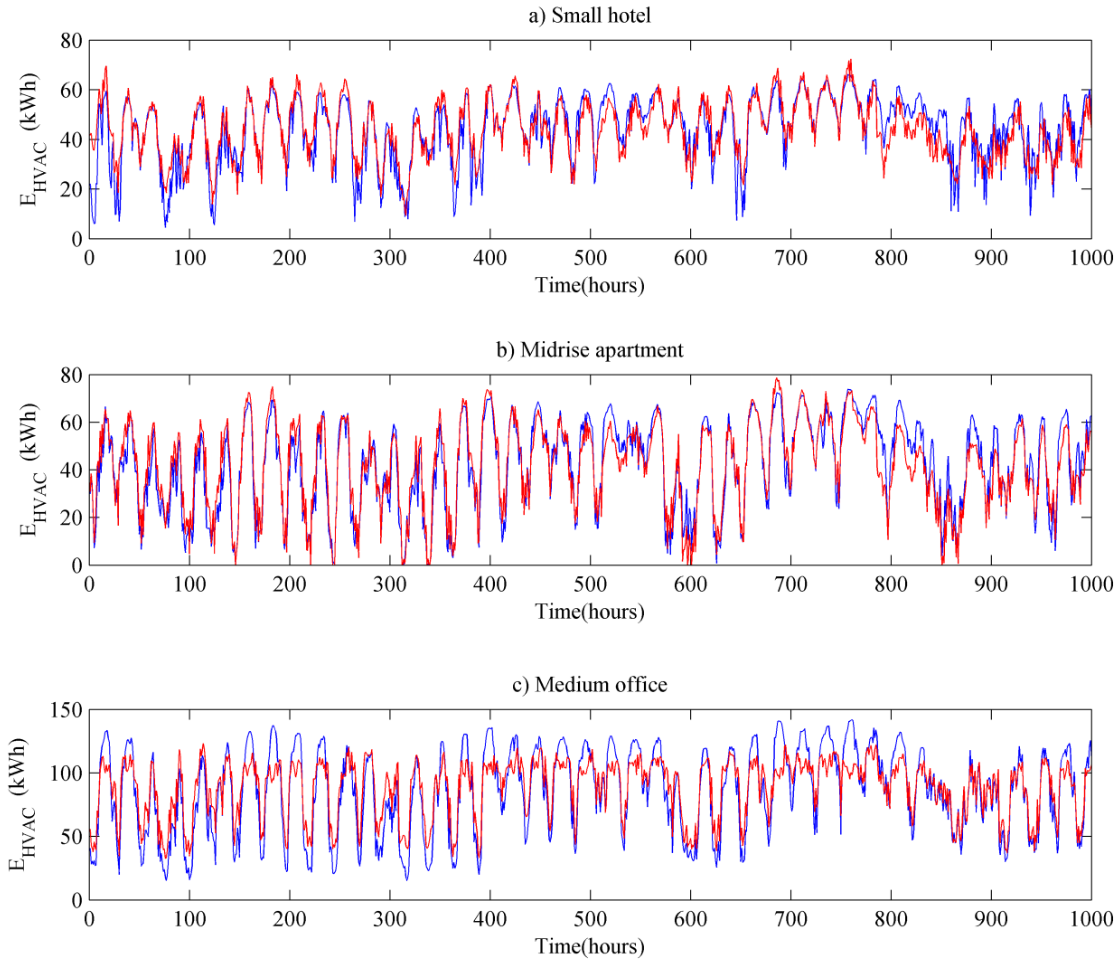


Figure 36 Electricity consumption across different buildings. Estimated values (red curves), simulated values (blue curves)

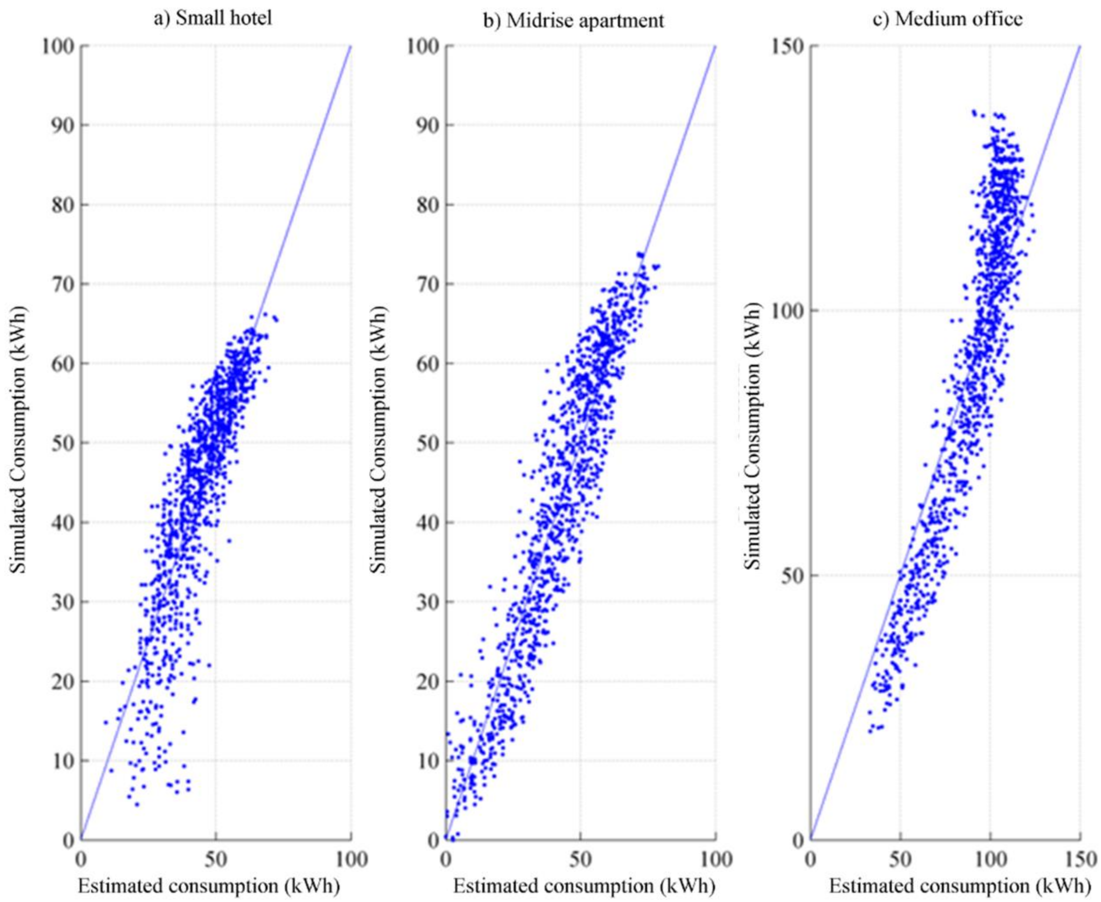


Figure 37 Scatterplots of estimated versus simulated consumption values for $\mathbf{E_{HVAC}}$

### 4.3.2 Lighting and Equipment Models

In this section, the lighting and equipment models for three building types, namely small hotel, mid-rise apartment, and medium office are described. These models will be eventually fed to the multi-objective optimization problem in order to adjust both lighting and equipment schedules. For the building with industrial load, such models are not considered due to the assumption of uncontrollable load. One way for calculating lighting and equipment loads is based on zonal operation schedules and total floor areas as in (3) and (4). This method is widely applied in energy simulation tools, such as EnergyPlus.

$$E_{LGHT}^{\phi}(t) = \sum_{z=1}^{Z(\phi)} PC_{LGHT}^{z} \times A_z \times SCH_{Z}^{\phi,LGHT^{0}}(t) \tag{3}$$

$$E_{EQPT}^{\phi}(t) = \sum_{z=1}^{Z(\phi)} PC_{EQPT}^{z} \times A_z \times SCH_{Z}^{\phi,EQPT^{0}}(t) \tag{4}$$

$$E_{\gamma}^{\phi}(t) = \sum_{z=1}^{Z(\phi)} \gamma_z \times SCH_{Z}^{\phi,\gamma^{0}}(t) \tag{5}$$

where, PC is the constant power consumption per square footage [$W/ft^2 \sim 0.092\ W/m^2$], $A_z$ is the zonal square footage, and $SCH_{Z}^{\phi,\gamma^{0}}$ is the predefined hourly schedule. One may consider them as a percentage of lights and equipment that are being used at each time step. Since in EnergyPlus Input Data Files (IDF), zonal areas are not provided, the lighting and equipment electricity consumptions are regressed against zonal operational schedules. This transforms equations (3) and (4) to the linear regression models as shown in (5).

### 4.3.3 Characteristics of the Building with Industrial Load (Uncontrollable Building)

As mentioned before, in this study a building with uncontrollable industrial load is considered. Daily electricity consumption profiles as well as a boxplot for such building are demonstrated in Figure 38 (electricity consumption data is adopted from [126]). It is observed that large industrial loads randomly occurred (peak loads) in the following hours: 9:00 a.m. – 10:00 a.m., 2:00 p.m. – 4:00 p.m. and 6:00 p.m. –7:00 p.m. Such large industrial loads are often uncontrollable and cannot be either shifted or curtailed. This is because such loads are consumed by large industrial equipment that typically work based on a set of internal schedules and are not necessarily controlled by the building manager. For example, in a university campus, students may use a large heater in a mechanical lab, which lead to large stochastic loads over time. The schedule of the mechanical lab is not supervised by the building manager. To overcome this problem, a statistical method called non-parametric bootstrapping method is used to estimate the sample distribution of hourly loads. In non-parametric bootstrapping method, a large number of bootstrapped samples e.g., 1000 with replacement are drawn from a population made up of the sample data. A sampling distribution for these two statistic measures is created by determining the mean and variance of each sample. It has been shown that by using non-parametric bootstrapping, the hourly sample mean distributions will be symmetric (see Figure 39) [131]. Using non-parametric bootstrapping will lead to hourly sample mean distributions, which are symmetric. This is demonstrated in Figure 39. In addition, it can significantly decrease the variance of the estimated values and provides more precise results.

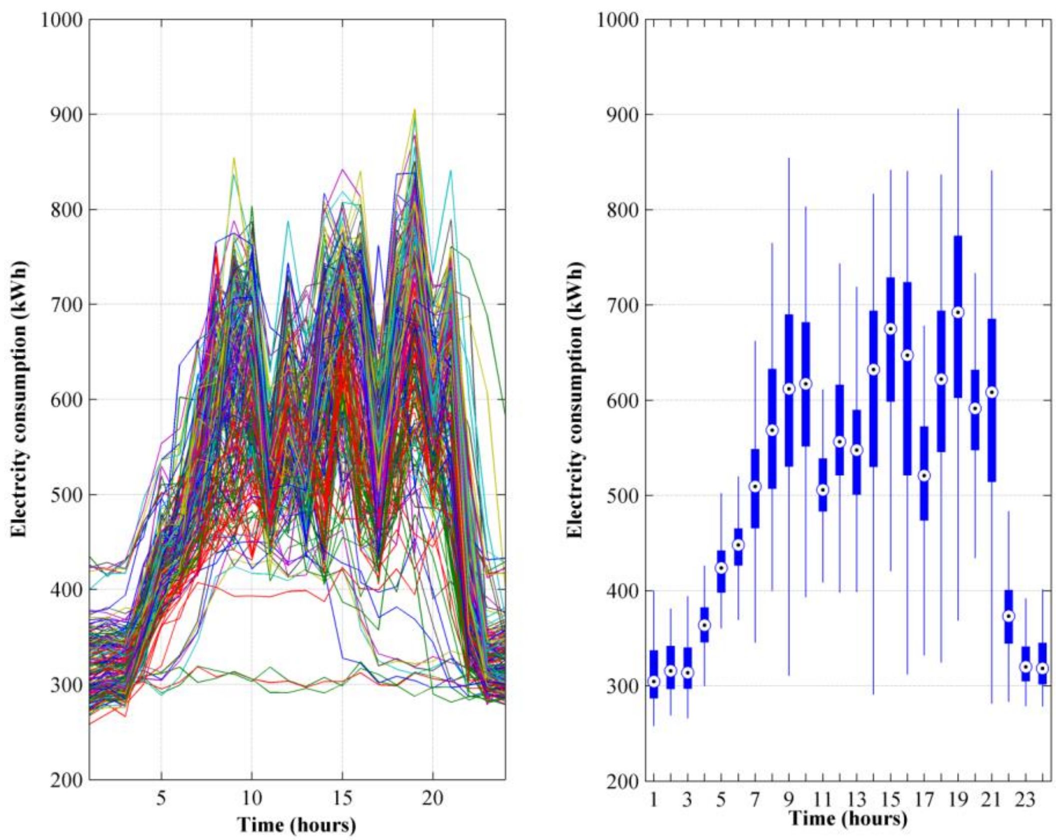


Figure 38 Daily electricity consumption profiles (left), Boxplot of hourly electricity consumption (right)

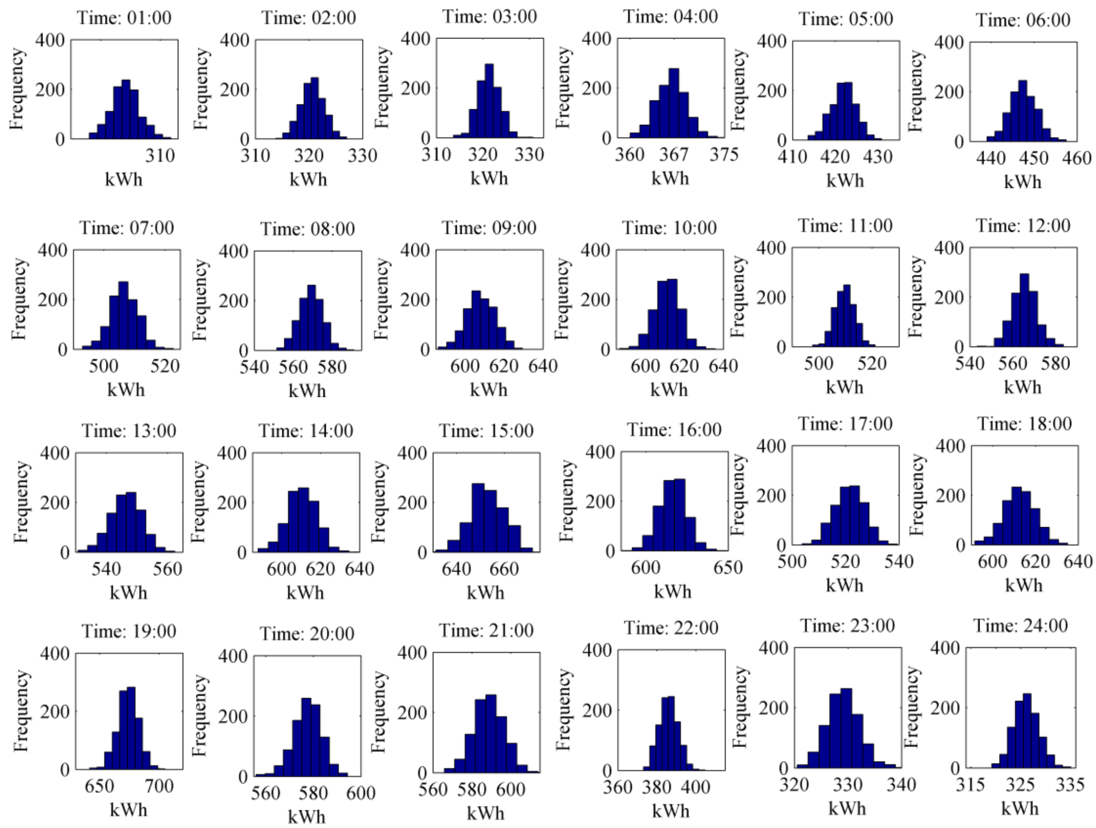

Figure 39 Hourly sample mean distributions of electricity consumption in a building with industrial load

### 4.3.4 Energy Market Dynamics

In this chapter, publicly available energy market data provided by Pennsylvania-New Jersey-Maryland (PJM) interconnection [132] is utilized in order to investigate the dynamics of uncertain energy market. PJM coordinates the buying, selling and delivery of wholesale electricity and balances the needs of suppliers, wholesale customers and other energy market participants. In analogy, the energy market operation is similar to a stock exchange, with market participants establishing a price for electricity by matching supply and demand. The market uses locational marginal pricing (LMP) that reflects the value of the energy at the specific location and time it is delivered. LMP will be same across the entire grid until regional transmission congestion happens to effect prices.

The Energy Market consists of both Day-Ahead and Real-Time markets. The Day-Ahead Market is a forward market in which hourly LMPs are calculated for the next operating day based on generation supplies, demand bids, and scheduled bilateral transactions. The Real-Time Market is a spot market in which current LMPs are calculated at five-minute intervals based on the actual grid operating conditions. This study is focused on the hourly market data for the year of 2014. At the present day, the day-ahead market is used as the forecasted price and availability of perfect information is assumed (real-time market for day-ahead). In Figure 40, the hourly day-ahead market (green curves) is plotted for each month along with the monthly average (red curve).

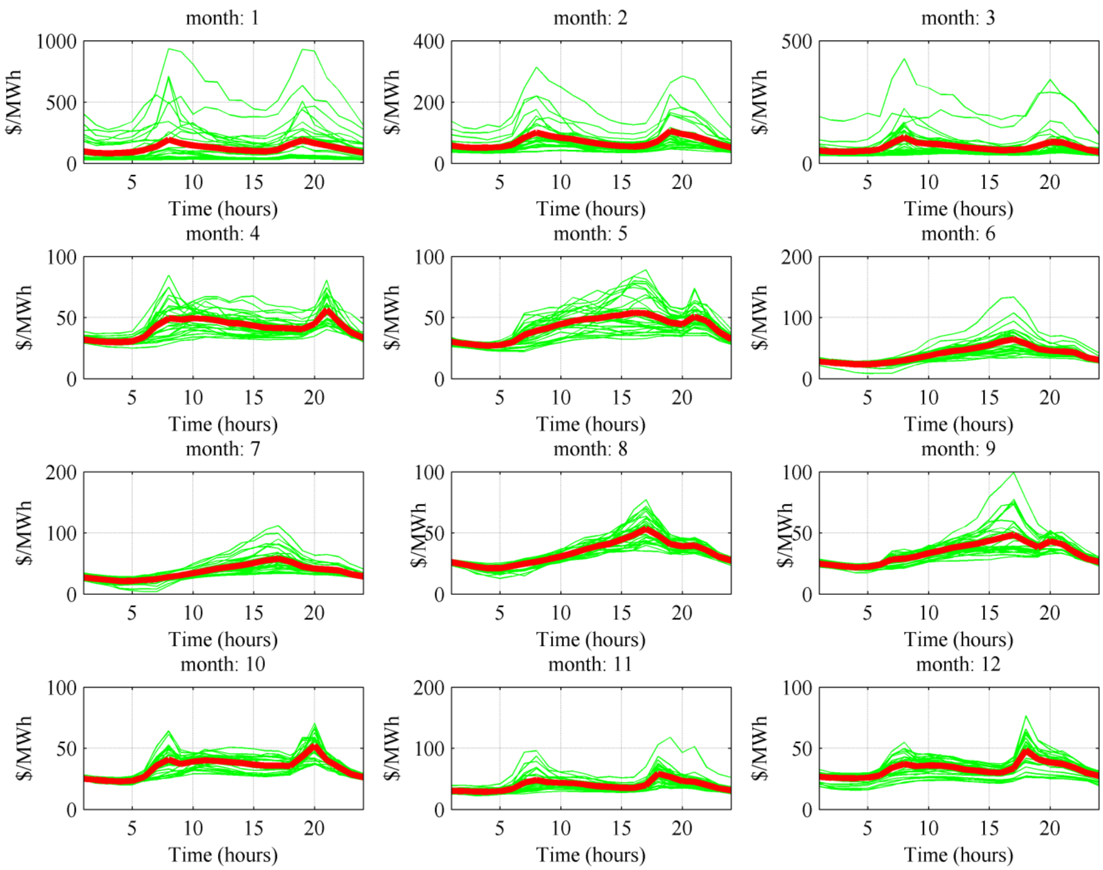


Figure 40 hourly day-ahead market (green curves) and monthly average (red curve)

From Figure 40, a clear trend in the day-ahead energy market can be observed. For months 1, 2, 3, 4, 10, 11, and 12 (non-summer) both morning and evening peaks happen. The Morning peak hour is consistent among non-summer months (8:00 a.m.) while evening peak ranges between 6:00 p.m. and 8:00 p.m. For months 5,6,7,8, and 9 (summer) only evening peak (at 5:00 p.m.) is observable. In the proposed day-ahead operational planning problem, Day-ahead Price (DAP) market data is used. Although DAP calculation methods are well-established and trustworthy, one should be cautious about price volatilities. Extreme price volatility, which can be up to two orders of magnitude higher than that of any other commodity or financial asset, forces energy market participants to hedge against price movements. Consumers who are able to forecast the volatile wholesale prices with a reasonable level of accuracy can adjust their bidding strategy and their consumption schedule in order to reduce the risk of system failures and/or maximize the profits in the day-ahead trading [133]. With the assumption that actual market data (RTP) is available, incorporating price volatility (Real Time Price (RTP) vs. Day Ahead Price (DAP)) into day-ahead planning is the point of interest. In Figure 41, one can observe the deviation of RTP from DAP in both summer and non-summer months. It is noticeable that the larger variation happens during peak hours, such as8:00 a.m. and 7:00 p.m. for non-summer months (Figure 41.a) and 5:00 p.m. for summer months (Figure 41.b).

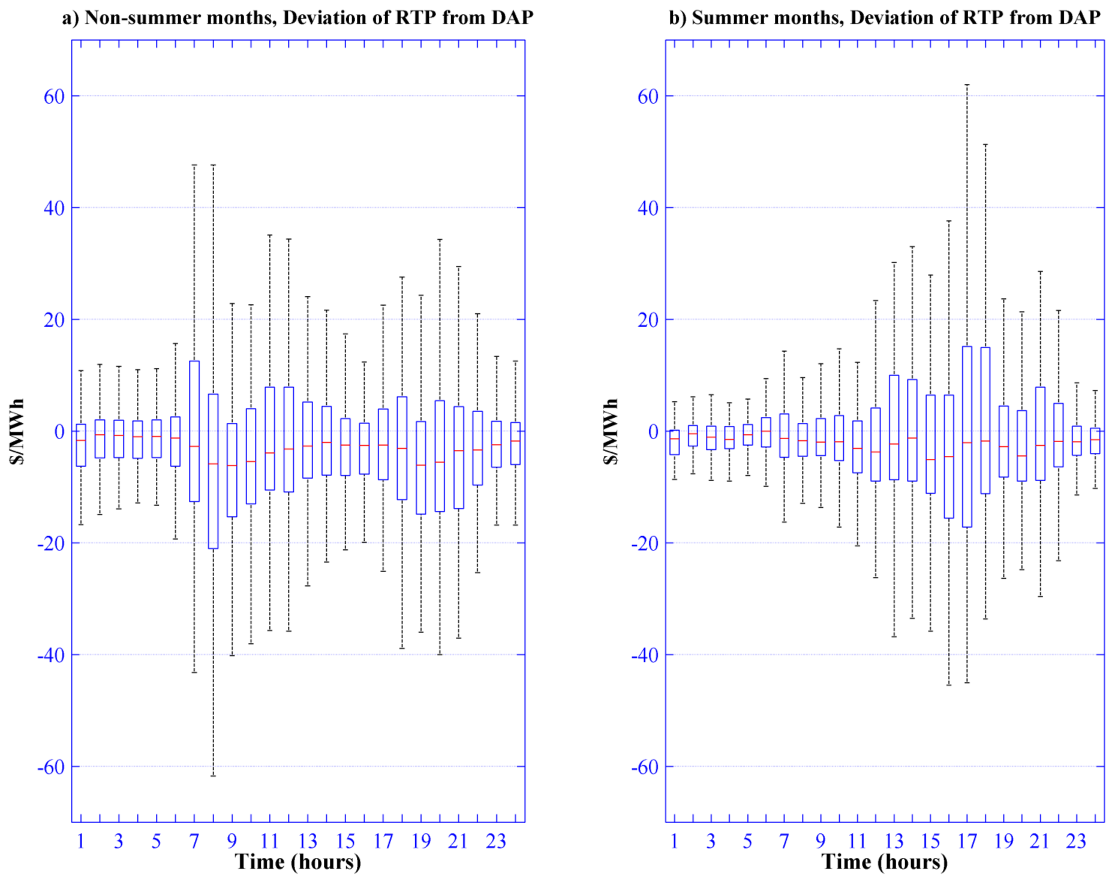


Figure 41 Deviation of RTP from DAP in both summer and non-summer months

### 4.3.5 Multi-objective Problem

The multi-objective problem of interest is to simultaneously minimize the total cost of electricity ($f_1$) and the occupant discomfort ($f_2$) as shown in the following equation:

$$\text{minimize}\{f_1(x), f_2(x)\}, \quad \text{s.t } x \in \Omega \tag{6}$$

where $\Omega$ is the feasible region and $f_1$ and $f_2$ along with operational constraints are defined as below:

$$f_1 \sim P^{\mathrm{DAP\ or\ RTP}} \times \sum_{\phi} \sum_{T} E^{\phi}_{HVAC}(t) + E^{\phi}_{LGHT}(t) + E^{\phi}_{EQPT}(t) \tag{7}$$

$$f_2 \sim \sum_{\phi} \sum_{\gamma=LGHT,EQPT} \sum_{Z} \sum_{T} (SCH_Z^{\phi,\gamma^0}(t) - SCH_Z^{\phi,\gamma^M}(t))^p . O_Z^{\phi}(t) \tag{8}$$

$E^{\phi}_{HVAC}$, is presented in (1) $E^{\phi}_{LGHT}$, $E^{\phi}_{EQPT}$ are also represented by (3), (4), respectively.

$$LB \le T_i^{z,\phi} \le UB \tag{9}$$

$$SRL \times SCH_Z^{\phi,\gamma^0} \le SCH_Z^{\phi,\gamma^M} \le SCH_Z^{\phi,\gamma^0} \tag{10}$$

In principal, electricity consumption can be shifted or curtailed at each time interval via:

1) Building thermal storage: This refers to pre-cooling capability. According to (4) and the lower and upper bounds of temperature (9), HVAC pre-cools the building (if any) with respect to building internal parameters (e.g., occupancy, internal zonal temperatures) and exogenous parameters such as ambient temperature and energy market.

2) Lighting and equipment adjustments: Electricity consumption of both lighting and equipment may be curtailed by modifying predefined schedules. Schedule modification takes into account zonal occupancy and occupant comforts (each zone in each building has its own schedule and occupancy pattern).

The weighted sum method is used which allows the multi-objective optimization problem to be cast as a single-objective mathematical optimization problem. This single objective function is constructed as a sum of objective functions $f_i$'s multiplied by weighting coefficients $w_i$'s. Hence, the problem (6) is reformulated to:

$$\begin{array}{l} \text{minimize} \sum_{i=1}^{k} w_i f_i(x), \\ \quad \text{s.t } x \in \Omega \end{array},$$

$$w_i \geq 1, \forall i = 1, \ldots, k \text{ and } \sum_{i=1}^{k} w_i = 1 \tag{11}$$

Under the convexity assumptions, the solution to (11) is Pareto optimal (the solution is unique if the problem is strictly convex). Decision maker (DM) often assigns weights of objective functions based on the intrinsic knowledge of the problem. However, as different objective functions can have different magnitude, normalization of objectives is required to get a Pareto optimal solution consistent with the weights assigned by the DM. The weights are computed as $w_i = u_i \Theta_i$ where $u_i$'s are the weights assigned by the DM and $\Theta_i$'s are the normalization factors. Normalization factors are calculated using utopia ($z_i^*$) and nadir points ($z_i^N$). The former is the lower bound of the Pareto optimal set, while the latter is the upper bound of the Pareto optimal set (see [134] for more details on normalization in multi-objective optimization). It should be noted that, the differences of optimal function values in the nadir and utopia points gives the length of the intervals where the optimal objective functions vary within the Pareto optimal set. That being said, one could calculate the normalization factors as follows:

$$z_i^* = f_i(x^{[i]}) = \text{argmin}_x\{f_i(x): x \in \Omega\} \tag{12}$$

$$z_i^N = \max_{1 \le j \le k} f_i(x^{[j]}), \forall i = 1, \dots, k \tag{13}$$

$$\Theta_i = {}^{1}/_{z_i^N - z_i^*}. \tag{14}$$

Pareto optimal sets for our optimization problem are illustrated in Figure 42. Any point on the Pareto frontier curve (contract curve) suggests that there is no better solution without compromising either of the objective functions. Hereafter, it is assumed that intrinsic knowledge of the problem exists: $w_1 = 0.59$ , $w_2 = 0.41$ .

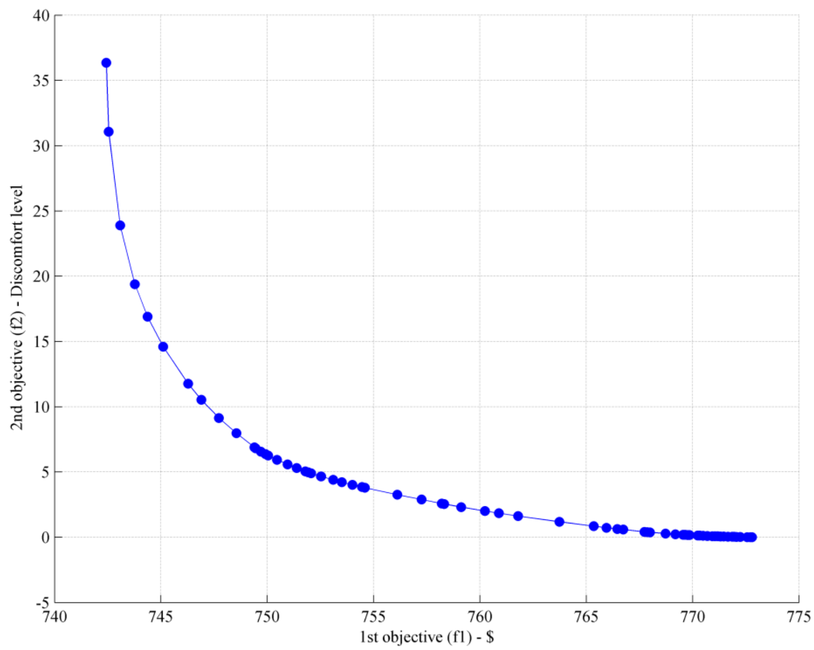


Figure 42 Pareto optimal sets

### 4.3.6 Day-ahead Operational Plans

In this section, first the effect of real-time price deviation from day-ahead price on operational plans and on responded load is investigated. Then the proposed approach to consider such price deviation into day-ahead operational planning problem will be explained.

#### 4.3.6.1 Effect of RTP Deviation from DAP

Figure 41 depicts the deviation of RTP from its forecasted values (DAP). The underlying causes of such variation are barely predictable due to their stochastic nature. The known causes are sudden outages e.g., generator, transmission outages, extreme weather conditions, and imbalance between generation and demand [135]. Market tries to motivate costumers to adjust their load according to these unexpected price variations. The larger the magnitudes of these variations are, the more load adjustment is needed. Due to this reason, elasticity in operational schedules is needed in order to for portfolio managers respond to new price signals and adjust load accordingly. To demonstrate the need of such elasticity in operational schedules, a day-ahead price profile for one summer day is picked and the variance of all real-time price profiles (153 days) against the selected day-ahead profile ($\mathrm{Var} = \widehat{\mathrm{E}}\left[\left(\mathrm{RTP}_{\mathrm{d,t}} - \mathrm{DAP}_{*,\mathrm{t}}\right)^2\right] - \widehat{\mathrm{E}}\left[\left(\mathrm{RTP}_{\mathrm{d,t}} - \mathrm{DAP}_{*,\mathrm{t}}\right)\right]^2$) is computed.

Var is used as a measure of RTP deviation form DAP. The results are provided in Figure 43. In this figure, the average optimal operational schedules of three buildings in response to real-time prices are presented. Each pixel represents an hour of the day. The reference colors for the temperature set-points (26°C) and the lighting/equipment schedule (0% reduction) are red and blue, respectively. The first row is the operational plan with the selected day-ahead price ($DAP_{*,t}$). It can be observed that by increasing the Var (moving upward in y-axis), the number of pixels in each line that have different colors than the reference color increases. This effect is more pronounced in the lighting and equipment schedules (The middle and right sections of Figure 43) than in the temperature set points. If such adjustment does not happen among end-uses, the real-time needs of the network would not be satisfied. In other words, the reliability of the whole system might be jeopardized.

Load management would be more effective if one could accurately predict the magnitude of the price variation. This would afford opportunities to plan the load adjustment accordingly in advance (day-ahead) instead of dealing with it in the real-time or near real-time bases. As mentioned earlier, the price variation and its magnitude are hardly predictable due to stochastic nature of underlying causes. Instead, inclusion of the price variability trend into decision making is suggested. For example, by looking at Figure 41, one may observe a systematic pattern in the price variation: larger variations occur around peak hours for both summer and non-summer months (summer: at times 3:00 p.m. – 6:00 p.m., and non-summer: at times 7:00 a.m. – 9:00 a.m. and 6:00 p.m. – 9:00 p.m.).

Foreseeing such systematic variation in conjunction with forecasted prices (DAP) in day-ahead planning, may provide an ability to accommodate real-time network needs (PHR, OLR, LF enhancement) better than by just utilizing forecasted process in day-ahead planning. Figure 44 shows the load response to both Day Ahead Price (DAP) and Real Time Price (RTP) for six different days. In this figure, the red solid and red dotted curves represent DAP and RTP respectively. The blue solid curve is the load response to

DAP. This is the solution of (6) where $P^{DAP}$ is utilized in (7). On the other hand, the blue dotted curve is the load response calculated by substituting $P^{RTP}$ with $P^{DAP}$ in (7). In this case, one may observe the unexpected spikes in RTP. Almost in all spike events, the shift of the load as the result of the pre-cooling is observed. However, no more curtailment in these events is detected. This is due to our defined lower limit for both the lighting and equipment schedule, which has already been achieved in DAP-based operational plans. By relaxing this assumption, one may experience both further load curtailment and load shift in host of RTP spikes.

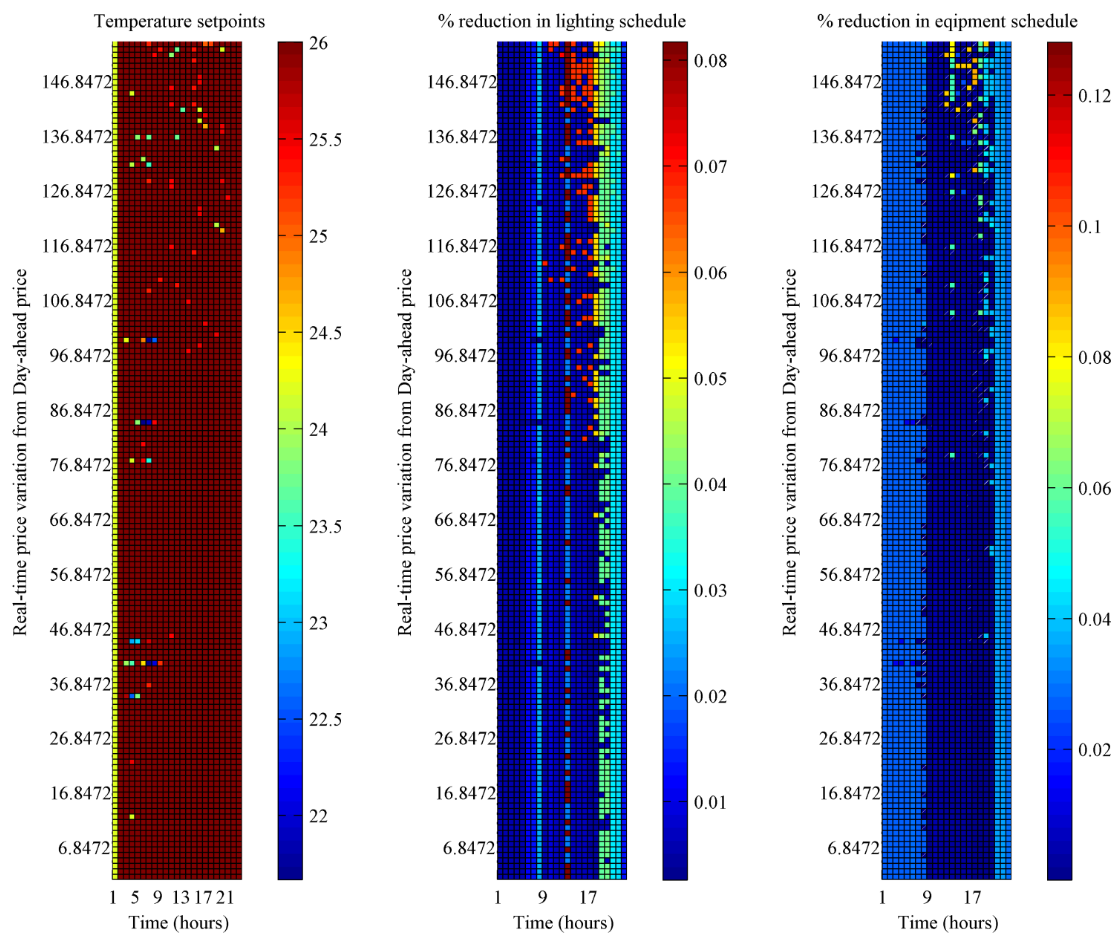


Figure 43 Impact of **Var** on average optimal operational schedule of three buildings

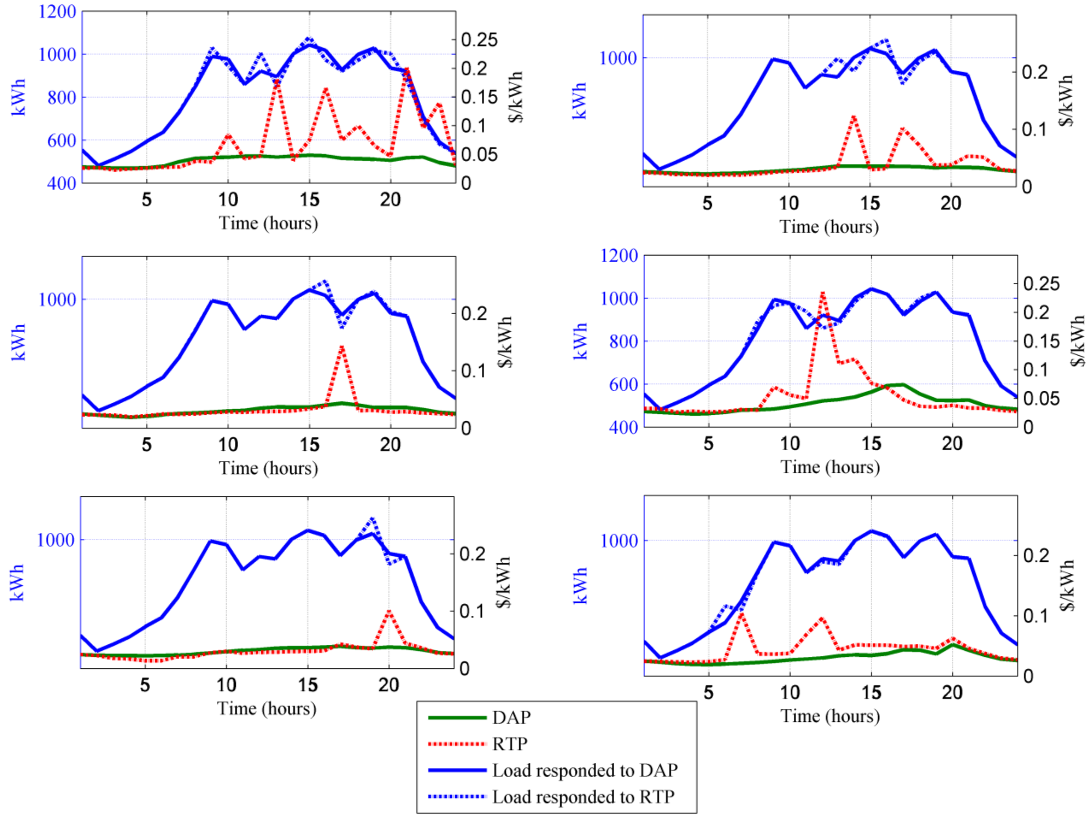


Figure 44 Responded load to both DAP and RTP for six different days

4.3.6.2 Incorporating Price Deviation into Day-ahead Operational Planning Problem

In this section, two new pricing schemes which can be used in day-ahead planning instead of using DAP are proposed. These schemes are namely; DAP&ED, and DAP&SSD. The former adds the expected market uncertainty trend to DAP schemes ($\widehat{\mathrm{E}}\left[\mathrm{RTP}_{\mathrm{d,t}} - \mathrm{DAP}_{\mathrm{d-1,t}}\right]$) while the latter includes standard deviation of market uncertainty trend into DAP schemes ($\sqrt{\widehat{\mathrm{E}}\left[\left(\mathrm{RTP}_{\mathrm{d,t}} - \mathrm{DAP}_{\mathrm{d-1,t}}\right)^2\right] - \widehat{\mathrm{E}}\left[\mathrm{RTP}_{\mathrm{d,t}} - \mathrm{DAP}_{\mathrm{d-1,t}}\right]^2}$). In both schemes, we conducted normalization in order to add expected value and standard deviation to DAP schemes:

$$\mathrm{DAP\&ED}_{d-1,t} = \frac{\mathbf{v}=(\mathrm{DAP}_{d-1,t}+\hat{\mathrm{E}}[\mathrm{RTP}_{d,t}-\mathrm{DAP}_{d-1,t}])-\min \mathbf{v}_{\forall t=t,\ldots,T}}{(\max \mathbf{v}-\min \mathbf{v})_{\forall t=t,\ldots,T}} \tag{15}$$

$$\mathrm{DAP\&SDD}_{d-1,t} = \frac{\mathbf{w}=(\mathrm{DAP}_{d-1,t}+\sqrt{\hat{\mathrm{E}}\left[(\mathrm{RTP}_{d,t}-\mathrm{DAP}_{d-1,t})^2\right]-\hat{\mathrm{E}}[\mathrm{RTP}_{d,t}-\mathrm{DAP}_{d-1,t}]^2})-\min \mathbf{w}_{\forall t=t,\ldots,T}}{(\max \mathbf{w}-\min \mathbf{w})_{\forall t=t,\ldots,T}} \tag{16}$$

In order to investigate the daily performance of different pricing schemes, multi-objective optimization is solved for price regimes namely; $\mathrm{DAP}_{d-1,t}$, $\mathrm{DAP\&ED}_{d-1,t}$, $\mathrm{DAP\&SDD}_{d-1,t}$. Responded loads are then compared with the case that load is responded to $\mathrm{RTP}_{d,t}$. As mentioned earlier, three performance indicators namely; PHR, OLR, and LF enhancement are considered in the comparison of different pricing schemes.

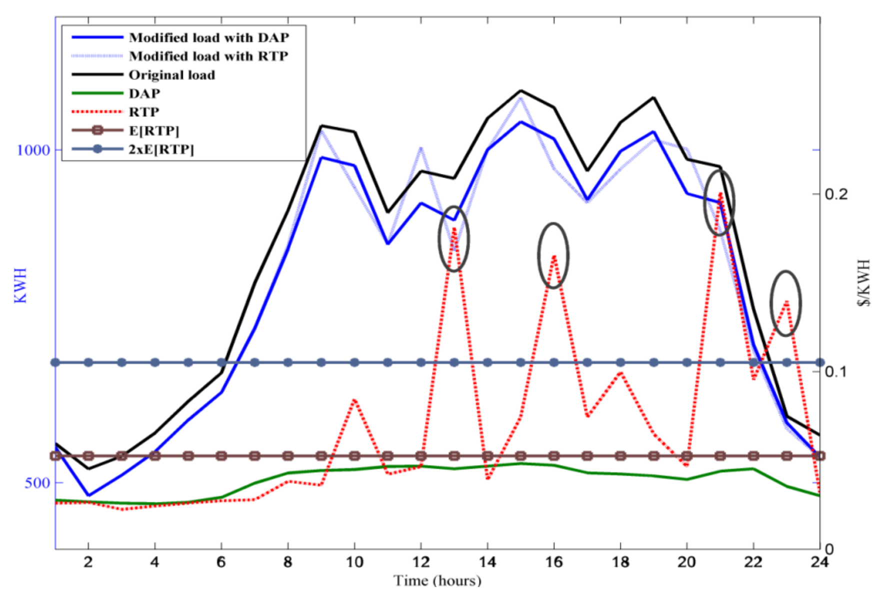


Figure 45 Illustration of candidate hours in PHR measure test

In the comparison test-bed, three measures are considered namely: peak hour reduction (PHR), overall load reduction (OLR), and daily load factor (LF) enhancement.

The latter refers to average daily load divided by the daily peak load. For all summer days, the multi-objective problem is solved for different price schemes. Given $d^{th}$ day, these are operational plans under following schemes: i) $RTP_d$, ii) $DAP_{d-1}$ iii) $DAP\&ED_{d-1}$ and iv) $DAP\&SDD_{d-1}$. For the peak hour reduction (PHR) measure, the hours where sudden spikes are realized in RTP are that of interest. In fact, these are moments (hours) that power network is under the stress. It is assumed that these are the hours where $RTP_t$'s are α times greater than the expected value of daily real-time prices).

$$\arg(RTP_t > \alpha \times \hat{E}[RTP]: t \in \{t = 1 \ldots T\}) \tag{17}$$

Here it is assumed that α=2. In Figure 45, hours that meet criteria in (17) are highlighted. Under each price scheme, the percentage of load reduction (R) for all candidate hours is calculated. To compare the performances, scatterplots as appeared in Figure 46 are constructed where in all of the subplots, x-axis corresponds to $R_{RTP}$ and y-axis corresponds to $R_{DAP}$,$R_{DAP\&ED}$, $R_{DAP\&SDD}$ respectively from left to right. OLR and LF calculations are on daily basis while PHR calculation is hourly (In Figure 46-a, each dot represents an hour while in 46-b and 46-c, each dot represents a day). In Table 15, statistics from Figure 46 in terms of percentage of points (%P) are provided. Considering the upper left subplot in Figure 46, these are percentage of points located above or beyond of $y = x$. Points above the line indicate superior performance of the scheme represented in y-axis than that's of x-axis and vice versa. As an example, in Figure 46-a, it is demonstrated that in terms of PHR using RTP surpasses DAP (Figure 46-a (Left)) while DAP&ED, and DAP&SSD surpass RTP (Figure 46-a (Middle)) and (Figure 46-a (Right)) respectively.

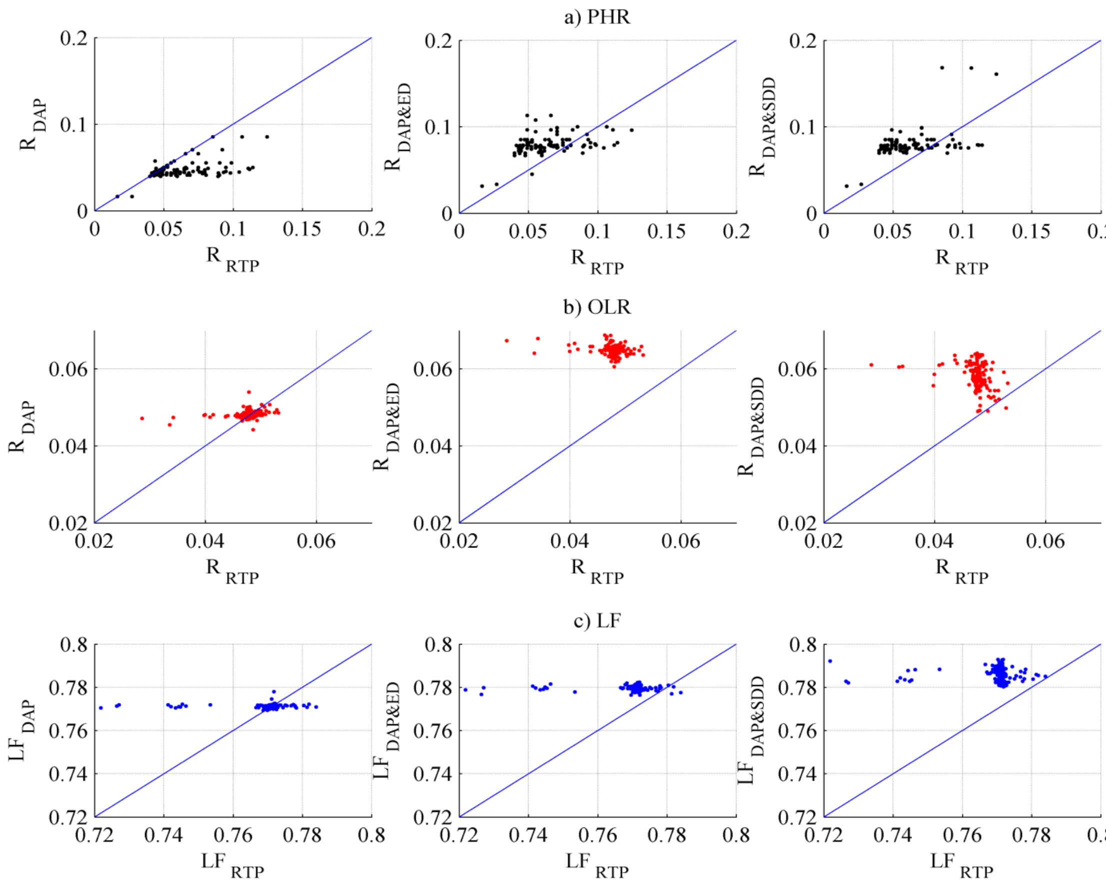


Figure 46 Scatterplot of PHR, OCL, and LF (blue curve: y=x)

Table 15 PHR, OLR and LF under all pricing schemes

| | | |
|---|---|---|
| Percentage of peak hour reduction | | |
| $\%P_{R_{DAP}> R_{RTP}}$ | $\%P_{R_{DAP\&ED}> R_{RTP}}$ | $\%P_{R_{DAP\&SDD}> R_{RTP}}$ |
| 30.9 | 93.4 | 94.5 |
| Percentage of overall load reduction | | |
| $\%P_{R_{DAP}> R_{RTP}}$ | $\%P_{R_{DAP\&ED}> R_{RTP}}$ | $\%P_{R_{DAP\&SDD}> R_{RTP}}$ |
| 62 | 100 | 96 |
| Load factor | | |
| $\%P_{LF_{DAP}> LF_{RTP}}$ | $\%P_{LF_{DAP\&ED}> LF_{RTP}}$ | $\%P_{LF_{DAP\&SDD}> LF_{RTP}}$ |
| 55.5 | 97 | 100 |

## 4.4 Discussions

In this research, a HVAC estimation model proposed in earlier work [137] is extended to improve the model robustness as well as practicality. The extension is made at three fronts: (i) One regression model relates the energy consumption to both exogenous and internal parameters. In a two-stage algorithm proposed in [137], an intermediate variable called sensible cooling/heating rate ($\dot{R}$) is estimated. The calculated $\dot{R}$ is used as an independent variable in the second model for estimation of HVAC energy consumption. $\dot{R}$ represents the sensible cooling/heating rate that is actually supplied by the system to the zone for the reported time step. From the practical point of view, developing a model independent of $\dot{R}$ is of great interest. This is because although $\dot{R}$ is available in energy simulation tools e.g., EnergyPlus, it is not necessarily practical to collect and measure such data in real buildings. (ii) In contrast to [136, 137] which focus on only one specific building, the proposed model is more robust and is tested and validated on multiple buildings with different use types. (iii) The time dependent effects are captured using mathematically meaningful variables (dummy time indicator variables) in [137]. In this work, real measure such as hourly building occupancy percentage is used instead of dummy variables.

In terms of day-ahead operational plans, one may observe a peak reduction from 5 to 10% and an overall load shedding of 4 to 6% for all pricing schemes. One may argue that such tiny figures are not significant. This is not true; in particular considering the total investment need for the electricity grid infrastructure worldwide until 2035 is estimated by the International Energy Agency (IEA) to be of the magnitude of $17 trillion [138].

Reducing or deferring only 1 % of this need would still affect an investment volume of \$170 billion.

In terms of the performance and effectiveness of different pricing schemes, Table 16 shows using either the proposed DAP&ED or DAP&SDD schemes results in load responses which can better satisfy all three demand management goals (PHR, OLR, and LF). It is demonstrated that for LF and PHR, the performance of DAP&SDD is superior to DAP while for OLR, DAP&ED outcomes are more suitable load responses. One cautionary note is that these observations are based on the presented case study and the results are not general. The main message out of this research is that if day-ahead planning incorporates insights about future market trends (Deviation of RTP from DAP), this can result in load responses which simultaneously satisfy power network needs and demand management aims better than just using the forecasted market data.

The models developed in this research can be improved in several ways. The proposed regression models can be significantly improved by considering the interaction between independent variables. To avoid the non-linearity in our mathematical programming, we did not incorporate such interaction. Furthermore, in the multi-objective framework, the defined penalty function for occupants discomfort can be more thoroughly investigated by using different functional forms.

## 4.5 Conclusion and Future Works

In this study, the day-ahead operational plans for a portfolio of multi-buildings are evaluated by experimenting with incorporating market uncertainty trend into the day-ahead planning. The portfolio of interest consists of two groups of buildings: controllable and uncontrollable. The load responses in the proposed pricing schemes are compared to the load responses where only Day-Ahead pricing scheme is considered. Three demand-side management goals, peak hour reduction (PHR), overall load reduction (OLR), and daily load factor (LF) enhancement, are considered as performance metrics. Hybrid physics-based and statistical models for HVAC system is developed along with models for lighting and electronic equipment for this purpose. The operational plans are generated by solving a multi-objective mathematical programming problem in which the objectives are minimal operational expenditure and minimal occupants' discomfort by considering variables related to building, market, and weather information. This research shows the day-ahead operational plans under the proposed pricing schemes result in 5% to 10% peak reduction and the overall load shedding is in the range of 4% to 6%. It is demonstrated that incorporating available insights about market uncertainty into day-ahead planning can result in load responses which may help to manage the underlying load more rigorously than just using market forecasts the forecasted market data. It is demonstrated that incorporating available insights about market uncertainty trend into day-ahead planning can lead to a load management strategies with higher performance than just using market forecasts. One direction for the future work is analysis and investigation of drivers that encourage companies and building owners to adopt efficiency improvements and sustainability policies. The other direction is inclusion of electricity storage network for building portfolio. One aspect of such study could be the dynamics and interaction between system of storages, and the other would be cost and benefit analysis. This could be in terms of comparing incentive-based programs to encourage occupants to consume accordingly e.g. according to utility signals to investing on electricity storage devices.

## ELSEVIER LICENSE
## TERMS AND CONDITIONS

Jul 05, 2016

This Agreement between farbod farzan ("You") and Elsevier ("Elsevier") consists of your license details and the terms and conditions provided by Elsevier and Copyright Clearance Center.

| | |
|---|---|
| License Number | 3902420460941 |
| License date | Jul 05, 2016 |
| Licensed Content Publisher | Elsevier |
| Licensed Content Publication | Energy and Buildings |
| Licensed Content Title | Operational planning for multi-building portfolio in an uncertain energy market |
| Licensed Content Author | Farbod Farzan,Seyed A. Vaghefi,Khashayar Mahani,Mohsen A. Jafari,Jie Gong |
| Licensed Content Date | 15 September 2015 |
| Licensed Content Volume Number | 103 |
| Licensed Content Issue Number | n/a |
| Licensed Content Pages | 13 |
| Start Page | 271 |
| End Page | 283 |
| Type of Use | reuse in a thesis/dissertation |
| Intended publisher of new work | other |
| Portion | full article |
| Format | both print and electronic |
| Are you the author of this Elsevier article? | Yes |
| Will you be translating? | No |
| Order reference number | |
| Title of your thesis/dissertation | Dynamic demand modeling, energy management, and investment strategies in uncertain energy markets |
| Expected completion date | Jul 2016 |
| Estimated size (number of pages) | 160 |
| Elsevier VAT number | GB 494 6272 12 |
| Requestor Location | farbod farzan<br>1507 azalea drive<br><br>NORTH BRUNSWICK, NJ 08902<br>United States<br>Attn: farbod farzan |

References

[1] F. Farzan,S.Lahiri,M. Kleinberg,K. Gharieh, F.Farzan, andM. Jafari, “Microgrids for fun and profit: The economics of installation investments and operations,” IEEE Power Energy Mag., vol. 11, pp. 52–58, Jul. 2013.

[2] Lasseter, R.H., A Akhil, C. Marnay, J Stephens, J Dagle, R Guttromson, A. Meliopoulous, R Yinger, and J. Eto, “The CERTS Microgrid Concept,” White paper for Transmission Reliability Program, Office of Power Technologies, U.S. Department of Energy, April 2002.

[3] R. L. Dohn, "The business case for microgrids - The new face of energy modernization," Siemens, 2011.

[4] World Energy Outlook 2010, International Energy Agency, ISBN: 978 92 64 08624 1

[5] P. Grahn, J. Munkhammar, J. Widén, K. Alvehag, and L. Söder, “PHEV Home-Charging Model Based on Residential Activity Patterns,” IEEE Transactions on Power Systems vol. 28, pp.2507, 2013.

[6] H. Chao, “Price responsive demand management for a smart gridworld,” Elsevier, The Electricity J., vol. 23, no. 1, pp. 7–20, 2010.

[7] Farzan, F,”Towards Uncertainty in Micro-grids: Planning, Control and Investment,” Ph.D. dissertation, Dept.Industrial & Systems Engineering, Univ. Rutgers, Piscataway, NJ 08854, 2013.

[8] T. Hoff, “Identifying distributed generation and demand side management opportunities” The Energy Journal 17 vol.4,1996.

[9] M. Albadi, E. El-Saadany, “A summary of demand response in electricity markets,” Electric Power Systems Research vol.78, 2008.

[10] Woo C, Greening L. Guest editors’ introduction. Energy April 2010;35(4).Demand response resources: the US and International Experience.

[11] US DOE, “Benefits of Demand Response in Electricity Markets and Recommendations for Achieving Them,” Report to the US Congress., Feb.2006. Available: http://eetd.idi.gov.

[12] Poudineh R, Jamasb T, “Distributed Generation, Storage, Demand Response and Energy Efficiency as Alternatives to Grid Capacity Enhancement,” Energy Policy vol.67, pp. 222–231, 2014.

[13] A. B. Philpott and E. Pettersen, “Optimizing demand-side bids in dayahead electricity market,” IEEE Trans. Power Syst., vol. 21, no. 2, pp 88–498, May 2006.

[14] N. Motegi, M. A. Piette, D. S.Watson, S. Kiliccote, and P. Xu, “Introduction to commercial building control strategies and techniques for demand response,” Lawrence Berkeley National Laboratory, Berkeley, CA, May 2007 [Online]. Available: http://drrc.lbl.gov/pubs/59975.pdf.

[15] “Development and evaluation of fully automated demand response in large facilities,” Demand Response Research Center, CEC-500-2005-013, Jan. 2005 [Online]. Available: http://drrc.lbl.gov/pubs/CEC-500- 2005-013.pdf

[16] U.S. Energy Information Adminstration. (2012). Electricity; Detailed State Data. Avaialable: http://www.eia.gov/electricity/data/state/.

[17] G. Kassakian, “The Future of the Electric Grid,“ Massachusetts Institute of Technology., Massachusetts, 2011.

[18] J. R. Brodick, “U.S. Lighting Market Characterization,” Navigant Consulting, Inc. Washington DC, 2002.

[19] Electric Drive Transportation Association. (2014). Electric Drive Sales Dashboard. Available: http://electricdrive.org/index.php.

[20] J. Campillo, F. Wallin, D. Torstensson, “Energy Demand Model Design for Forecasting Electricity Consumption and Simulating Demand Response Scenarios in Sweden,” in International Conference on Applied Energy ICAE, Suzhou, China, 2012.

[21] V. Richard, “Demand Shaping: Achieving and Maintaining Optimal Supply and Demand Alignment,”Practice, 2010.

[22] L. G. Swan, V. I. Ugursal, “Modeling of End-use Energy Consumption in the Residential Sector: A Review of Modeling Techniques,” Renewable Sustainable Energy Rev., vol. 13, pp. 1819–1835, 2009.

[23] D. L. O’Neal, E. Hirst’ “An Energy Use Model of the Residential Sector,” IEEE Transactions on Systems, Man and Cybernetics vol.10, pp. 749-755, 1980.

[24] G. Raffio , O. Isambert , G. Mertz, C. Schreier, “Targeting Residential Energy Assistance,” In Proceedings of energy sustainability conference, pp. 489–95, 2007.

[25] R. A. Douthitt, “An Economic Analysis of the Demand for Residential Space Heating Fuel in Canada,” Energy vol.14, pp.187–97, 1989.

[26] D.J. Aigner, C. Sorooshian, P. Kerwin, “Conditional Demand Analysis for Estimating Residential End-use Load Profiles,” Energy vol.5, pp.81–97, 1984.

[27] D.W. Caves, J.A. Herriges, K.E. Train, “A Bayesian Approach to Combining Conditional Demand and Engineering Models of Electricity Usage,” Economics and Statistics vol.69, pp.438–48, 1987.

[28] M. Aydinalp, V.I Ugursal, A. Fung, “Modeling of the Appliance, Lighting, and Spac-ecooling Energy Consumptions in the Residential Sector Using Neural Networks,” Applied Energy vol.72, pp. 87–110, 2002.

[29] G. Mihalakakou, M. Santamouris, A. Tsangrassoulis, “On the Energy Consumptionin Residential Buildings,” Energy and Buildings vol.34, pp. 727–736, 2002.

[30] A. Capaso, W. Grattieri, R. Lamedica, “A Bottom-up Approach to Residential Load Modeling,” IEEE Transactions on Power Systems vol.9, pp. 957–64, 1994.

[31] R. Kadian, R.P Dahiya, H.P. Garg, “Energy-related Emissions and Mitigation Opportunities from the Household Sector in Delhi,” Energy Policy vol.35, pp. 6195-6211, 2007.

[32] N. Kohler, B. Schwaiger, B. Barth, M. Koch, “Mass Flow, Energy Flow and Costs of the German Building Stock,” 2nd International Conference on Buildings and the Environment, Paris, France, 1997.

[33] Y. Huang, J. Broderick J, “A Bottom-up Engineering Estimate of the Aggregate Heating and Cooling Loads of the Entire US Building Stock” Lawrence Berkeley National Laboratory, Berkely, CA. Report LBNL-46303, 2000.

[34] B. M. Larsen, R. Nesbakken, “Household Electricity End-use Consumption: Results From Econometric and Engineering Models,” Energy Economics vol.26, pp.179–200, 2004.

[35] R. Ramirez, F. Sebold, T. Mayer, M. Ciminelli, “A Building Simulation Palooza: The California CEUS Project and DrCEUS,” IBPSA, 9th International Conference, Montreal, Canada, pp. 1003–1010, 2005.

[36] I. Richardson, M. Thomson, D. Infield, “A High-resolution Domestic Building Occupancy Model for Energy Demand Simulations,” Energy and Buildings vol.40, pp.1560–1566, 2008.

[37] J. Widén , E. Wäckelgård , “A high-resolution Stochastic Model of Domestic Activity Patterns and Electricity Demand,” Applied Energy vol.87, pp. 1880–1892, 2010.

[38] M. Muratori, M. C. Roberts, R. Sioshansi, V. Marano, “A Highly Resolved Modeling Technique to Simulate Residential Power Demand,” Applied Energy, vol. 107, pp. 465–473, 2013.

[39] J. Aghaei, M. Alizadeh, "Demand response in smart electricity grids equipped with renewable energy sources: a review," Renewable Sustainable Energy Rev vol.18, pp.64-72, 2013.

[40] P. Cappers, C. Goldman, D. Kathan, "Demand Response in U.S. Electricity Markets: Empirical Evidence." Energy vol.35(4) , pp.1526–35, 2010.

[41] M. Muratori, CY. Chang, G. Rizzoni, W. Zhang," Dynamic Energy Management of a Residential Energy Eco-system." In: Proceedings of the ASME2013 dynamic systems & control conference, Oct 21-23, 2013.

[42] M. Muratori, CY. Chang, E. Serra, W. Zhang, G. Rizzoni, "Impact of Electricity Price Structures on Residential Demand Response," In: Proceedings of the26th international conference on ECOS, July 16-19, 2013.

[43] M. Muratori, BA. Schuelke-Leech, G. Rizzoni, "Role of Residential Demand Response in Modern Electricity Markets," Renewables and Sustainable Energy Reviews vol.33, pp. 546-553, 2014.

[44] A Conejo, J. Morales , L. Baringo, "Real-time demand response model," Smart Grid IEEE Trans vol.1(3), pp.236–42, 2010.

[45] U.S. Energy Information Administration, "Today in Energy" Available: http://www.eia.gov/todayinenergy/.

[46] S. M. Pandit, S. M. Wu, Time Series and System Analysis with Applications, Wiley, New York, 1983.

[47] D. S. Hamermesh, H. Frazis, J. Stewart, "Data Watch The American Time Use Survey," Economic Perspectives vol.19, pp. 221–232, 2005.

[48] Y. S. Chiou, "Deriving U.S. Household Energy Consumption Profiles from American Time Use Survey Data – A Bootstrap Approach," Eleventh International IBPSA Conference, Glasgow, Scotland, July 27-30, 2009.

[49] D. L. Coe, P. A. Ryan, L. R. Chinkin, "Weekday/Weekend Activity Patterns for Residential and small Commercial area Sources in Los Angeles," 11th Annual Emission Inventory Conference, April 16-18, Atlanta, Georgia, 2002.

[50] R. Curtin, Y. Shrago, J. Mikkelsen, (2009), Plug-in Hybrid Electric Vehicles, University of Michigan, Available: http://www.sca.isr.umich.edu/fetchdoc.php?docid=39427.

[51] J. Min, L. Azevedo, W. Bruin, "Labeling Energy Cost on Light Bulbs Lowers Implicit Discount Rates," Ecological Economics vol.97, pp.42–50, 2014.

[52] S. Attari, M. DeKay, C. Davidson, W. de Bruin, "Public Perceptions of Energy Consumption and Savings," In Proceedings of the National Academy of Sciences, 2010.

[53] Residential Energy Consumption Survey, Available: http://www.eia.gov/consumption/residential/data/2009/index.cfm.

[54] Appliances and Electronics, Available: http://energy.gov/public-services/homes/saving-electricity/appliances-electronics.

[55] S. Gail, R. De Dear, "Climate, Comfort & Natural Ventilation: A new adaptive comfort standard for ASHRAE Standard 55, Moving Thermal Comfort Standards into the 21st Century" Oxford Brookes University, Windsor, UK, 2001.

[56] C. Reinhart, "Lightswitch-2002: A Model for Manual and Automated Control of Electric Lighting and Blinds," Solar Energy vol.77, pp. 15–28, 2004.

[57] Green Building Operations and Maintenance Manual, Green Seal, Inc. Washington, D.C. Available: www.greenseal.org/Portals/0/Documents/IG/PHA%20Manuals/Chapter4_Green_Building_OM_Manual_PHA.pdf.

[58] U.S Department of Energy, "Reduce Hot Water for Energy Savings" Available: http://energy.gov/energysaver/articles/reduce-hot-water-use-energy-savings.

[59] U.S. Department of Transportation; Federal Highway Administration, "Drivers"Available: http://www.fhwa.dot.gov/policyinformation/pubs/pl08021/pdf/onh_chap4.pdf.

[60] P. Grahn, J. Munkhammar, J. Widén, K. Alvehag, L. Söder, "PHEV Home-Charging Model Based on Residential Activity Patterns," IEEE Transactions on Power Systems vol. 28, pp.2507, 2013.

[61] U.S. Department of Transportation; Federal Highway Administration, "Licensed Drivers by Age and Sex" Available: https://www.fhwa.dot.gov/ohim/onh00/onh2p4.htm

[62] J. Axsen, A. Burke, K. Kurani, “Batteries for Plug-in Hybrid Electric Vehicles (PHEVs): Goals and the State of Technology,” Institute of Transportation Studies University of California Davis, CA UCD-ITS-RR-08-14, 2008.

[63] A. Pesaran, T. Market, H. Tataria, D. Howell, “Battery Requirements for Plug-in Hybrid Electric Vehicles: Analysis and rationale,” 23rd Int. Elect. Veh. Symp. Expo, Anaheim, CA, 2007.

[64] U.S. Energy Information Administration, “Residential Energy Consumption Survey End-Use Models,” Available: http://www.eia.gov/consumption/residential/methodology/2009/pdf/faqs-enduse-models022013.pdf.

[65] EnergyPlus Energy Simulation Software, Weather Data, Available: http://apps1.eere.energy.gov/buildings/energyplus/cfm/weather_data3.cfm/region=4_north_and_central_america_wmo_region_4/country=1_usa/cname=USA.

[66] S. Schey, D. Scoffield , J. Smart, “A first look at the impact of electric vehicle charging on the electric grid in the evproject. In:26th Electric vehicle symposium (EVS-26), Los Angeles, 2012.

[67] A. Vaghefi, M.A. Jafari, E. Bisse, J. Brouwer, Y. Lu, “Modeling and Forecasting of Cooling and electricity load demand”, Applied Energy vol.136, pp. 186-196, 2014.

[68] Reprinted, with permission, from F Farzan, F Farzan, M Jafari, J Gong, Integration of demand dynamics and investment decisions on distributed energy resources, IEEE publication title, 2015

[69] H. Liang, W. Zhuang, "Stochastic Information Management in Microgrid Operations," IEEE Commun.Surveys & Tutorials, vol. 16, 2014.

[70] A. Bhattacharya, "Optimal Microgrid Energy Storage Strategies in the Presence of Renewables," Proc. of Ind. and Systs. Eng. Research Conf., 2014.

[71] F. Farzan, S. Lahiri, M. Kleinberg, K. Gharieh, F. Farzan, and M. Jafari, "Microgrids for fun and profit: The economics of installation investments and operations," Power and Energy Mag., IEEE, vol. 11, pp.52–58, 2013.

[72] US DOE, "Benefits of Demand Response in Electricity Markets and Recommendations for Achieving Them," Report to the US Congress., Feb.2006. Available: http://eetd.idi.gov.

[73] R. Poudineh , T. Jamasb, "Distributed Generation, Storage, Demand Response and Energy Efficiency as Alternatives to Grid Capacity Enhancement," Energy Policy vol.67, pp. 222–231, 2014.

[74] T.Hoff, "Identifying Distributed Generation and Demand-side Management Opportunities," Energy, vol.4, 1996.

[75] M. Albadi, F. El-Saadany, "Demand Response in Electricity Markets: An Overview", IEEE Power Eng. Society General Meeting, 2007.

[76] C. Woo, L. Greening “Demand response resources: the US and International Experience” Energy, vol.35 2010.

[77] F. Farzan, M A. Jafari, Micro-grid Portfolio Optimization Under Uncertainty, IEEE Trans. on SmartGrid, 2014.

[78] L. Costa L, G. Kariniotakis, “A Stochastic Dynamic Programming Model for Optimal Use of Local Energy Resources in a Market Environment,” IEEE Power Tech, Lausanne, pp. 449-454, 2007.

[79] P. Beraldi, D. Conforti, “A New Solution Approach for Nonlinear Stochastic Integer Programming Problems,: Technical Report; DOE; Informatics and Systems, University of Calabria, 2005.

[80] P. Beraldi, D. Conforti, A. Violi, “A Two-Stage Stochastic programming Model for Electric Energy Products”, Computers & Operations Research vol. 35, pp 3360-3370, 2008.

[81] https://analysis.nrel.gov/homer/.

[82] W. El-Khattam, K. Bhattacharya, Y. Hegazy,“Optimal Investment Planning for Distributed Generation in a Competitive Electricity Market,” IEEE Trans. Power Systs, vol. 19, pp. 1674-1684, 2004.

[83] T. Logenthiran, D. Srinivasan, “Optimal Capacity and Sizing of Distributed Energy Resources for Distributed Power Systems,” Renewable and Sustainable Energy vol.4, 2012.

[84] S. Bruno, S, “Optimization of Real Asset Portfolio using a Coherent Risk Measure: Application to Oil and Energy Industries,” Int. Conf. Eng Optimization, Rio de Janiero, Brazil, 2008.

[85] F. Farzan, F. Farzan, K. Gharieh, M. A. Jafari, and R. Masiello, “Closing the Loop between Short-term Operational Volatilities and Long-term Investment Risks in Microgrids,” ” In Proc. IEEE ISGT Conf., Feb. 2014.

[86] A. Siddiqui, M. Stadler, C. Marnay, and J. Lai, “Optimal Control of Distributed Energy Resources and Demand Response Under Uncertainty,” In Proc. Int. Assoc. for Energy Econ., June. 2010.

[87] P. Centolella,” The Integration of Price Responsive Demand into Regional Transmission Organization Wholesale Power Markets and System Operations”, Energy vol.35 ,pp.1568–1574, 2010.

[88] C. Cecati, C. Citro, A. Piccolo, and P. Siano,”Smart Grids Operation with Distributed Generation and Demand Side Management,” Modeling and Control of Sustainable Power Systems,pp.27-46.2012.

[89] B. Nordman, “Networks in Buildings” In Proc. ACEEE Summer Study on Energy Efficiency in Buildings, 2008.

[90] J. G. Roos and I. E. Lane, “Industrial Power DR Analysis for One Part Real-time Pricing,” IEEE Trans. on Power Syst., vol. 13, pp. 159-164, 1998.

[91] T. M. Calloway and C. W. Brice, "Physically-based Model of Demand with Applications to Load Management Assessment and Load Forecasting," IEEE Trans. on Power App. Syst., vol.101, pp. 4625-4631, 1982.

[92] T. Hubert, S. Grijalva, "Realizing Smart-grid Benefits Requires Energy Optimization Algorithms at Residential Level," In Proc. of IEEE Innovative Smart Grid Technologies (ISGT), pp. 1-8, 2011.

[93] G. Xiong, C. Chen, S. Kishore and A. Yener, "Smart (in-home) Power Scheduling for Demand Response on the Smart-grid," In Proc. of Innovative Smart Grid Technologies (ISGT), pp. 1-7, 2011.

[94] C. Liu, J. Wang, A. Botterud, Y. Zhou, A. Vyas, "Assessment of Impacts of PHEV Charging Patterns on Wind-Thermal Scheduling by Stochastic Unit Commitment" IEEE Trans. on SmartGrid, vol.3. 3, 2012.

[95] J. Ma, J. Deng, L. Song, Z. Han, "Incentive Mechanism for DSM in Smart Grid Using Auction", IEEE Trans. on SmartGrid, vol. 5, 2014.

[96] G. Costanzo, A. Zhu,"A System Architecture for Autonomous Demand Side Load Management in Smart Buildings" IEEE Trans. on SmartGrid, 2013.

[97] Outstanding Efficiency, Siemens Wind Turbine SWT-2.3-93, Available: http://www.energy.siemens.com/hq/pool/hq/power-generation/wind-power/E50001-W310-A102-V6-4A00_WS_SWT-2.3-93_US.pdf

[98] Environmental Protection Agency. (2008). "Technology Characterization:Fuel Cells," Available at: http://www.epa.gov/chp/documents/catalog_chptech_fuel_cells.pdf

[99] F. Farzan, K. Mahani, M. A. Jafari, F. Farzan, and W. Katzenstein, "A Simple Approximate Approach to Optimal Sizing and Investment Timing of Distributed Energy Resources". In Press 18th Real Option group Conference, Medellin Colombia, 2014.

[100] R. Walawalkar, S. Fernands, N. Thakur, K. Chevva, "Evolution and Current Status of Demand Response (DR) in Electricity Markets: Insights from PJM and NYISO," Energy vol.35, 2010.

[101] F. Farzan, M. A.Jafari, J. Gong, F. Farzan, A. Stryker, "A Multi-Scale Adaptive Model of Residential Energy Demand" Applied Energy vol.150 pp. 258-273, 2015.

[102] Air Pollution Control Technology Fact Sheet, EPA-452/F-03-009, Available: http://www.epa.gov/ttn/catc/dir1/fscr.pdf

[103] R. Poore, and C. Walford, "Development of an Operations and Maintenance Cost Model to Identify Cost of Energy Savings for Low Wind Speed Turbines," In: Subcontract Report, NREL/SR-500-40581, 2008.

[104] Catalog of CHP Technologies,U.S. Environmental Protection Agency, Available at: http://www.epa.gov/chp/documents/catalog_chptech_full.pdf.

[105] F Farzan, A Vaghefi, K Mahani, M Jafari, J Gong, "Operational planning for multi-building portfolio in an uncertain energy market" Energy and Buildings 103, 271-283, 2015.

[106] F. Farzan, S. Lahiri, M. Kleinberg, K. Gharieh, F. Farzan, M.A Jafari, "Microgrids for fun and profit: The economics of installation investments and operations", IEEE Power Energy Mag 11 52–58, 2013.

[107] U.S. Energy Information Administration / Monthly Energy Review (2015), Available at: http://www.eia.gov/totalenergy/data/monthly/pdf/sec2_3.pdf.

[108] M. A. Piette, S. Kiliccote, G. Ghatikar,"Field Experience with and Potential for Multi-time Scale Grid Transactions from Responsive Commercial Buildings", ACEEE Summer Study on Energy Efficiency in Buildings, 2014. Available: https://www.aceee.org/files/proceedings/2014/data/papers/3-499.pdf.

[109] T A. Nguyen, M. Aiello, "Energy intelligent buildings based on user activity: A survey" Energy and Buildings 56 244–257, 2013.

[110] L.P Lombard, J. Ortiz, C. Pout, "A review on buildings energy consumption information" Energy and Buildings 40 394–398, 2008.

[111] Z. Nagy, F. Yong, M. Frei, A. Schlueter, "Occupant centered lighting control for comfort and energy efficient building operation" Energy and Buildings 94 100–108, 2015.

[112] K. Aduda, W. Zeiler, G. Boxem, "Smart Grid-BEMS: The Art of Optimizing the Connection between Comfort Demand and Energy Supply" In IEEE Fourth International Conference in Intelligent Systems Design and Engineering Applications 565-569, 2013.

[113] F. Oldewurtel, A. Ulbig, M. Morari, G. Andersson, "Building control and storage management with dynamic tariffs for shaping demand response", 2nd IEEE PES Innovative Smart Grid Technologies, 2011.

[114] R. Yang and L. Wang, “Multi-objective optimization for decision-making of energy and comfort management in building automation and control,” Sustainable Cities and Society 2  1-7, 2012.

[115] P M. Valdésa, A F Tlacuahuaca, V M. Zavalab, “Analyzing the effects of comfort relaxation on energy demandflexibility of buildings: A multiobjective optimization approach” Energy and Buildings 85  416–426, 2014.

[116] H. Liu, S. Lee, M. Kim, H. Shi, J.T. Kim, K.L. Wasewar, C.K. Yoo, “Multi-objective optimization of indoor air quality control and energy consumption minimization in a subway ventilation system” Energy and Buildings 66 553–561, 2013.

[117] A. Rackes, M S. Waring, ” Using multi-objective optimizations to discover dynamic building ventilation strategies that can improve indoor air quality and reduce energy use ” Energy and Buildings 75 272–280, 2014.

[118] L. Klein, G. Kavulya, F. Jazizadeh, J. Kwak, B. Becerik-Gerber, M. Tambe, Towards optimization of building energy and occupant comfort using multi-agent simulation, International Symposium on Automation and Robotics in Construction ,2011.

[119] A J. Majumdar, J. L. Setter, J R. Dobbs, B M.Hencey. Energy-comfort optimization using discomfort history and probabilistic occupancy prediction. In IEEE Green Computing Conference (IGCC), 1-10, 2014.

[120] V. Zavala, C. Thomas, M. Zimmerman, and A. Ott, “Next-generation building energy management systems and implications for electricity markets.” Argonne National Laboratory (ANL), Tech. Rep, 2011.

[121] E. Oh, J. Park, S Y. Son, "Group Building based Power Consumption Scheduling for the Electricity Cost Minimization with Peak Load Reduction" Journal of Electrical Engineering & Technology 9 742-749, 2014.

[122] Business Case for Energy Efficient Building Retrofit and Renovation, McGraw-Hill Construction, 2013, Available at: http://energy.gov/sites/prod/files/2013/12/f5/business_case_for_energy_efficiency_retrofit_renovation_smr_2011.pdf.

[123] J.L. Mathieu, P.N. Price, S. Kiliccote, A. Ann Piette, Quantifying changes in building electricity use, with application to demand response, IEEE Trans. on Smart Grid 3 507–518, 2011.

[124] G. Boris, V. Laraa, M. Luis, C. Molinab, M. Yanes , "Modeling and identification of the cooling dynamics of a tropical island hotel" Energy and Buildings 92 19–28, 2015.

[125] Deru, M.; Field, K.; Studer, D.; Benne, K.; Griffith, B.; Torcellini, P; Halverson, M.; Winiarski, D.; Liu, B.; Rosenberg, M.; Huang, J.;Yazdanian, M.; Crawley, D "U.S. Department of Energy Commercial Reference Building Models of the National Building Stock" Washington, DC: U.S. Department of Energy, Energy Efficiency and Renewable Energy, Office of Building Technologies, 2010.

[126] A. Vaghefi, F. Farzan, M. A. Jafari, "A Risk-based Approach to Modeling Industrial Loads in Non-Residential Buildings" Submitted to Applied Energy, 2015.

[127] C. Diakaki, E. Grigoroudis, D. Kolokotsa, “Towards a multi-objective optimization approach for improving energy efficiency in buildings” Energy and Buildings 402 1747–1754, 2008.

[128] L. W, M. Shahidehpour, “A Hybrid Model for Day-Ahead Price Forecasting” IEEE Trans. Power Systems, 25(3), 2010.

[129] P. Areekul, T. Senju, H. Toyama, S. Chakrabort, A. Yona, N. Urasaki, “A new method for next-day price forecasting for PJM electricity market” International Journal of Emerging Electric Power Systems, 11, 2010.

[130] R. Weron, “Electricity price forecasting: A review of the state-of-the-art with a look into the future” International Journal of Forecasting 30 1030–1081, 2014.

[131] J.L Horowitz, “The bootstrap” The Handbook of Econometrics 5 3463–3568, 2001.

[132] PJM Energy Market, Available at: http://www.pjm.com/markets-and-operations/energy.aspx

[133] R. Weron, “Electricity price forecasting: A review of the state-of-the-art with a look into the future” International Journal of Forecasting 30 1030–1081, 2014.

[134] O. Grodzevich, O. Romanko, Normalization and other topics in multiobjective optimization, in: Proceedings of the First Fields-MITACS Industrial Problems Workshop. The Fields Institute 89-102, 2006.

[135] E. Hirst, “Real time balancing operations and markets: key to competitive wholesale electricity markets” (2001) Available at: http/ www.ksg.harvard.edu/hepg/Papers/Hirst%204-01.rtmreport.pdfS.

[136] F. Farzan, M.A.Jafari, J. Gong, F. Farzan, A. Stryker, “A Multi-Scale Adaptive Model of Residential Energy Demand” Applied Energy 150 258-273, 2015.

[137] A. Vaghefi, M.A. Jafari, E. Bisse, J. Brouwer, Y. Lu, “Modeling and Forecasting of Cooling and electricity load demand”, Applied Energy 136 186-196, 2014.

[138] International Energy Agency (IEA), “World Energy Outlook (WEO) 2014”, London, 2014.